



**UNIVERSITY OF L'AQUILA**  
**DEPARTMENT OF BIOTECHNOLOGICAL AND APPLIED CLINICAL SCIENCES**

Research Doctorate in Experimental Medicine  
Curriculum Clinic, Endocrinology and Experimental Medicine  
XXXV cycle

Functional and molecular characterization of pharmacological inhibitors with anti-histone-deacetylase activity, in Rhabdomyosarcoma *in vivo* and *in vitro* models

SSD MED/50

PhD Student  
Alessandra Rossetti

PhD Coordinator  
Prof. Mariagrazia Perilli

Tutor  
Prof. Giovanni Luca Gravina

Co-Tutor  
Dott. Claudio Festuccia

A.A. 2021/2022





# INDEX

INDEX	1
ABSTRACT	3
INTRODUCTION	4
1. Sarcomas	4
2. Rhabdomyosarcoma	4
2.1 Diagnosis and treatments	6
2.2 Genetic predisposition to RMS	8
3. Alveolar Rhabdomyosarcoma	8
3.1 Molecular genetics of ARMS	9
3.2 PAX-FOXO1 oncogenicity	10
3.3 Therapeutic targetability of genetic aberrations	13
3.3.1 Targeting PAX3-FOXO1 expression	13
4. Embryonal Rhabdomyosarcoma	14
4.1 Molecular genetics of ERMS and their targetability	14
5. RMS and radioresistance	16
5.1 Mechanism of action	18
5.2 RT and epigenetic remodeling	20
6. Epigenetic	21
7. Histone Deacetylases	21
7.1 HDACs role in transcription and translation	22
7.2 HDACs in cancer	23
8. HDAC inhibitors	24
9. RMS and HDACi	27
10. Romidepsin	27
10.1 Mechanism of action	29
11. Entinostat	29
11.1 Mechanism of action	30
AIM OF RESEARCH	33
MATERIALS AND METHODS	34
1. Cell lines and pharmacological treatments	34
2. Class I HDACs activity	34
3. RNA isolation and qRT-PCR	34
4. Cell viability assay	35
5. Cell cycle analysis by Flow Cytometry	35
6. Apoptosis and PARP1 activity assays	35
7. Mitochondrial superoxide anion ( $O_2^-$ ) production assessment	35
8. Radiation exposure and Clonogenic assay	36

9. Protein extraction and Western blotting	36
10. Animal research ethics statement and <i>in vivo</i> xenograft experiments	37
11. Evaluation of treatment response <i>in vivo</i>	37
12. Statistical analysis and data analysis	37
<b>RESULTS</b>	39
<i>IN VITRO</i>	39
1. Activity levels of class I HDACs in RMS subtypes	39
2. Viability assay of RMS cell lines	39
2.1 FK228 treatment reversibly and not efficiently controls tumor proliferation	39
2.2 MS275 treatment induces growth arrest and cell death	40
3. FK228 reduced the mRNA expression levels of HDACs	41
4. MS275 downregulated transcript levels of HDACs	42
5. Cell cycle distribution and related molecular signature in RD and RH30 cells	42
5.1 FK228 did not control efficiently tumor proliferation	42
5.2 MS275 affected cell cycle distribution	44
6. Apoptosis and PARP1 activity	45
6.1 RMS cells activate anti-apoptotic and pro-surviving signals against FK228	45
6.1.1 MS275 induced non-apoptotic cell death	46
7. <i>In vitro</i> radiosensitive effects of HDACs in RMS cell lines	48
7.1 FK228 radiosensitize FP-RMS	48
7.1.1. FK228 maintains DNA damage	48
7.1.2. FK228 reduce antioxidant ability of RMS	49
7.1.3. FK228 impairs DSBs repair ability	50
7.2 MS275 radiosensitize FP-RMS	52
7.2.1 MS275 increase apoptosis in combination with RT	52
7.2.2 MS275 is able to induce DNA damage	53
7.2.3 MS275 impaires DNA damage repair system of FP-RMS from ROS accumulation induced by RT	54
<i>IN VIVO</i>	56
8. <i>In vivo</i> radiosensitive effects of HDACis in RMS cell lines	56
8.1 FK228 radiosensitizes ARMS	56
8.2 MS275 radiosensitizes FP-RMS cells	57
<b>DISCUSSION</b>	60
<b>CONCLUSIONS</b>	65
<b>BIBLIOGRAPHY</b>	66

## ABSTRACT

Rhabdomyosarcoma is a malignant soft tissue sarcoma typical of children and adolescents. Standard treatments are a combination of surgery, radiotherapy (RT) and chemotherapy. Unfortunately, RT promotes the formation of metastases, due to the proliferation of RT-resistant cell populations. RMS derives from mesenchymal precursors and is divided into two histological subtypes: Alveolar (ARMS) and Embryonal (ERMS). ARMS expresses the fusion proteins PAX3- or PAX7-FOXO1 (therefore they are considered, fusion-positive FP). ERMS is fusion-negative (FN) but is characterized by various mutations and genomic aberrations at the level of the RAS and RTK pathways. However, the two subtypes have anomalous pathways in common. For example, aberrant epigenetic regulation appears to play a critical role in RMS progression and survival.

Histone acetylation is tightly controlled by epigenetic mechanisms regulated by acetyltransferases (HATs) and histone-deacetylases (HDACs), which make the chromatin structure transcriptionally active or inactive, respectively. This means that deregulation of HDAC expression and/or activity may be involved in the development and progression of several cancers, including RMS. It has been seen that class I and IV HDACs are deregulated in the RMS. Thus, HDAC inhibitors (HDACis) are already used with good results for hematological tumors, but not for solid tumors. They could be useful, instead, in combination with classical therapies (e.g. RT). But several studies shown that using a pan-HDAC inhibitor could be responsible for the low therapeutic efficiency of this type of drug.

FK228, or Romidepsin, is a potent natural selective HDACi for class I and II. MS275, or Entinostat, is a potent selective HDACi for class I and IV. Romidepsin induces cell cycle arrest and apoptosis in various solid tumors. Entinostat appears to induce cell cycle arrest in the G<sub>0</sub>/G<sub>1</sub> phase and promotes apoptosis. It downregulates proteins related to cell cycle progression and upregulates proapoptotic proteins. It can reduce the expression of p38 and p65 (NFκβ), thus inhibiting the pathway of MAPKs.

The purpose of this work was to observe the behavior of FK228 and MS275 alone and in combination with RT *in vivo* and *in vitro* models of RMS: RH30 (ARMS) and RD (ERMS). About, FK228 as single therapy shows limited effects but appears to radiosensitize ARMS when combined with RT. It does not show many effects in ERMS; this may be due to the inability of FK228 to inhibit HDAC3, which are the major representatives of class I HDACs in ERMS and plays a crucial role in ERMS oncogenicity.

MS275 has been shown to influence tumor survival by inducing non-apoptotic death and cell cycle arrest in the G<sub>1</sub> phase. In RH30 cells it has irreversible effects, while they are reversible in RD cells. In combination with RT, the molecule is able to prevent growth even *in vivo*, but only in RH30 cells, because in RD cells it showed a partial inhibitory effect. However, it is important to note that targeting HDACs class I and IV may be a potential therapeutic strategy to raise awareness of the most aggressive type of RMS (FP-RMS).

## INTRODUCTION

### 1. Sarcomas

Sarcomas are a group of rare and heterogeneous mesenchymal tumors and represent the 12-15% of tumors occurring in pediatric age. Most of them are characterized by an aggressive biological behavior, highly relapsing and metastatic after treatment. Multimodal therapies have been optimized involving surgery, chemotherapy, radiotherapy (RT) and targeted therapeutics, but sarcomas remain lethal in one-third of patients. Therefore, new therapeutic approaches are needed to improve patients' outcome<sup>1</sup>. Sarcomas are classified according to both molecular and pathological features. Genetically, sarcomas can be divided into two major groups:

- One characterized by simple genetic alterations and nearly diploid karyotypes, usually showing specific alterations such as reciprocal chromosomal translocations or point mutations which have diagnostic significance and often arise *de novo*,
- One exhibiting nonspecific genetic lesions and complex unbalanced karyotypes characteristic of severe genomic instability<sup>2</sup>.

The most common and aggressive forms of sarcoma in childhood are:

- fusion positive (FP),
- Ewing's sarcoma family of tumors (ESFTs),
- FP rhabdomyosarcoma (FP-RMS), known as Alveolar RMS,
- synovial sarcoma (SS).

These sarcomas represent prototypic examples of solid tumors driven by pathognomonic chromosomal translocations<sup>3</sup>.

### 2. Rhabdomyosarcoma

Rhabdomyosarcomas (RMSs) is a heterogeneous group of high-grade malignant neoplasms with a propensity for myogenic differentiation. It characterized pediatric soft tissue tumors associated with the skeletal muscle lineage<sup>4</sup>. Indeed, RMS is more common in children and representing about 50% of all sarcomas and 5% of malignant solid tumors in children aged 0-14 years. Adolescents and more rarely adults may also be affected<sup>5</sup>. It is characterized by an annual incidence of 4.5 cases per million children in the United States, which corresponds to roughly 350 cases *per year*<sup>6</sup>. With the development and refinement of multimodal treatment regimens, survival has improved substantially for many children with RMS. However, the survival of those diagnosed with widely metastatic or relapsed disease continues to be very low<sup>7</sup>.

RMS arise in primitive fetal mesenchyme even at sites that do not contain skeletal muscle. Histologically, the tumor resembles fetal striated muscle. It also manifest immunohistochemical expression of myosin, actin, desmin, myoglobin and Z-band protein. Tumor tissue expresses a DNA binding protein, MTOD1, which may turn out to be a lineage marker for RMS<sup>8</sup>.

The World Health Organization (WHO) recognizes several RMS hystotypes that arise in young people:

1. Embryonal RMS (ERMS),
2. Alveolar RMS (ARMS),
3. Pleomorphic RMS (PRMS),
4. Spindle cell sclerosing RMS (SRMS).

These pose distinct challenges in diagnostic classification and treatment<sup>9</sup>.

Whereas the historical classification based on histological and light microscopic features recognized Alveolar RMS (ARMS) and Embryonal RMS (ERMS) as the two main RMS subtypes, the current classification distinguishes RMS in FP-RMS and fusion-negative RMS (FN-RMS) based on the presence or absence of chromosomal translocations. This molecular stratification more accurately reflects the biological and clinical behavior of these malignancies and FP-RMSs represent the higher risk subtype characterized by a less favorable prognosis<sup>10</sup>. ARMS accounts for 20-30% of RMS, affects children as well as adolescents and young adults, and usually occurs in the extremities and torso. In contrast, ERMS represents 70-80% of all RMS cases. ERMS generally affect younger children (0-4 years), occurring more commonly in the head and neck and genitourinary tract (fig. 1). ARMS' more aggressivity and its association with an unfavorable prognosis, could is partially attributable to its propensity for early dissemination, poor response to therapy and frequent relapses following therapy. Indeed, the 5-year overall survival for ARMS is around 50% compared to 75% for ERMS<sup>11</sup>.

In 80% of cases with Alveolar histology, balanced chromosomal translocations involving chromosomes 2 o 1 and chromosome 12 result in expression of the fusion oncoproteins PAX3-FOXO1 or PAX7-FOXO1, respectively, that drive the malignant phenotypes of these tumors. Pathological, clinical and molecular diversity is noted in the Embryonal subtype of RMS with genetic aberrations including frequent chromosomal gains (chromosomes 2, 8 and 13), mutations of genes such as those in the RAS pathway and specific regions of the loss of heterozygosity and imprinting<sup>12</sup>.



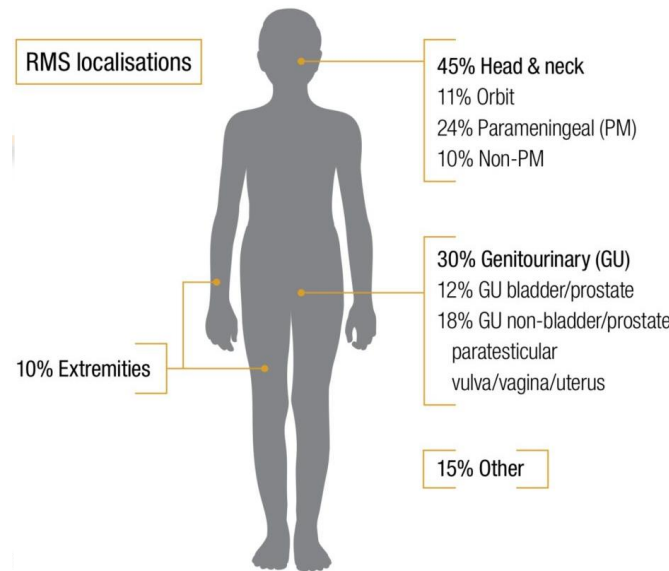


**Fig. 1** Distribution of primary sites for rhabdomyosarcoma. The head and neck site may be subdivided as 7% orbit, 8% other head, 23% parameningeal, and 9% non-parameningeal. The pelvic sites may be subdivided as 11% bladder and prostate, and 5% female genital or 12% male non-bladder/prostate<sup>13</sup>

The 70% of children with localized disease survive with conventional treatment, including surgery, RT and chemotherapy. However metastatic RMSs are frequently resistant or present relapse after initial response, with a 5-years event-free survival rate at about 30%. Therefore, the outcome for high-risk RMS patients remains very poor<sup>14</sup> and the discovery of innovative therapies is an absolute priority to improve therapeutic efficacy and reduce toxicity.

We strongly believe that RMS biology should directly inform clinical trial design. In recent years, insights into the genetics and molecular biology of RMS have provided much-needed opportunities to improve disease classification, risk stratification, assessment of treatment response and opportunities for targeted therapies. The collection of biomaterials as part of clinical trials is critically important to correlate molecular characteristics with clinical parameters and response to treatment. The translation of preclinical findings into clinical trials and, ultimately, standard-of-care recommendations are coordinated by cooperative groups. The International Soft Tissue SaRcoma ConsorTium (INSTRuCT), a cooperation of the European pediatric Soft tissue sarcoma Study Group (EpSSG), created in 2004 by the merge of the International Society of Pediatric Oncology-Malignant Mesenchymal Tumor Committee (SIOP-MMT) and the Associazione Italiana di Ematologia e Oncologia Pediatrica Soft Tissue Sarcoma Committee, the Children's Oncology Group (COG) and the Cooperative Weichteilsarkom Studiengruppe (CWS) offer a platform to harmonies prospective molecular testing and coordinate investigations as part of large clinical trials<sup>7</sup>.

### 2.1. *Diagnosis and treatments:*

The thorough history and physical examination are followed by initial laboratory evaluation consisting of a complete blood count (CBC), urinalysis, renal and liver function studies and a bone marrow biopsy. Computerized tomography (CT) scans and/or magnetic

resonance imaging (MRI) of the primary lesion help to determine size and invasiveness of the tumor. Further testing is based on the location of the primary tumor as examination of cerebral spinal fluid (CSF) for cranial parameningeal lesions, evaluation of the spinal cord in paraspinal tumors and intravenous urography, cystography, cystoscopy and vaginoscopy for genitourinary tumors. Diagnosis is confirmed by biopsy of the primary tumor<sup>8</sup>.

Recent technological developments have extended molecular testing of tumors to include the analysis of circulating tumor-derived material shed by tumors into bodily fluids such as blood, urine and saliva. This approach, known as a “liquid biopsy”, may help to overcome the limitations associated with tissue biopsies. In this way, they can obtain information about tumor cells which may not have been sampled because of their anatomical location. Furthermore, as a minimally invasive technique, liquid biopsies can be collected at multiple time points throughout patient treatment and follow-up. This may remove the need for serial tissue biopsies and thus helps to reduce children’s exposure to anaesthesia and imaging procedures (fig. 2). So, liquid biopsies hold enormous potential for RMS screening, diagnosis, risk stratification and monitoring<sup>7</sup>. Prognosis can be determined by stage, histological classification, age, and site of origin. Staging, in children, is accomplished by clinical evaluation (Intergroup Rhabdomyosarcoma Study Group (IRSG) Stage) and / or surgicopathological evaluation (IRSG Group). The IRSG subdivides RMS into low, intermediate and high risk groups for purposes of protocol based therapy. Younger patients (1-9 years) tend to have a more favorable prognosis than infants and adolescents. ERMS have a better prognosis than ARMS. ERMS with diffuse anaplasia may have a worse outcome than the other subsets of embryonal rhabdomyosarcoma<sup>15</sup>.

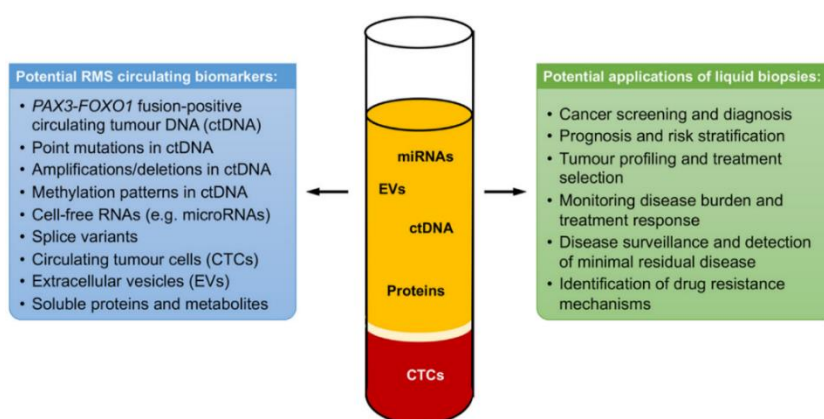


**Fig. 2** Overview of liquid biopsy components and potential biomarkers and applications in RMS. CTCs → circulating tumour cells; ctDNA → circulating tumour DNA; EVs → extracellular vesicles; miRNAs → microRNAs.<sup>7</sup>

If the tumor can be completely excised it should be resected. If uncertainly exists regarding the margins or microscopic residuals remain after excision, re-excision of the tumor site is indicated prior to adjuvant therapy, as chemotherapy and RT<sup>8</sup>. RT, by using ionizing radiations (IR), is able to kill cancer cells directly by inducing DNA double strand breaks

(DSBs), and indirectly by promoting immunogenic cell death (ICD), which consists of recruiting the host immune system by the release of several mediators, including cytokines. However, cancer cells can efficiently escape from RT-induced cell death through different mechanisms, such as resistance to apoptosis, high DNA repair capacity, antioxidant capacities and ICD escape<sup>16</sup>. Notably, radioresistance has been shown to be higher in cancer stem cells (CSCs), known to be the critical driving force of cancer and the real target of any antitumoral therapeutic approach. However, several studies have identified molecular mechanisms implicated in radioresistance<sup>17</sup>.

## 2.2. *Genetic predisposition to RMS:*

Having a cancer predisposition syndrome is one of the strongest risk factors for developing RMS. The genetic syndromes that have been implicated in susceptibility to RMS include:

- Li-Fraumeni (frequently associated with pathogenic TP53 germline variants),
- Neurofibromatosis type 1 (associated with pathogenic variants in NF1),
- Nevoid basal cell carcinoma syndrome (frequently associated with pathogenic PTCH1 and SUFU germline variants),
- DICER1,
- Costello (frequently associated with pathogenic HRAS germline variants),
- Noonan (a RASopathy linked to pathogenic variants in several germline genes including CBL),
- Beckwith-Wiedemann (associated with abnormal regulation of genes encoded by two imprinting centres at 11p15),
- Nijmegen Breakage Syndrome with mutations in NBN,
- Rubinstein Taybi Syndrome with mutations in CREBBP and EP300<sup>7</sup>.

Heritability of RMS may be even higher and caused by variants in genes not yet recognized as relevant cancer predisposition genes, rare variants and/or interactions between variants. Parallel tumor/germline sequencing studies and subsequent functional investigations are needed to further delineate the landscape of pathogenic germline variants that contribute to the RMS development. The most frequent pathogenic/likely pathogenic (P/LP) germline variants identified in patients with young-onset RMS were detected in TP53, NF1 and BRCA2 (table 1)<sup>18</sup>. Additional studies are needed to fully evaluate the role of these genes on RMS susceptibility.

## 3. Alveolar Rhabdomyosarcoma

Alveolar rhabdomyosarcoma (ARMS) is a high grade neoplasm that can metastasize to the regional lymph nodes. Histologically it is composed by a monomorphous population of primitive

cells with round nuclei, with fibrovascular septa that separate the tumor cells into discrete nests and features of arrested myogenesis. These nests contain central clusters of cells with loss of cohesion around the periphery, giving an ‘alveolar’ appearance. The male:female ratio is approximately the same and no geographic or racial predilection is reported. ARMS commonly arise in the extremities. Additional sites of involvement include the paraspinal and the perineal regions and the paranasal sinuses. Clinically, ARMS typically present as rapidly growing extremity masses, tend to be high stage lesions at presentation and form expansile, rapidly growing soft tissue tumors. Tumors at other sites such as paranasal, perirectal and paraspinal mainly cause symptoms of compression of the surrounding structures. Immunohistochemically, ARMS stain strongly for desmin. Myogenin and MyoD1 typically show a diffuse, strong nuclear staining pattern<sup>19</sup>.

### 3.1. Molecular genetics of ARMS:

ARMSs belong to FP-RMS, and they are associated with balanced chromosomal translocations which involve chromosomes 2 or 1 and chromosome 13 [t(2;13)(q35;q14), t(1;13)(p36;q14) less common], how shows in figure 3, resulting in fusion oncoproteins consisting of the N-terminal DNA-binding domains of paired box gene 3 (PAX3) or paired box gene 7 (PAX7) [encoding highly homologous members of the paired box family of transcription factors] fused to the C-terminal transactivation domain of the Forkhead Box O1 (FOXO1) gene [encoding a member of the O subfamily of forkhead box transcription factors], generating PAX3-FOXO1 and PAX7-FOXO1 oncogenes, respectively<sup>5</sup>. The presence of the PAX3-FOXO1 fusion gene has been shown to be associated with significant negative prognostic value in RMS in several studies and is more frequent in adolescents than younger patients<sup>20</sup>.

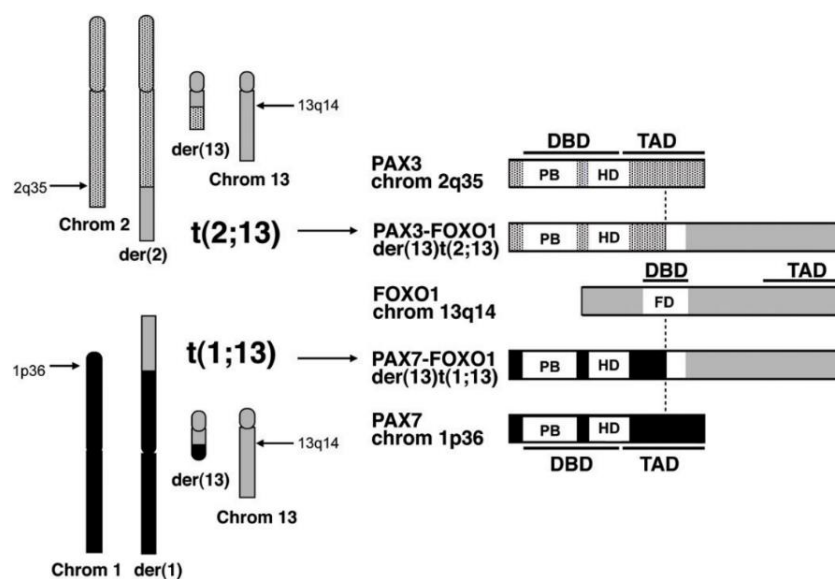


**Fig. 3** Schematic depiction of t(2;13)(q35;q14) and t(1;13)(p36;q14) chromosomal translocations and resultant PAX3/7-FOXO1 chimeric fusion products. The vertical dashed line denotes the fusion point. DBD: DNA binding domain; FD: Forkhead domain; HD: Homeobox domain; PB: Paired box; TAD: Transcriptional activation domain.<sup>6</sup>

Molecular pathology studies of the chimeric products reveal that around 60% of ARMS tumors are PAX3-FOXO1-positive, 20% are PAX7-FOXO1-positive and 20% are fusion-negative (FN)<sup>6</sup>. Interestingly, FN-ARMS demonstrates genetic changes characteristic of ERMS, which is consistent with the similar expression patterns and clinical outcomes of FN-ARMS and -ERMS cases<sup>21</sup>. In rare cases, alternative translocations were found, as PAX3 is rearranged with widely expressed alternative partners such as Forkhead Box O4 (FOXO4), Nuclear Receptor Coactivator 1 or 2 (NCOA1 or NCOA2) and INO80D encoding the INO80 Complex Subunit D present in the INO80 chromatin remodeling complex<sup>22</sup>. The partner gene fused to FOXO1 may hold additional prognostic significance, with PAX7-FOXO1 tumors possibly having superior overall survival compared to PAX3:FOXO1-translocated tumors<sup>23</sup>.

### 3.2. *PAX-FOXO1 oncogenicity:*

PAX3 and PAX7 are highly related members of the paired box transcription factor family, acting as important regulators of lineage commitment during embryogenesis and development of neural tube, neural crest and skeletal muscle<sup>24</sup>. Whereas PAX3 exerts a major role in early skeletal muscle formation, PAX7, a marker of satellite cells, is predominantly implicated in muscle postnatal growth and regeneration in the adult. In skeletal muscle progenitors, PAX3 and PAX7 direct cells into a myogenic program by transcriptional and epigenetic regulation of myogenic determinant genes. The most frequent fusion partner in RMS, FOXO1, encodes a ubiquitous member of the FOXO transcription factor subfamily involved in a variety of processes during both embryogenesis and adult tissue homeostasis<sup>25</sup>. FOXO1 regulates transcription and DNA repair and because of their antiproliferative and proapoptotic functions, FOXO proteins are considered tumor suppressors. The enhanced transcriptional activity of the chimeric proteins was shown to rely on the decreased sensitivity of the FOXO1 transactivation domain to the inhibitory effects of PAX3 or PAX7 N-terminal domain<sup>26</sup>. The PAX-FOXO1 fusion products have altered expression, subcellular localization and function, compared to the wild-type. In contrast to the wild-type, FOXO1 protein can shuttle between the nucleus and cytoplasm, while the PAX3- or PAX7-FOXO1 protein is localized exclusively in the nucleus<sup>6</sup> (fig. 4). The oncoproteins promote an aberrant transcription factor driving malignant transformation and progression by altering multiple cellular pathways and biological processes. In particular, through the two PAX3 DNA binding domains, PAX3-FOXO1 causes transcriptional activation of hundreds of PAX3 target genes, including myogenic and neural marker genes and also act as key factor driving the transcription through looped myogenic super-enhancers, contributing to freeze cells in a myoblastic status. It is important to specify that, to date, most functional studies have

concentrated on PAX3-FOXO1, though many findings can be extended in conception to include PAX7-FOXO1.

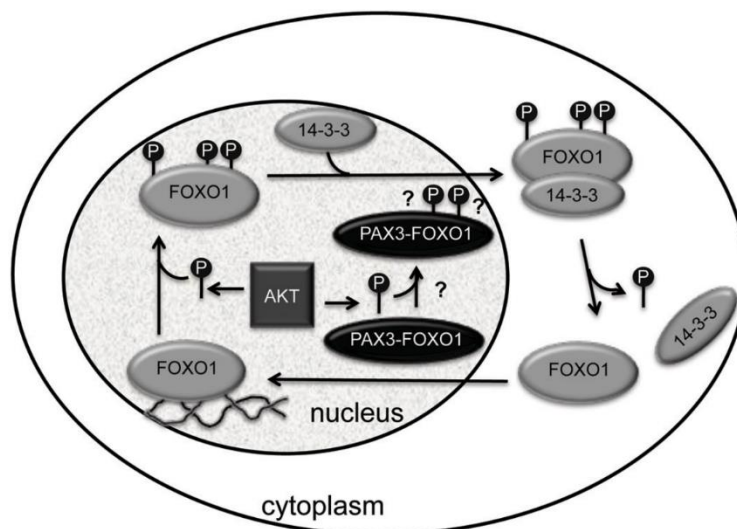


**Fig. 4** Phosphorylation-mediated regulation of FOXO1, but not PAX3-FOXO1, subcellular localization. Wild-type FOXO1 contains three evolutionarily conserved AKT phosphorylation sites (P). AKT-driven phosphorylation at these FOXO1 residues promotes 14-3-3 protein docking and binding, resulting in inactivation of FOXO1 transcriptional activity via cytoplasmic sequestration. PAX3-FOXO1 is resistant to AKT-mediated regulation by phosphorylation as evidenced by its constant nuclear localization.<sup>6</sup>

A higher expression of PAX3/7-FOXO1 mRNA and protein, compared with the wild-type fusion partners, appears to be relevant for FP-RMS development. Indeed, whereas PAX3 protein is rapidly degraded during early myogenic differentiation, PAX3-FOXO1 expression has been suggested to participate in the heterogeneous expression of the fusion gene in primary and metastatic tumors<sup>10</sup>. About this, it was demonstrated that upregulation of PAX3-FOXO1 during the G<sub>2</sub>/M phase of cell cycle triggered a transcriptional program allowing checkpoint adaptation under stress conditions, such as irradiation<sup>27</sup>. The cells origin of these FP-RMS, as well as the contribution of further genetic alterations to the pathogenesis and disease progression remain elusive and highly debated. Indeed, several transgenic and knock-in animal models demonstrated that PAX3-FOXO1 by itself cannot cause FP-RMS whereas additional genetic lesions are necessary to recapitulate oncogenic transformation and sarcoma development<sup>28</sup>.

Amplification of the chromosomal regions 2p24 and 12q13-q15 involves the N-Myc protooncogene (MYCN) and cyclin-dependent kinase 4 (CDK4), respectively, as well as TP53 mutations and CDKN2A deletion. The amplicon containing CDK4 has been associated with a poor prognosis in FP-RMS<sup>29</sup>; the amplicon containing the MYCN oncogene is associated with an inferior outcome<sup>30</sup>. So, CDK4 and MYCN amplification will be assessed for prognostic value independent of PAX3-FOXO1 status.

The FOXO1 protein shuttles between the nucleus and cytoplasm, with its subcellular localization regulated by the canonical PI3K/AKT signaling pathway. Phosphorylation of

FOXO1 confers cytoplasmic sequestration, and dephosphorylation allows nuclear translocation<sup>31</sup> (fig. 5).

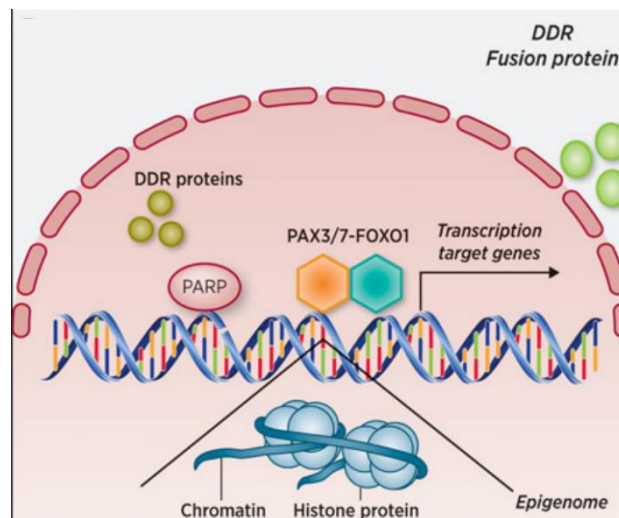


**Fig. 5** Overview of the cellular processes used in the targeted therapy-based combination treatments in ARMS. In particular, the intranuclear processes: DNA damage response (DDR) (PARP), and the epigenome that are used as therapeutic targets in (pre)clinical combination treatments in ARMS.<sup>37</sup>

While multiple serine/threonine kinases, such as members of the AGC protein kinase family, CDK1, CDK2, CK1, and DYRK1 have been reported to phosphorylate FOXO1 at various sites, AKT is regarded as the primary kinase involved in phosphorylation-dependent modulation of FOXO1 subcellular localization and consequent transcriptional activity. FOXO1 harbors three evolutionarily conserved AKT phosphorylation sites located at threonine 24, serine 256, and serine 319. Upon activation, AKT translocates to the nucleus and directly phosphorylates FOXO1 74–76<sup>6</sup> (fig. 4).

In addition, direct or indirect interactions of PAX3-FOXO1 with chromatin-related proteins such as HATs, HDACs, bromodomain-containing protein 4 (BRD4) and ATP-dependent chromodomain helix DNA-binding protein 4 (CHD4), have been demonstrated to participate in the oncoprotein-driven epigenetic reprogramming<sup>31</sup>(fig. 6).

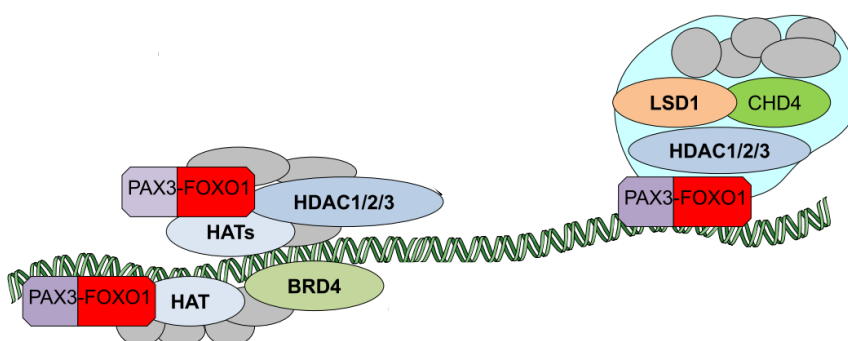


**Fig. 6** Schematic representation illustrating examples of the reported investigational combinatorial strategies targeting HDACs and other epigenetic regulators in FP-RMS.<sup>10</sup>

The poorer prognosis associated with PAX3-FOXO1-positive tumors coupled with the ARMS-specific nature of PAX3-FOXO1 expression make this oncogenic chimera a very interesting therapeutic target. Despite some tentative approaches, the development of agents specifically targeting fusion oncoproteins remains extremely challenging, also because FP-RMS are considered mutationally quiet compared with other malignancies<sup>6</sup>.

### 3.3. *Therapeutic targetability of genetic aberrations:*

Specific genetic aberrations in RMS, identified through sequencing analyses of tumor samples or liquid biopsies, may indicate targets for therapeutic intervention. Indeed, in pediatric sarcomas, translocation fusion products have long been regarded as potential tumor antigens<sup>7</sup>.

#### 3.3.1. *Targeting PAX3-FOXO1 expression:*

Even if PAX3-FOXO1 expression is typically not sufficient for full oncogenic transformation, the fusion protein plays a necessary and fundamental role in ARMS tumorigenesis. Indeed, its inhibition can reduce cellular proliferation, decreased motility and invasion, increased myogenic differentiation<sup>32</sup>. PAX3-FOXO1 is an intrinsically disordered protein with no catalytic activity or drug binding pockets which to date has precluded direct pharmacologic targeting. Early efforts in PAX3-FOXO1 biology were directed at inhibiting the downstream transcriptional targets (effectors) of the fusion protein. Moreover, many studies have shown that the inhibition of even catalytically PAX3-FOXO1 targets did not effectively impair FP-RMS cell growth due to the not enough modulation of signaling pathways that results not sufficient for full inhibition of PAX3-FOXO1 activity<sup>33</sup>. Recent efforts have shifted to targeting proteins that modulate or co-regulate PAX3-FOXO1 activity such as proteins that control the life cycle of the fusion protein (synthesis, activation or degradation). Targeting BRD4, that is required for PAX3-FOXO1 activity, contributes to the decompaction of chromatin and the stability of the fusion protein<sup>34</sup>. Also, AKT, that phosphorylates FOXO1 in a positive way, could be an indirect target that leads to the inactivation of FOXO1 transcriptional function<sup>6</sup>.

Nevertheless, immunotherapy represents a plausible strategy to antagonize the PAX3-FOXO1 oncoprotein, including targeting the oncoprotein breakpoint epitope using vaccine or targeting cell surface effector proteins of PAX3-FOXO1 through monoclonal antibodies, Chimeric Antigen Receptor T Cell (CAR-T) or CAR-NK cells<sup>7,27</sup>. However, further studies are required to determine the best approach to apply immunotherapy to RMS.



#### 4. Embryonal Rhabdomyosarcoma

ERMS is a primitive, malignant soft tissue tumor that recapitulates the phenotypic and biological features of embryonic skeletal muscle. It is the most common subtype, occurring in 2.6 per million children ages less than 15 years in the United States, with children less than 5 years of age being most commonly affected. They are more common in males than females with a ratio of 1.4:1.25. The tumors occur in equal proportion in the head and neck and the genitourinary system. Besides these two general regions, ERMS occur in the biliary tract, retroperitoneum, pelvis, perineum, and abdomen and have been reported in various visceral organs, such as the liver, kidney, heart, and lungs<sup>35</sup>.

Histologically, ERMS show primitive oval to spindle cells with minimal cytoplasm. The background can be loose myxoid or the cells can be compactly arranged in sheets. Some areas show small blue round cell morphology. As these cells differentiate, they progressively acquire more cytoplasmic eosinophilia and elongate shapes, varyingly described as “tadpole”, “strap”, and “spider” cells and deemed to be evidence of rhabdomyoblastic differentiation. Immunohistochemically, markers of skeletal muscle differentiation are positive in ERMS. Desmin is the most frequently diagnostic marker used and shows diffuse staining. ERMS typically shows patchy positivity for Myogenin and MYO-D1<sup>17</sup>.

ERMS do not show any gene fusions. Molecular analyses typically show aneuploidy with multiple copy number gains and losses noted. Whole chromosome gains with polysomy of chromosome 8 are common. Whole chromosome losses of 10 and 15 are noted. The specific genes associated with ERMS include RAS family genes (HRAS, NRAS, KRAS), FGFR4, PIK3CA, NF1 and FBXW7<sup>36</sup>.

##### 4.1. *Molecular genetics of ERMS and their targetability:*

The RAS pathway is altered in the majority of FN-RMS, involving HRAS, KRAS or NRAS genes<sup>37</sup>. Candidate compounds in current clinical trials include farnesyl protein transferase inhibitors (FT-ases), which are designed to prevent the lipidation of RAS proteins, preventing binding to the plasma membrane where RAS activation occurs. More recently, small molecule inhibitors have been designed to specifically and irreversibly bind KRAS<sup>G12C</sup> and trap it in its inactive GDP-bound state<sup>7</sup>. It is hoped that future compounds will target a more expansive array of RAS mutant proteins. The use of mutant-specific inhibitors allows tumor cells to adapt by upregulating signaling through any normal unmutated RAS alleles present. Overcoming this adaptation by using an inhibitor against SHP2 (which mediates signaling from many tyrosine kinase receptors in combination with a mutant specific RAS inhibitor) proved effective in a preclinical study and suggests that use of vertical pathway inhibition strategies may be necessary to prevent rapid resistance to mutation-specific RAS inhibitors<sup>38</sup>. The most common finding in FN tumors was that at least one member of the RAS

pathway was mutated, affecting over half of all cases. Approximately a third of all FN tumors presents mutations in one of the RAS genes (not only predominant NRAS but also HRAS and KRAS) (fig.7.A). Also, it was described a non-random distribution of these RAS mutations with age, as HRAS strongly associated with under one-years old, KRAS more frequent in toddlers and NRAS in adolescents<sup>39</sup>. Beyond the RAS genes, there are many mutations in its pathway genes that contribute to activation of RAS as copy number gain or mutation of RTK-encoding genes, as well as mutations in downstream signal transducers, all of which can be targeted by approved drugs<sup>40</sup>. Although more frequent in FN-RMS, TP53 mutations have been found to correlate with outcome and represents a potentially important biomarker of risk. Small molecules which can bind and cause the refolding of mutant TP53 are a clinical candidate currently in clinical trials in adult patients<sup>39</sup>.

Perturbation of the PI3K pathway in RMS is also evident, due to mutations in PIK3CA and loss of PTEN, and the pathway is active in the majority of RMS<sup>7</sup> suggesting PI3K/mTOR targeted agents may be broadly effective (fig. 7. A).

Defects in the DNA damage response are another major class of genetic aberrations in RMS. MDM2 amplification occurs in 5% of cases<sup>36</sup> indicating that MDM2 antagonists may be of therapeutic value. MYOD1 is a member of the basic helix-loop-helix muscle regulatory factor family and is required for muscle differentiation. A particular missense mutation (L122R) has been associated with around a third of the spindle/sclerosing morphologic subtype of RMS, although, importantly, it has also been found in ERMS histology. This mutation is more frequently seen in tumors from older patients with RMS and represent highly aggressive tumors with a very poor outcome<sup>40</sup>.

Adaptation of RMS cells to the transcription factors such as the fusion proteins, MYCN and MYOD1 may create dependency on the ATR-CHEK1-WEE1 axis (fig. 7. B). This is supported by the inhibition of WEE1 that has shown potential in a preclinical study<sup>41</sup>. Patients with MYOD1 mutant tumors are not effectively treated by current protocols and urgently require new personalized treatment options. These may be due to the cooperating mutations in PI3K and RAS pathway genes and/or targeting MYOD1<sup>L122R</sup> and its role in tumorigenesis. However, directly targeting mutant MYOD1 while leaving the wild-type molecule unaffected would be very challenging<sup>42</sup>.

Finally, the use of proteolysis-targeting chimeras (bifunctional molecules containing two ligands, one to the target molecule to be degraded and one to the E3 ubiquitin ligase) makes the ubiquitin-proteasome system able to degrade any desired molecule. This will increase therapeutic options for RMS and allow targeting of traditionally undruggable proteins such as transcription factors.

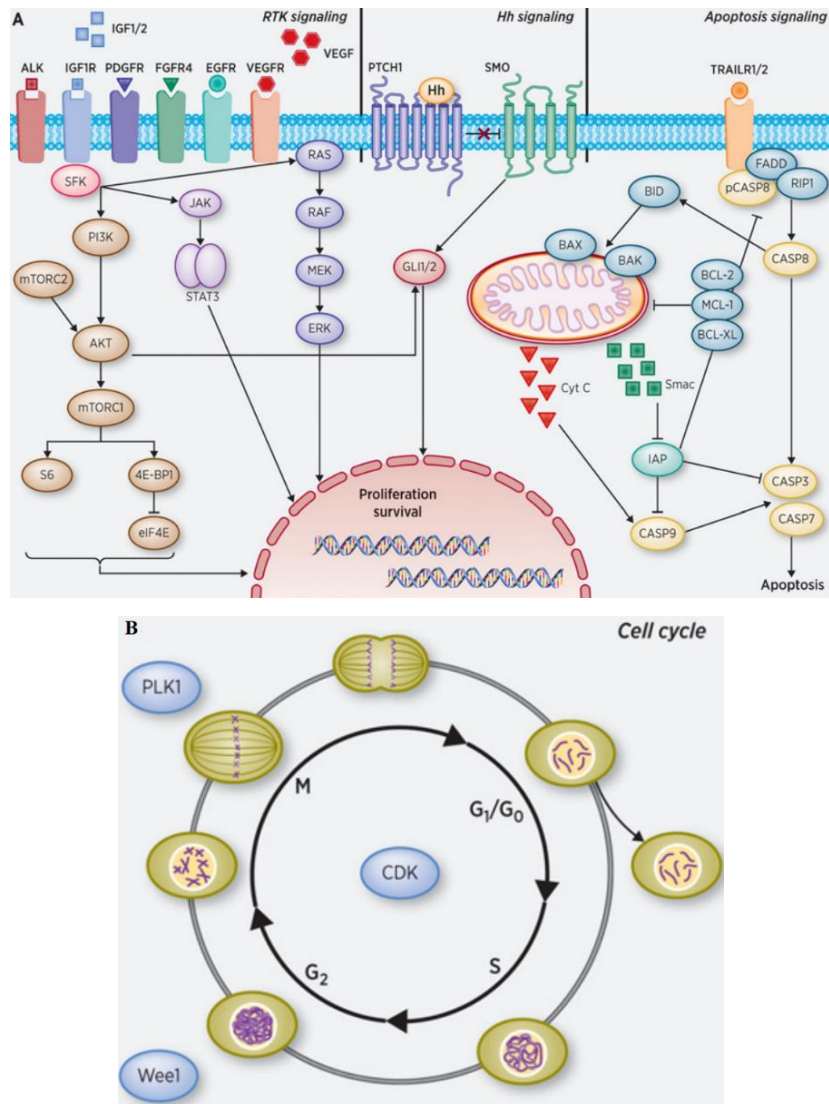


**Fig. 7** Overview of the cellular processes used as targets in the targeted therapy-based combination treatments in ARMS and ERMS.

- A.** Membrane-bound growth factor receptors IGF1R, ALK, PDGFR, FGFR4, EGFR, VEGFR, Patched 1 (PTCH1), SMO, and TRAILR1/2; ligands IGF1/2, VEGF and (Sonic, Indian, Desert) Hh; intracellular signaling proteins of the PI3K/AKT/mTOR, JAK/STAT3, RAS/MEK/ERK, Hh and apoptosis pathway (4E-BP1, eukaryotic translation initiation factor 4E-binding protein 1; eIF4E, eukaryotic translation initiation factor 4E; JAK, Janus kinase; FADD, Fas-associated protein with death domain; CASP, caspase; RIP1, receptor-interacting serine/threonine-protein kinase 1; BID, BH3 interacting-domain death agonist; BAX, Bcl-2-associated X protein; BAK, Bcl-2 homologous antagonist killer; BCL-2, B-cell lymphoma 2; MCL-1, induced myeloid leukemia cell differentiation protein; BCL-XL, B-cell lymphoma-extra large; Smac, second mitochondria-derived activator of caspases; Cyt C, cytochrome C, IAP, inhibitor of apoptosis protein).
- B.** Intranuclear processes: the cell cycle that are used as therapeutic targets in (pre)clinical combination treatments in ARMS and ERMS.<sup>10</sup>

## 5. RMS and radioresistance

RT is crucial for local control at primary and metastatic sites in pediatric RMS, preventing in-field progression in both cases<sup>43</sup>. Although innovative technologies greatly improve the irradiation delivery and reduce general toxicity, allowing complete remission in many RMS patients. RT induces cancer cell death by the direct or indirect action of radiation on the DNA molecules. Indeed, this therapy can disrupt the DNA structure through direct molecule breaks or indirectly by increasing the water solvent temperature that leads to the generation of reactive oxygen species (ROS), causing

DNA damage. However, treatment frequently fails resulting in disease progression, probably due to the ability of RMS cells to become radioresistant<sup>44</sup> (fig. 8).

RMS cells can efficiently escape from RT-induced cell death through different mechanisms, identified by different studies over the last years. Several key cellular and molecular factors, including resistance to apoptosis, high DNA repair capacity, antioxidant capacities, tumor microenvironment, seem to be important for radioresistance capability<sup>45</sup>. Notably, tumor heterogeneity and the presence of cancer stem cells (CSCs) are implied in RMS radioresistance, and they are known to be the critical driving force of cancer and the real target of any antitumoral therapeutic approach<sup>46</sup>. For example, the FP-RMS resistance is caused by the upregulation of the fusion oncoprotein, that during the G<sub>2</sub> phase promoted a cell cycle checkpoint adaptation allowing cells to transit from G<sub>2</sub> to mitosis despite DNA damage induced by radiation.

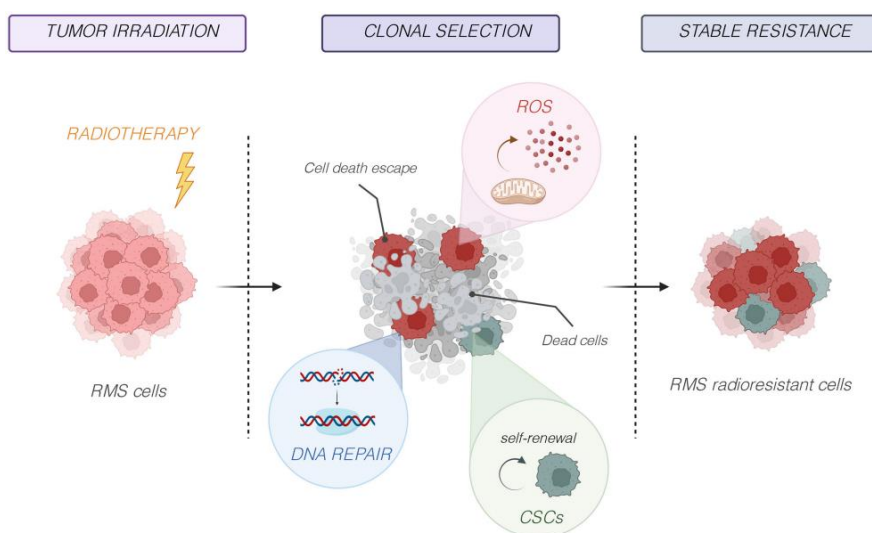


**Fig. 8** Molecular mechanisms responsible of radioresistance. Several key cellular and molecular factors, including DNA damage and repair, oxidative stress, tumor microenvironment, cancer stem cells (CSCs), and tumor heterogeneity, are implied in RMS radioresistance<sup>13</sup>

Furthermore, recent preclinical evidence indicates that RT could promote the formation of distant metastases due to the emergence of these RT-resistant cell populations<sup>47</sup>. Thus, together with the development of more sophisticated and effective technologies, overcoming radioresistance seems to be not just a question of dose but rather of understanding the cellular mechanisms that support radioresistance to identify future radiosensitizing strategies<sup>45</sup>. Indeed, radiosensitizer agents (chemical or pharmaceutical) can improve the RT-killing effect by enhancing the induction of DNA damage and the production of ROS. Mostly, mechanisms of action, that can improve the RT-killing effect, involve the:

- enhancement of DNA damage through the inhibition of the DNA repair pathways NHEJ and HR,
- impairment of cell cycle progression at a radiosensitive phase (G<sub>2</sub>/M),
- gene expression alteration of radioresistance and radio-sensitive genes<sup>48</sup>.

### 5.1. *Mechanism of action:*

DSBs, caused by the production of ROS, are the most lethal form of DNA damage and a primary cause of cell death induced by RT. They can be divided in simple and complex types. Contrary to SSBs and simplex DSBs (two-ended breaks of DNA, usually directly consequent to the action of radiation), complex DSBs are clusters of different DNA damages including single-base mutations, insertions, and deletions and/or SSBs around DSBs. They are generally indirectly induced by radiation through the production of ROS, are usually inefficiently repaired, determining genomic instability and cell death<sup>49</sup>. However, cancer cells can activate specific DNA damage repair mechanisms, surviving the following irradiation<sup>50</sup>. Studies described how RT mainly kills cancer cells by modulating oxidative stress and which genes and miRNAs are involved. However, the two main RMS subtypes efficiently activate an antioxidant stress response, able to protect themselves against ROS injury during RT exposure. They counteract RT by upregulating the expression of antioxidant-enzymes, such as superoxide dismutases (SOD), catalase (CAT) and glutathione peroxidases 4 (GPx4), and several miRNAs (miR-22, -126, -210, -375, -146a, -34a)<sup>45,51</sup>. Studies also shown that radiation increased the expression of NRF2 (nuclear factor erythroid 2-related factor), a transcription factor known to regulate the expression of pro- and anti-oxidant proteins, which protects cells and from the oxidative stress. Indeed, NRF2 silencing counteracted the expression of antioxidant enzymes and miRNAs and so enhanced the RT-mediated toxicity, which may represents a potential target for new radiosensitizing therapies in RMS tumors. So, radioresistance could really depend by the ability of RMS cells to upregulate the expression of several antioxidant molecules by the activation of specific antioxidant-related transcription factors to protect DNA from ROS-induced lethal damages<sup>51</sup>. Furthermore, it is recently shown that CAV-1, a tumor promoter sustaining rhabdomyosarcomagenesis, promotes radioresistance in RMS through increased oxidative stress protection and that RMS surviving to RT more efficiently detoxifies from ROS<sup>52</sup>.

The homologous recombination (HR) and the non-homologous end joining (NHEJ) mechanisms represent the most prominent pathways, orchestrating the DNA damage response (DDR) and NHEJ is the major DDR pathway activated by RT<sup>45</sup>. Several studies noted in RMS biopsies an overexpression of PARP1, PARP2, and PARP3 mRNAs compared with normal skeletal muscle and PARPi have been demonstrated to affect growth, survival, and radiation susceptibility of human ARMS and ERMS cell lines. Therefore, using PARPi could radiosensitize RMS independently of HR pathway because conventional RT, causing thousands of SSBs, would saturate the HR mechanisms inducing, in the presence of PARPi, RMS death, as already shown for other cancer types<sup>53</sup>.

About NHEJ mechanism, DNA-dependent Protein Kinase catalytic subunit (DNA-PKcs) is the key regulator of this repair process. Moreover, DNA-PKcs has been shown to interplay with HR pathway, suggesting its pleiotropic role in regulating DDR. Several studies suggest a role for DNA-PKcs in RMS radioresistance. Specifically, it promotes sarcomagenesis and sustains the activity of c-Myc and AKTs, which are known to support radioresistance in ERMS and ARMS tumors<sup>54</sup>. Thus, targeting DNA-PKcs has been supposed to be a critical radiosensitizing strategy and, nowadays, several inhibitors, with a high selectivity and a valid pharmacokinetics, are available across a variety of cancer types<sup>49</sup>.

Another potential target to affect ERMS radiosensitivity is c-Myc, whose downregulation through the inhibition of the MEK/ ERK pathway has been demonstrated to *in vitro* and *in vivo* cause cell death by promoting the radiation-induced DNA DSB damage and impairing the DNA DSB repair machinery<sup>55</sup>.

Recent evidence suggests that CSCs of several malignancies, also comprehending RMS, can resist ionizing radiation because of a high expression of genes and pathways (fig. 9) related to stem-like features, activated DNA repair mechanisms and altered levels of free radical scavenger levels<sup>56</sup>. Specifically, the molecular pathways contributing to the CSC intrinsic radioresistance are PI3K/Akt/mTOR and NOTCH ones, which upregulates ROS scavenging enzymes. Thus, inhibiting NOTCH could be the efficient strategy to radiosensitize CSCs, bypassing their ability to detoxify from ROS<sup>57</sup>.

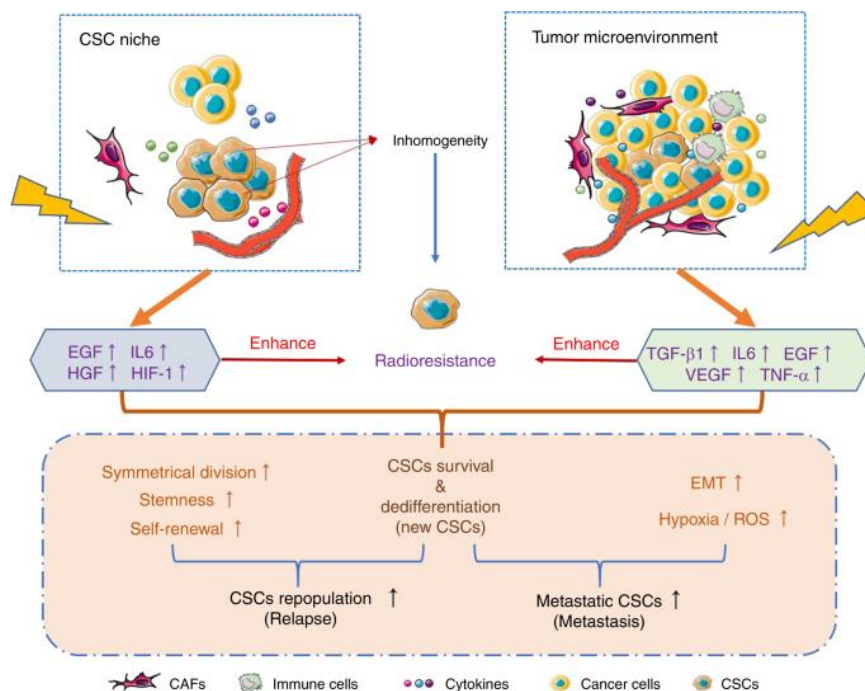


**Fig. 9** Potential mechanisms by which CSCs induce relapse and metastasis. CSCs have innate radioresistance. Both the CSC niche and tumour microenvironment can enhance the radioresistance of CSCs and support CSC survival during radiotherapy through the expression of multiple cytokines that contribute to increased stemness and self-renewal of CSCs and induce EMT and hypoxic conditions, resulting in higher migration and invasion of CSCs, further leading to tumour recurrence and metastasis. CAF = Cancer Associated Fibroblasts<sup>58</sup>

## 5.2. RT and epigenetic remodeling:

Deregulated epigenetic mechanisms have been shown to sustain different mechanisms of radioresistance including DNA repair, antioxidant response, cancer cell life and death decisions, as well as anti-cancer immune response<sup>59</sup>. Therefore, identifying the molecules and epigenetic reprogramming pathways used by cancer cells could lead to the development of promising targeted therapies able of weakening the different mechanisms of radioresistance, also in the context of RMS. Indeed, targeting specific DNMTs or HDACs has been demonstrated to reverse RMS phenotype, counteracting stemness and inducing radiosensitization<sup>60</sup>.

It is important to find some therapies that can enhance the radiosensitivity of ARMS and ERMS cells by inducing a drastic G<sub>2</sub> cell cycle arrest, which was correlated to a permanent DNA damage (upregulation of  $\gamma$ -H2AX) and to the inability of tumoral cells to repair it (alteration of RAD51, ATM, and DNA-PK protein expression), targeting class I and IV HDACs in RMS cells (fig. 10). Thus, growing evidence suggests that radiation exposure is also related to substantial epigenetics changes of cancer cells. Different studies demonstrated that RT could affect DNA methylation patterns and promote a decrease in the expression level of DNMTs and HDACs, with that genomic hypomethylation resulting in enhanced radiation sensitivity in several cancer types<sup>61</sup>.

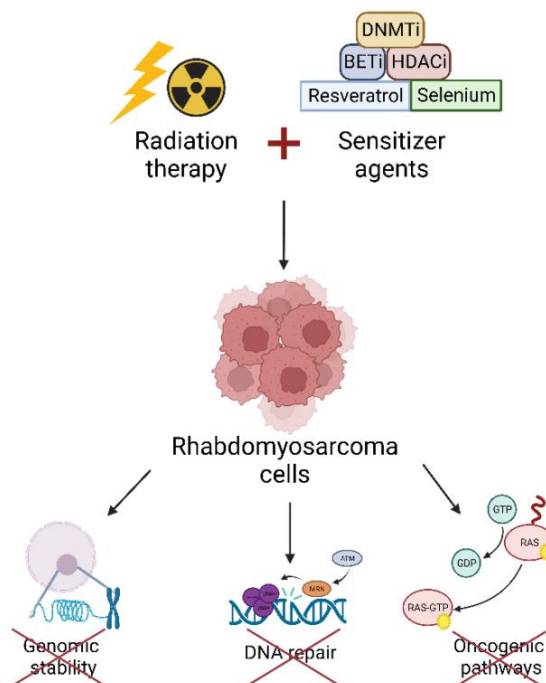


**Fig. 10** The combination of radiation therapy and sensitizer agents able to target epigenetic enzymes, transcription factors etc., sensitizes RMS cells to ionizing radiation by impairing genomic stability, DNA repair, and oncogenic pathways. DNMTi: DNA Methyltransferase inhibitors; BETi: Bromo- and extra-terminal domain inhibitors; HDACi: Histone Deacetylase inhibitors.<sup>44</sup>

## 6. Epigenetic

Epigenetic dysregulation represents an important mechanism driven by the specific alterations present in tumors<sup>62</sup>. Indeed, the chromatin remodeling induced by the chimeric proteins causes transcription alterations leading to aberrant expression of oncogenes and repression of tumor suppressors. However, the epigenetic rewiring also provides potentially druggable targets in these malignancies with histone deacetylases (HDACs) playing a pivotal role<sup>63</sup>.

## 7. Histone Deacetylases (HDACs)

Chromatin is composed of DNA and histones. The core histones comprise 2 copies of H2A, H2B, H3 and H4 wrapped around 146 base pairs of DNA with H1 functioning as a linker. Acetylation and deacetylation of lysine residues of nuclear histones are a reversible post-translational modification and so they are the most important epigenetic processes that influence chromatin epigenetics and gene expression<sup>63</sup>. The acetylation and deacetylation of histone proteins is a tightly regulated process driven by the action of two enzymes (fig. 11):

- Histone acetyl transferases (HATs) or lysine acetyl transferases (KATs),
- Histone deacetylases (HDACs)<sup>64</sup>.

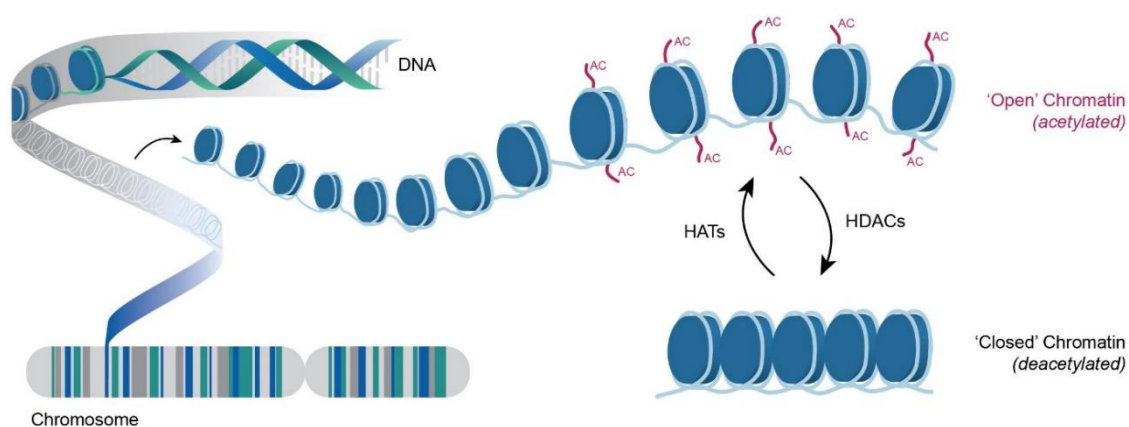


**Fig. 11** Schematic representation of the balance between acetylation and deacetylation of lysine residues on both histone and non-histone proteins regulated by histone acetylases (HATs) and histone deacetylases (HDACs). HATs are grouped in three superfamilies (i.e. GNAT, P300/CBP and Myst) and HDACs in four classes. The picture illustrates the impact of histone acetylation on chromatin relaxation and structural/functional changes consequent to acetylation of non-histone proteins.<sup>10</sup>

HDAC enzymes remove N-acetyl groups (deacetylation) from acetylated lysine residues of both histone and non histone proteins, causing chromatin condensation and transcriptional suppression, influencing a variety of cellular processes as differentiation, development and cellular homeostasis<sup>65</sup>. On the other hand, acetylation of histones caused by HATs or KATs induce an open chromatin conformation and provides access for various transcription factors, regulating the gene expression at the corresponding genomic loci. A balance between the opposing activities of HATs and HDACs is crucial in the regulation of gene expression. Thus, HDACs play a crucial role on transcription. The mammalian family of HDACs comprises 18 isoforms grouped into 4 classes:



1. Class I are HDAC-1, HDAC-2, HDAC-3 and HDAC-8,
2. Class II are further classified into class - IIa (HDAC-4, HDAC-5, HDAC-7, HDAC-9)  
- IIb (HDAC-6 and HDAC-10),
3. Class III are Sirtuins (SIRT) that includes SIRT 1-7, which require NAD<sup>+</sup> for their activity. SIRT proteins are localized in the nucleus (SIRT1, SIRT6, SIRT7), cytoplasm (SIRT2) and mitochondria (SIRT3, SIRT4, SIRT5),
4. Class IV includes HDAC11<sup>62,63,66</sup>.

Classes I, II and IV include the classic HDACs harboring a Zn<sup>2+</sup> ion in the catalytic pocket, are Zn<sup>2+</sup>-dependent enzymes (fig. 12). All tissue types ubiquitously express class I HDACs whereas only select tissues express class IIa HDACs. Initially, researchers believed all HDACs and SIRTs could deacetylate lysine substrates. However, two studies showed that only HDACs 1, 2, 3, and 6 had sufficient catalytic activity toward acetylated substrates<sup>67</sup>. Similar to the HDACs, SIRTs 1, 2, and 3 possess the most robust deacetylase activity of the sirtuin family; instead, SIRTs 4–7 all have very weak deacetylase activity. SIRT5 can deacylate succinylated and malonylated lysine at far greater rates than acetylated substrate, and SIRT6 has greater catalytic activity for long-chain fatty-acids as such as myristoylated and palmitoylated lysine<sup>66</sup>.

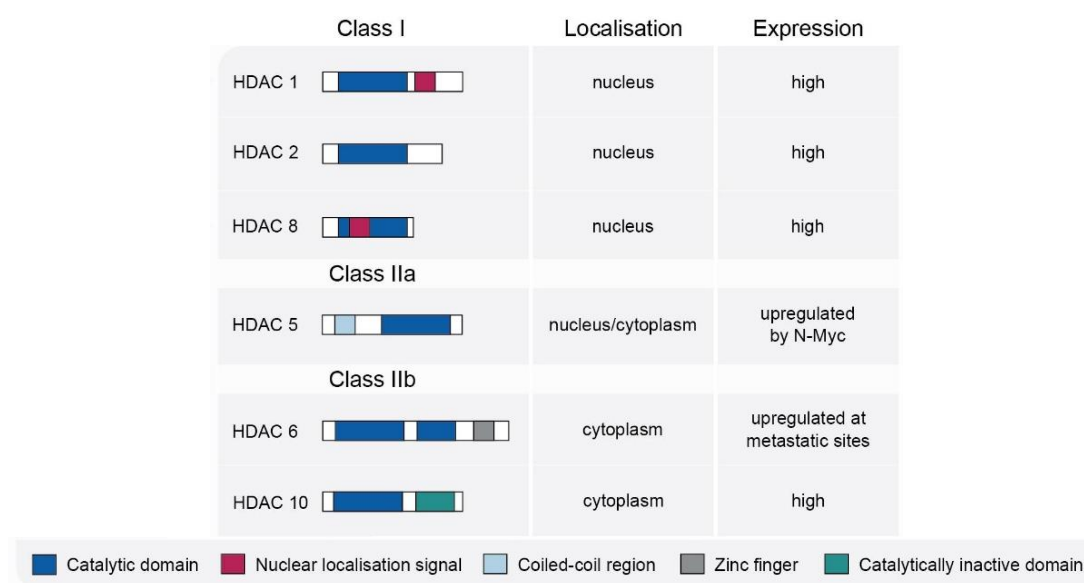


**Fig. 12** Structure and localization of Class I and II HDAC<sup>68</sup>.

### 7.1. HDACs role in transcription and translation:

In general, transcription of protein-coding genes involves initiation, elongation process of transcription and is mainly regulated by RNA polymerase II (RNA P2). The elongation step of transcription is tightly regulated by proteins that positively regulate transcription such as positive transcription elongation factor  $\beta$  (P-TEF $\beta$ ) as well as proteins that negatively regulate the transcription such as negative elongation factor (NELF) and dichloro-1- $\beta$ -D-

ribofuranosylbenzimidazole (DRB)-sensitivity inducing factor (DSIF)<sup>64</sup>. Interestingly, HDACs facilitate the perfect binding of elongation factors to the acetylated promoters and enhancers for efficient transcription. The enzymatic activity of HDAC proteins is tightly regulated by several cellular events such as post-translational modifications, protein-protein interactions and targeted recruitment. Ongoing studies continue to identify the key biological roles performed by HDACs and the relevance of these roles in different pathological conditions<sup>66</sup>.

## 7.2. HDACs in cancer:

The overexpression of HDACs is closely associated with a great variety of cancers, neurological diseases, inflammatory diseases, metabolic disorders and so on. It is interesting to note that the deletion of any one of class I HDAC genes has no significant effect on tumor cell viability. But, combined deletion of HDAC-1 and HDAC-2 leads to cell death<sup>69</sup>. Thus, aberrant epigenetic regulation through acetylation in cancer represents a field of interest and intense cancer research. In fact, HDAC activity can control the expression of oncosuppressors as well as of genes regulating cell cycle, DNA damage response, apoptosis, autophagy and other cellular processes (fig. 13). Moreover, HDACs can act as components of corepressor complexes and can be recruited by oncoproteins to drive tumorigenesis<sup>62</sup>. For instance, HDAC1 overexpression was observed in gastric, ovarian and prostate cancer, HDAC3 in ovarian and HDAC2 and HDAC3 in colorectal cancer<sup>68</sup>.

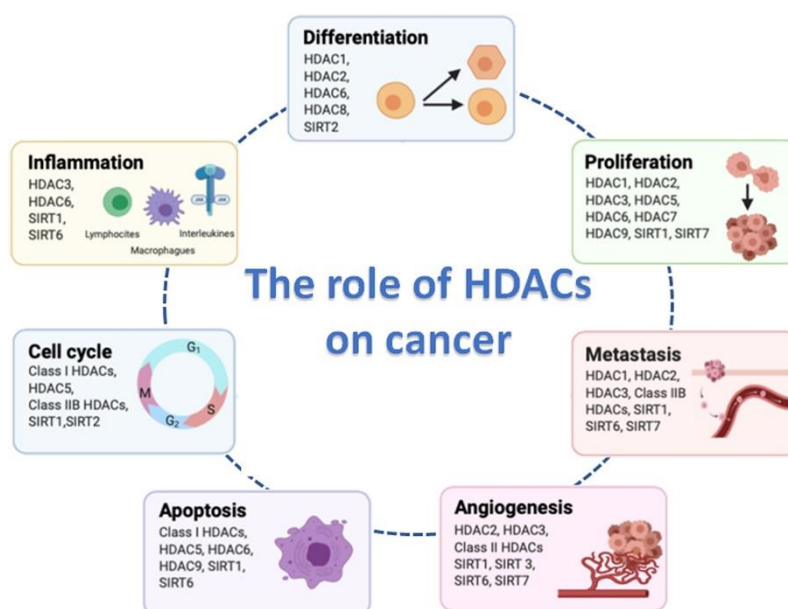


**Fig. 13** HDAC inhibitors modulate various biological processes in cancer cells. They induce histone acetylation preferentially at promoters of tumor suppressor microRNA, lncRNA, p21 and cause cell-cycle and apoptosis in cancer cells. HDACi also acetylate several non-histone proteins such as p53, c-myc, tubulin, STAT-3, regulating cancer cell proliferation. HDACi also cause acetylation of p53 and cause increased p53 activity and apoptosis in cancer cells. They also modulate Aurora kinase involved in the cell cycle.<sup>61,69</sup>

Studies reporting deregulated expression/function of specific HDAC isoenzymes, their direct interaction with fusion oncoproteins and their participation in multiprotein transcriptional

complexes as well as the aberrant recruitment to target gene promoters paver the way to investigation of HDAC targeting approaches in FP-sarcomas<sup>70</sup>. In preclinical models, inhibition of HDACs can reverse aberrant sarcoma epigenetic states resulting in reduced growth, cell cycle arrest, apoptosis and also reprogramming towards differentiation. Therefore, targeting these enzymes would facilitate the identification of promising anti-cancer agents and the development of HDAC inhibitors has become a promising therapeutic strategy.

## 8. HDAC inhibitors

HDAC inhibitors (HDACis) modulate and modify both the histone and non-histone proteins, inhibit cancer cell invasion, sensitize the cancer cells to chemotherapy, induce apoptosis and immunogenicity, induce cell cycle arrest, reduce angiogenesis and metastasis<sup>65,70</sup>. However, the mechanism of action of HDAC inhibitors varies with individual cancer types, and even if they gave very promising results in the preclinical setting, efficacy of HDACi monotherapies has been found largely restricted to hematologic malignancies in the clinic<sup>62</sup>. Initially hybrid polar compounds (HPC) were synthesized to enhance apoptosis or differentiation in cancer cells. Later second-generation HDAC inhibitors were synthesized. Those HDAC inhibitors are classified based on the chemical structure as:

- hydroxamic acids,
- aliphatic acid-based,
- benzamide based,
- cyclic peptides<sup>64</sup>.

These HDACis modulate gene expression not only by influencing histone acetylation and methylation but also restoring the acetylation of various non histone proteins (as p53, STAT-3, tubulin etc.), mechanism that was drastically reduced in the transition from non-cancerous to cancerous state. For example, HDACis cause histone modifications at p21 promoter, regulate the expression of cell-cycle genes such as cyclin D1, Cdk4, Cdk6 (fig. 14). Thus, they induce cell cycle arrest in actively or abnormally proliferating cancer cells.

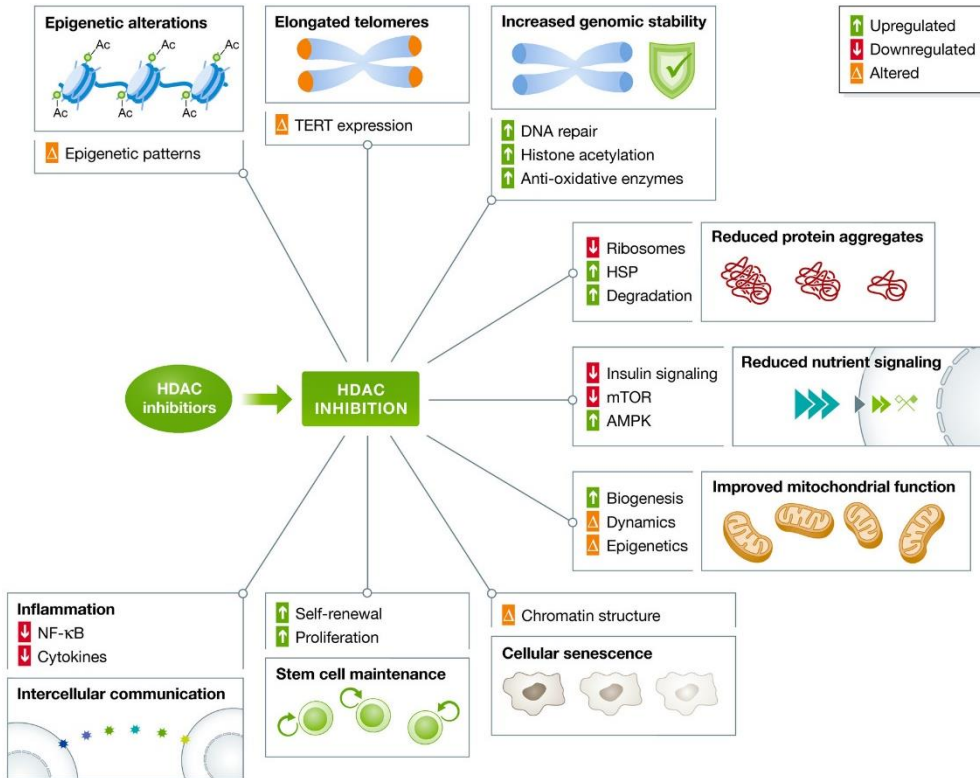


**Fig. 14** Hallmarks of aging in which HDACs are involved: epigenetic alterations, telomere attrition, genomic instability, loss of proteostasis, deregulated nutrient sensing, mitochondrial dysfunction, cellular senescence, stem cell exhaustion, and altered intercellular communication, and up- or downregulated processes are generally in line with beneficial changes for the health of the organism, while altered changes are indicative of potential synergies and interactions.<sup>61,71</sup>

This indicates that histone acetylation acts as a key marker for chromatin remodeling induced by HDACi<sup>64</sup> (fig. 15).

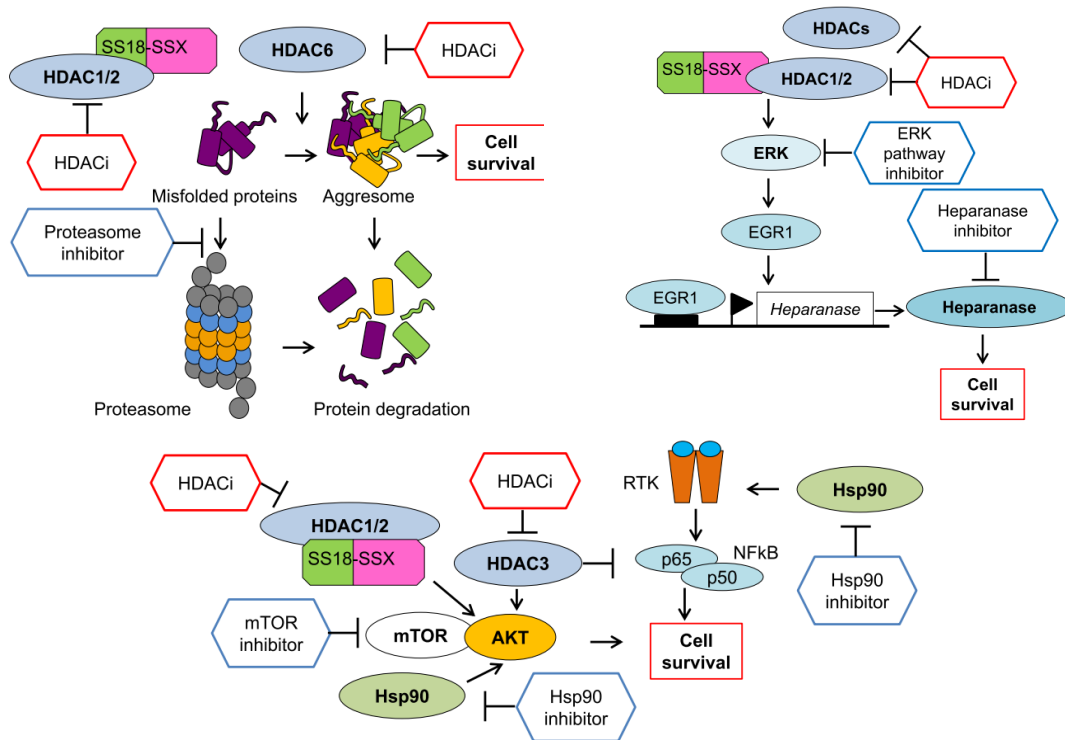


**Fig. 15** Simplified scheme illustrating examples of the reported investigational co-treatments targeting HDACs and different signaling pathway effectors.<sup>10</sup>

Thus far, five HDACis have been approved by US Food and Drug Administration (FDA) or China FDA (CFDA):

- Vorinostat (SAHA),
- Romidepsin (FK228),
- Belinostat (PXD101),
- Panobinostat (LBH589),
- Chidamide (CS055),

for the treatment of several hematological malignancies. There are also a great number of HDACis undergoing clinical trials, such as Entinostat (MS-275)<sup>68,70</sup> (tab. 1).

Hydroxamic acid-based were the first class of HDACi to be developed. Vorinostat, the first inhibitor, has nanomolar affinity toward HDACs. Initially, researchers believed that this compound was able to inhibit all HDACs. Instead, further testing demonstrated that it could only inhibit HDACs 1, 2, 3, and 6 at reasonable concentrations<sup>67</sup>. Owing to its potency in an orphaned disease, Vorinostat rapidly moved through preclinical and clinical studies. After completion of these studies, it earned FDA approval for the treatment of cutaneous T-cell lymphoma (CTCL).

Tetra/depsipeptides were also found to be capable of inhibiting HDACs. Romidepsin, a natural product isolated from the *Chromobacterium violaceum*<sup>72</sup>, gained approval to treat both CTCL and peripheral T-cell lymphomas (PTCL).

Amino-benzamide-based HDACis were the first inhibitors to target class I HDACs selectively. Enzyme kinetic studies of these inhibitors demonstrated that the amino-benzamide motif possesses a tight-binding mechanism (slow-on/slow-off), unlike the classic fast-on/fast-off kinetics associated with hydroxamic acid-based HDACis<sup>66</sup>. Entinostat (MS-275) is the first amino-benzamide-based HDACi to reach clinical trials. Interestingly, Entinostat has a lower therapeutic index than Vorinostat in the clinic. This is rather surprising, because Entinostat possesses much more selectivity toward HDACs compared to Vorinostat. Entinostat's low therapeutic index is probably due to lower affinity for targeted HDACs, off-target toxicity, and poor erratic pharmacokinetic properties<sup>72</sup>.

The major problem given by these inhibitors is that they have side effects; thus, there is an urgent need to discover novel HDAC inhibitors. Also, for effective anti-cancer therapy, it is highly important to focus on identifying the small molecules that are isoform-selective<sup>73</sup>. This will be a key turning point for HDAC therapeutics to improve the selective killing of cancer cells with limited side effects and will likely significantly improve the outcome of future HDAC inhibitor clinical trials.

**Tab. 1** Clinical trials of HDACi in solid tumors.<sup>63</sup>

	Cancer Type	Phase	Grade $\geq$ 3 Adverse Events
Vorinostat	Nonsmall cell lung cancer (NSCLC). Breast cancer, colorectal cancer, thyroid carcinoma, head and neck cancer, ovarian or primary peritoneal carcinoma, glioblastoma multiforme.	II	Thrombocytopenia, anemia, asthenia, nausea, fatigue, dehydration, ataxia, pneumonia, bruises and deep vein thrombosis.
Romidepsin	Renal cell carcinoma (RCC) lung cancer, colorectal cancer, prostate cancer, small cell lung cancer, malignant glioma, thyroid carcinoma, head and neck cancer.	II	Atrial fibrillation and tachycardia, anemia, neutropenia, thrombocytopenia, hypoxia
Belinostat	Malignant pleural mesothelioma, ovarian cancer, thymic epithelial tumors, hepatocellular carcinoma.	I+II	Leucopenia, neutropenia, thrombocytopenia anemia.
Panobinostat	High-grade glioma, RCC, pancreatic cancer	I+II	Hyperglycemia, thrombocytopenia, nausea, vomiting, diarrhea, anorexia, hypertension.
Entinostat	Pretreated metastatic melanoma, NSCLC	II	Hyponatremia, neutropenia, anemia, hypophosphatemia and hypoalbuminemia.

## 9. RMS and HDAC inhibitors

The multidisciplinary treatment of RMS includes surgery and/or RT and intensive cytotoxic chemotherapy based on alkylating agents. Despite many advances, the chance of cure for patients with widely metastatic and recurrent disease remains very low<sup>70</sup>. Novel and less toxic therapeutic approaches are needed to improve patients' outcome. Obviously, in FP- and FN-RMS, fusion proteins and specific pathways represent primary therapeutic targets, with the use of molecular targeting approaches (e.g. siRNA, antisense oligonucleotides or CRISPR/Cas9-based genome editing techniques)<sup>69</sup>.

The ability of fusion proteins and deregulated genes to reprogram the chromatin landscape through direct or indirect interaction with chromatin-related proteins suggest the way for the evaluation of epigenetic modulators such as HDACis. Indeed, in RMS HDAC inhibition has been shown to reverse oncogenic features and induce cell death, exert antiproliferative, proapoptotic, anti-invasive, pro-differentiating activities. In recent years, a broad range of inhibitors of epigenetic modifiers, with different structure and selectivity profile, has been developed<sup>66</sup>.

## 10. Romidepsin

FK228, also known as Romidepsin, Depsipeptide, FR901228 or NSC 630176, is the second HDACi to receive FDA approval, and the only natural HDACi used for the treatment of cutaneous (in 2009) and peripheral T-cell lymphoma, in 2011, (CTCL/PTCL) and multiple myeloma (MM)<sup>73</sup>. FK228 was originally isolated from the fermentation product of culture broth of *Chromobacterium*

*violaceum* No. 968 and belong to a small family of uncommon cage-shaped bicyclic pentapeptide (as chromopeptide A from *Chromobacterium*, sp. HS-13-94, or largazole from *Cyanobacterium Symploca* sp. The exact yield and conditions of industrial production remain proprietary. This bicyclic peptide framework was produced biosynthetically by a hybrid nonribosomal peptide synthetase (NRPS)-polyketide synthase (PKS) assembly line with multiple accessory enzymes<sup>74</sup>.

This natural product features a unique disulfide bond for mediating a new anticancer mode of action: mechanistically, the reduced thiol on the long aliphatic chain is able to chelate the Zn<sup>2+</sup> in the catalytic pocket of HDACs<sup>75</sup>. Thus, inhibiting the enzyme activity, which leads to a cascade of epigenetic consequences. In addition, the reduction of FK228 produces a reactive oxygen species which exerts its cytotoxicity against cancer cells<sup>76</sup>. FK228 has a novel chemical structure composed of four aminoacids (D-valine, D-cysteine, dehydrobutyrine and L-valine) and a novel acid (3-hydroxy-7-mercapto-4-heptenoic acid) configured in a cage-shaped bicyclic depsipeptide (fig. 16). Molecular formula of depsipeptide is C<sub>24</sub>H<sub>36</sub>N<sub>4</sub>O<sub>6</sub>S<sub>2</sub>, molecular weight of 540,71, and chemical name is (E)-(1S,4S,10S,21R)-7-[(Z)-ethylidene]-4,21-diisopropyl-2-oxa-12,13-dithia-5,8,20,23-tetraazabicyclo[8,7,6]-tricos-16-ene-3,6,9,19,22-pentanone<sup>77</sup>. It originally was developed as an anti-RAS compound, later was found to interfere with mitogen-induced signaling pathway and recently has been shown to a HDAC inhibitor.

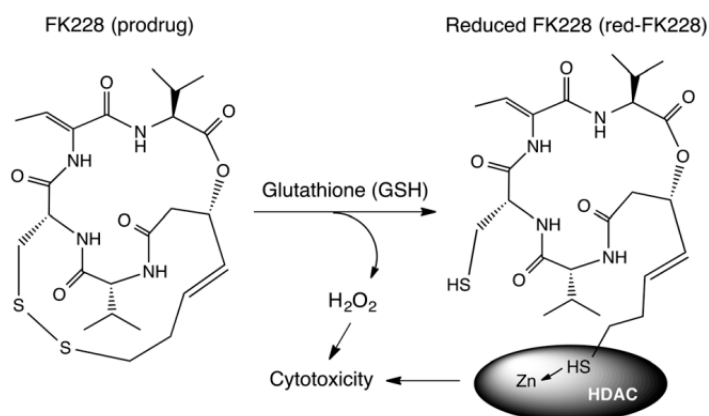


**Fig. 16** Structure and the formation of FK228 active metabolite (redFK228) following reduction by glutathione (GSH).<sup>73</sup>

Romidepsin works in a selective way, inhibiting HDACs 1 and 2; it has been reported to induce cell cycle arrest and apoptosis in various solid tumor cells (as ovarian cancer and hepatocarcinoma)<sup>78</sup>. In addition to direct cytotoxicity, FK228 can cause a wide range of immune changes like other HDACi, through the expression of costimulatory molecules (PD-L1), MHC, tumor antigens and cytokines<sup>79</sup>. FK228 forms non-hygroscopic white crystals, soluble in dehydrated ethanol, slightly soluble in water and insoluble in ether<sup>80</sup>. Romidepsin's insolubility in water necessitates its injection only dosage form. This drug showed a high clearance of 12.2 L/m<sup>2</sup> /h in mice<sup>76</sup> coupled with a relatively longer half-life of 348 min. Upon administration, Romidepsin is highly bound by proteins, 92%–94% in humans from its package insert. Furthermore, it is a substrate of P-glycoprotein<sup>77</sup>. Last, extensive

metabolism of FK228 occurs by the liver, in particular cytochrome p450 3A4. However, it does not appear to affect CYP activity in humans. Taken together, Romidepsin's poor kinetics, high levels of protein binding, and efflux via P-glycoprotein prevent this compound from working as efficaciously as it could and leaves much to be desired in clinic<sup>80</sup>.

FK228 exhibits promising results in the treatment of CTCL/PTCL, its expended applications have been limited as a result of the unresolved cardiotoxicity problems, episodes of neutropenia and thrombocytopenia. The most common non hematological toxicities associated with FK228 treatment were fatigue, nausea, vomiting and anorexia. Hypocalcemia was also noted but it was not associated with symptoms or significant clinical findings<sup>19</sup>. In recent years, combinatorial biosynthesis has become a promising strategy to develop new FK228 derivatives with low toxicity and high efficacy<sup>71</sup>.

#### 10.1. *Mechanism of action:*

FK228 is converted to its active form by reduction of an intramolecular disulfide bond by intracellular antioxidants involving glutathione. It has been suggested that one of the sulfhydryl groups of the reduced form of depsipeptide interacts with zinc ions of the active site of various enzymes, thus preventing the access of the substrate<sup>75</sup>. Reduced FK228 (redFK228) more strongly inhibited HDAC1 and HDAC2 class I enzymes than HDAC4 and HDCA6 class II enzymes. Precisely, it inhibits the removal of acetyl groups from lysine tails of histones and helps to maintain DNA in the more transcriptionally active open chromatin state. This chromatin conformation may facilitate access to DNA-binding transcription factors, thereby increasing gene transcription<sup>74</sup>. It has been reported that FK228 induces both a p53- independent/p21-dependent G<sub>1</sub> and a p21-independent G<sub>2</sub>/M arrest. The G<sub>1</sub> arrest is accompanied by decreased phosphorylation of the mitogen-activated protein (MAP) kinase and the retinoblastoma protein (Rb). Other possible mechanisms involved in the growth cell inhibition include the altered expression of cycline A, cyclin D and p27/Kip1, resulting in a reduction in CDK2 and CDK4 activities<sup>75</sup>. Also downregulates c-Myc expression. In addition, FK228 may suppress tumor expansion by inhibition of neovascularization by decreasing expression of angiogenic-stimulating factors, such as vascular endothelial growth factor (VEGF) or kinase insert domain receptor, and induces angiogenic-inhibiting factors, such as von Hippel Lindau and neurofibromin 2<sup>76</sup>.

## 11. Entinostat

Entinostat (SNDX-275, 3-pyridylmethyl-N-{4-[(2-aminophenyl)carbamoyl]- benzyl} carbamate; previously known as MS-275 and MS-27-275) is a synthetic benzamide (fig. 17) derivative established by Mitsui Pharmaceuticals (Chiba, Japan) in the late 1990s. It is an inhibitor of primarily class I histone deacetylases (HDACs) 1 and 3, but not 8<sup>81</sup>. This HDACi is currently being evaluated



in multiple Phase I and II trials as therapy for advanced and/or refractory solid tumors and hematologic malignancies<sup>82</sup>. It utilizes a similar strategy mechanistically to the other HDACis; however, unlike the hydroxamic acid-based inhibitors, its binding kinetics *in vitro* are more complicated. Entinostat, among other benzamide inhibitors, exhibits a moderate lipophilicity and moderate plasma protein binding (40%) in nonhuman animals<sup>83,84</sup>.

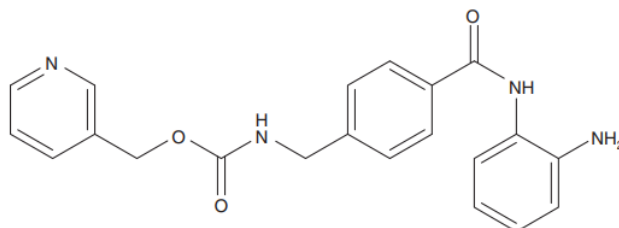


Fig. 17 Structure of the HDAC inhibitor MS275.<sup>84</sup>

MS275 is administered orally and is systemically distributed, but poor brain penetration as demonstrated by a study using positron emission tomography and the radiolabeled drug<sup>81</sup>. Its oral bioavailability is quite high at 85%; however, its interpatient variability in pharmacokinetics makes it rather difficult to dose in clinic. Patients displayed a time to maximal concentration ( $t_{max}$ ) values between 0.25 and 60 h. Interestingly, Entinostat had a relatively short half-life of approximately 1 h in mice, rats, and dogs. Notably, its elimination half-life ( $t_{1/2}$ ) in humans is approximately 52 h<sup>82,84,85</sup>. This may be, in part, due to increased plasma protein binding of the drug in humans compared to other mammals; maybe because of its much lower susceptibility to metabolism in humans. Indeed, radiolabeling Entinostat, it was not accumulated in cells expressing organic anion transporting polypeptides and in liver microsomes. These results strongly suggested that hepatic metabolism is a minor pathway of elimination in humans<sup>83,86</sup>. It is important to point out that the drug has been proven safe and well tolerated in multiple clinical trials<sup>87</sup>.

### 11.1. Mechanism of action:

Due to Entinostat's ability to inhibit HDACs, the primary method of clinical pharmacodynamic testing has been the evaluation of acetylated histones H3 and H4 in peripheral blood mononuclear cells (PBMCs) and/or bone marrow mononuclear cells (BMMCs). The drug increased p21 expression and caspase-3 activation and also the acetylation persisted for 2-3 weeks after the last dose. Increased acetylation was found to be dose-dependent in some cases<sup>88</sup>. MS275 has demonstrated antitumor activity alone or in combination with other agents in multiple *in vitro* and *in vivo* models of human malignancies. It mediated suppression of regulatory T cells (Tregs) and myeloid-derived suppressor cells (MDSCs) in combination with immunotherapies. Indeed, preclinically, Entinostat was shown to promote tumor necrosis and induce potent suppression of MHC-I<sup>+</sup> tumors, increases antigen-experienced T cell responses and decreases immune-suppressive populations and promotes an inflamed tumor microenvironment<sup>89</sup>.

In combination, it also potentiates the drug-induced DNA damage. For example, in ovarian cancer is able to repress BRCA1 expression decreasing radio-resistance gene expression, which leads to irreparable DSBs and ultimately cell death<sup>60</sup>. Entinostat's inhibition of primarily class I HDACs 1 and 3 that results in increased histone and non-histone protein acetylation, in turn, results in gene re-expression and de-repression of key cellular functions (fig. 18). Its apoptotic effects result from the generation of reactive oxygen species (ROS), which causes mitochondrial damage and from the induction of caspase-dependent apoptosis by the activation of caspase-3 and, to a lesser extent, caspase-8<sup>88</sup>. It increases cellular sensitivity to TNF-related apoptosis inducing ligand (TRAIL) and down-regulates the expression of the anti-apoptotic genes Bcl-2 and XIAP<sup>90</sup>. It also exhibits antiproliferative activity decreasing S-phase cells and increasing G-phase cells. These events are mediated by the transcriptional activation of the tumor suppressors cyclin-dependent kinase inhibitor (CDKI) p21WAF1/CIP1. The downregulation of cyclin D1 also leads to growth arrest<sup>91</sup>. Several other antineoplastic molecular and cellular functions are altered by Entinostat treatment. It has been shown to increase the levels of the transforming growth factor- $\beta$  type 2 receptor (TGF- $\beta$  RII) mRNA levels and E-cadherin expression. Also, anti-angiogenic properties due to decreased expression of pro-angiogenic genes have been attributed to the drug<sup>77</sup>. Also, multiple combination therapy studies that exploit Entinostat's mechanisms of action have proven successful. Most notable of these combinations are those where the drug was given in conjunction with DNA methyltransferase (DNMT) inhibitors, hormonal agents, retinoic acid or immunotherapy<sup>88</sup>.

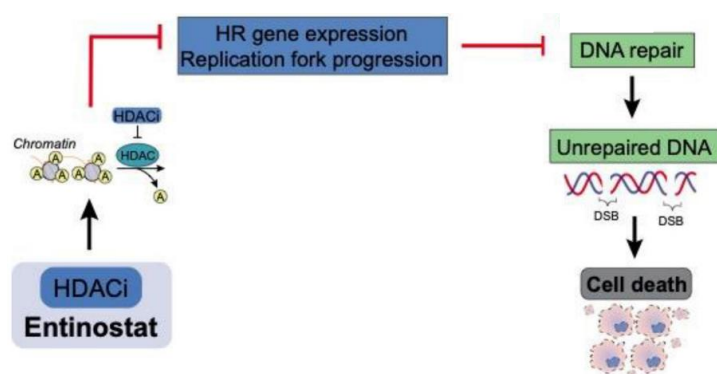


**Fig. 18** Entinostat causes breakdown of HR-DNA repair pathway crippling the cell's potential to repair SSBs. This in turn leads to accumulation of DSBs, which the cell is unable to repair due to defective HR repair pathway, accumulating unrepaired DNA ultimately resulting in cell death.<sup>89</sup>



## AIM OF THE RESEARCH

This PhD research has the purpose to observe potential antitumoral ability of HDACi in *in vitro* and *in vivo* models of RMS.

RMS is the most common soft tissue sarcoma of childhood. The two major histological subtypes are the “Alveolar” (ARMS) and “Embryonal” (ERMS) variants. ARMS is characterized by the expression of the PAX3- or PAX7-FOXO1 oncogenic “fusion proteins” (FP) and often has poor prognosis. ERMS, the most frequently subtype, hasn’t fusion genes (“fusion negative”, FN). Standard treatment for localized and locally advanced RMS requires the combination of surgery, RT and CHT. Despite advances in the cellular and genomic classification of RMS and the introduction of combined modality therapy, outcomes for patients at high risk for treatment failure remain suboptimal. In addition, patients who survive their disease are at high risk of developing long-term complication as a result of systemic and local therapies. However, new therapies are lacking and functional approaches and new molecular targets will be needed to further improve the outcome of this disease. In the last years several research groups discovered that RMS is also characterized by an aberrant epigenetic regulation because of high levels of HDACs that repress tumor suppressor gene expression. HDACs are enzymes whose expression and activity are implicated in cancer formation. Inhibition of HDAC result in apoptosis, inhibition of cancer cell invasion, cell cycle arrest. But the success of HDAC inhibitor drugs was found to be limited due to lack of specificity and toxic side effects. Thus, there is an urgent need to discover target specific HDAC inhibitor to prevent cancer. Therefore, we decided to target these deacetylases with specific inhibitors, studying their effects as single agents on the two main representative cell lines of RMS subtypes: RD (ERMS) and RH30 (ARMS). But a key part of this study was to combine HDACi with RT and to observe their radiosensitizing ability, both in *in vitro* and *in vivo* models.

## MATERIALS AND METHODS

### 1. Cell lines and pharmacological treatments

RD (ERMS) and RH30 (ARMS) human cell lines were purchased American Type Culture Collection (Manassaa, VA). Human multipotent mesenchymal stromal cells (HMSC) were isolated from Wharton's jelly of the umbilical cord deprived of vessels (WJMSC) obtained from the "Azienda Policlinico Umberto I" of Rome, upon written parental informed consent, in accordance with the Declaration of Helsinki. Cells were maintained in medium containing Dulbecco's Modified Eagle Medium low glucose (EuroClone, MI, Italy) supplemented with 10% Fetal Bovine Serum (FBS South America, EuroClone), 1% non-essential aminoacids (Sigma-Aldrich, Saint Louis, MO, USA), 1% antibiotic-antimycotics (Gibco by Life Technologies, Grand Island, NY, Usa) and 2 mM L-Glutamine (EuroClone); were plated into tissue-culture flasks, incubated at 37°C in 5% CO<sub>2</sub>. WJMSC from passages 7-10 were used for the experiments. RD and RH30 were cultured respectively using Dulbecco's Modified Eagle's Medium high glucose (DMEM, EuroClone) and RPMI medium (EuroClone) containing 10% FBS, supplemented with 1% L-glutamine and 1% penicillin/streptomycin (EuroClone); were plated into tissue-culture flasks and incubated at 37°C in 5% CO<sub>2</sub>. GenePrint 10 System (Promega Corporation, Madison, WI, USA) was used to authenticate cell cultures by comparing the DNA profile of our cell cultures with those found in GenBank. The cells were splitted using Trypsin solution (EuroClone) and resuspendend into a fresh medium once every 3-4 days. Romidepsin (FK228, Depsipeptide) and Entinostat (MS-275) were purchased from Selleckchem.com (Houston, TX, USA).

### 2. Class I HDACs activity

To assess HDACs activity, the day after planting, cells were exposed to treatments (IC<sub>50</sub>) and harvested after 4 days. Histone Deacetylase (HDAC) Activity Assay Kit (Fluorimetric) (from AbCam, Cambridge, UK) was used to test Class I HDACs activity, accordingly with the manufacturer's instructions.

### 3. RNA isolation and qRT-PCR

TriPure Isolation Reagent (Euroclone) was used to extract total RNA. The concentration and quality of RNA were evaluated by NanoDrop 2000 (ThermoFisher Scientific, Inc., Waltham, MA). QuantiTect Reverse Transcription Kit (Qiagen, Hilde, Germany) was used to perform the reverse transcription for target genes (NRF2, SOD, CAT and GPx4). A real-time PCR (qRT) was performed to analyze target genes. Each sample was run in triplicate, in at least two independent experiments, on a StepOne Real Time System (Applied Biosystems) machine. For data analysis, the C<sub>t</sub> values in

each sample and the efficiencies of the primers set were calculated using LinReg Software and then converted into relative quantities (RQ) and normalized according to the Pfaffl model. Normalization was carried out using, as housekeeping genes, HPRT-1 for mRNA targets.

#### 4. Cell viability assay

To assess cell viability, the day after planting, cells were exposed to FK228 (0, 1, 5, 10 and 20 $\mu$ M) and MS-275 (0.01, 0.1, 1 and 10  $\mu$ M) for 24 h. Trypan blue (ThermoFisher) exclusion was used and the Countess II Automated Cell Counter (ThermoFisher) was used to assess the number of the cells. SigmaPlot (Systat Software, Inc, San Jose, CA, USA) software was used to calculate IC<sub>50</sub> values.

#### 5. Cell cycle analysis by Flow Cytometry

Cell cycle analysis was performed by using a BD FACSCalibur (BD Biosciences, Franklin Lakes, NJ). Cells were harvested by trypsin and washed; pellets were then resuspended in formaline (4% paraformaldehyde) and left at room temperature for 10 minutes. The fixed cells were then washed with PBS twice, resuspended in PBS, in addition with 70% ethanol and left at room temperature for 5 minutes. An exceed of PBS was added and then samples were centrifugated. After the centrifuge pellets were resuspended in PBS and left at 4°C in the dark for no longer than 2 days before FACS analysis. ModFit LT 3.0 program (Verity Software House) was used to quantify flow cytometry data.

#### 6. Apoptosis and PARP1 activity assays

Annexin V/PI assay (AbCam, Cambridge, UK) was used to quantified apoptotic cells. After 24 h from treatments, cells were harvested, counted and Annexin-V labeling was performed. Approximate fluorescence excitation maxima: 488 and 540 nm. The early and late apoptotic cells were analyzed with a flow cytometer. PARP1 Enzyme Activity Assay (Sigma-Aldrich) was used to test PARP1 activity. Assay were performed according to the manufacturer's instructions.

#### 7. Mitochondrial superoxide anion (O<sup>2-</sup>) production assessment

To measured mitochondrial superoxide anion (O<sup>2-</sup>) production, MitoSOX Red (ThermoFisher) was used. 5 $\mu$ M MitoSox Red was added in a pre-warmed medium and then it was used for 15 minutes at 37°C with cultured cells. After incubation, cells were washed twice, first with complete medium and then with PBS, trypsinized and centrifuges at 1200 rpm; the pellet was resuspended in PBS with 3% FBS for immediate analysis in a BD FACS.

## 8. Radiation exposure and Clonogenic Assay

Radiation was delivered at room temperature using an x-6 MV photon linear accelerator. The total single dose of 4 Gy was delivered with a dose rate of 2 Gy/min using a source-to-surface distance (SSD) of 100 cm. A plate of Perspex thick 1.2 cm was positioned below the cell culture flasks in order to compensate for the build-up effect. Tumor cells were then irradiated placing the gantry angle at 180°. Non-irradiated controls were handled identically to the irradiated cells with the exception of the radiation exposure. The absorbed dose was measured using a Duplex dosimeter (PTW). For clonogenic survival assay, exponentially growing RD and RH30 cells in 25 cm<sup>2</sup> flasks were harvested by exposure to trypsin and counted. They were diluted serially to appropriate densities and plated in triplicate in 6 multi-well plates with 2 ml of complete medium each well in the presence or absence of the treatments or vehicle for 24h. After incubation, the cells were exposed at room temperature to various doses of radiation as already described. The cells were then washed with PBS, cultured in a drug-free medium for 14 days, fixed with methanol and stained with crystal violet. Colonies containing >50 cells were counted. The plating efficiency (PE), was defined as the number of colonies observed/the number of cells plated; the surviving fraction (SF) was calculated as follows: colonies counted/cells seeded.

## 9. Protein extraction and Western blotting

Cells were lysed using Lysis Buffer and sonicated for 1 min. protein concentration was estimated by BCA assay (Bicinchoninic Protein Assay kit, EuroClone) and an equal amounts were separated on SDS-PAGE. The proteins were transferred to a nitrocellulose membrane (ThermoFisher Scientific) by electroblotting. The balance of total protein levels was confirmed by staining the membranes with Ponceau S (Sigma-Aldrich). Membranes were blocked for 1h in 10% non-fat dry milk (ChemCruz, Santa Cruz Biotechnology, USA) in tris-buffered saline and Tween-20 (TBS-T) and then incubated at 4°C overnight with primary antibodies. The primary antibodies used were: p21<sup>WAF1</sup> (C-19), p27<sup>KIP1</sup> (F-8), Cyclin A (BF683), Cyclin D1 (M-20), Cyclin B1 (H-20), c-Myc (9E19), N-Myc (B.8.4.B), ERK1/2 (c-14), ERK1/2<sup>PO4</sup> (E-4), H2AX (C-20), GAPDH (6-C5),  $\alpha$ -Tubulin (TU-02), p-ATM (10H11.E12, Ser1981), ATM (H-248), DNA-PKCs (E-6), by Santa Cruz Biotechnology (Dallas, MA, USA).  $\gamma$ H2AX (Ser139) (2577), Bcl2 (D55G8) (4223), Bcl-xL (54H6) (2764), Caspase 3 (D3R6Y) by Cell Signaling Technology (Danvers, MA). p-DNA-PKCs (Thr2609) (10B1) by AbCam. Appropriate horseradish peroxidase (HRP)-conjugated secondary antibodies were used for 1h at room temperature. Quantification of Western blot data was performed by using ChemiDoc MP (Bio-Rad) imager.

## 10. Animal research ethics statement and *in vivo* xenograft experiments

The recommendations of the European Community (EC) guidelines (2010/63/UE and DL 26/2014 for the use of laboratory animals) and the Istituto Superiore di Sanità guidelines (Board Regulations on the use of laboratory animals, Italian government regulation n.116 27 January 1992) were considered to perform *in vivo* experiments. Six-week-old female CD1 nu/nu mice were purchased from Charles River Laboratories Italy, SRL (Calco, Italy). Before any invasive manipulation, mice were anesthetized with a mixture of ketamine (25 mg/ml)/xylazine (5 mg/ml). For xenotransplants were used RD or RH30 cells resuspended in saline solution at cell density  $1 \times 10^6/200 \mu\text{l}$ . When the tumor volume reached  $\sim 0.5 \text{ cm}^3$  ( $T_0$ ), mice were randomly assigned to 4 experimental groups. Each group was composed of 8 mice; one control group that received intraperitoneal injection (IP) of carrier solution; one group received IP of the HDACi solution; one group received RT; one group received drug solution and RT. 21-gauge needle on a tuberculin syringe was used to perform subcutaneously injecting. Treatments started when tumors reached a volume of  $0.5 \text{ cm}^3$ . FK228 injection IP (1.2 mg/kg body weight) started the day before the irradiation and then treatments were performed after the animals had received RT scheduled for that day. Five fractions of 2 Gy were daily delivered for a total dose of 10 Gy. MS-275 was administered 2.5 mg/kg/day by IP injection for 5 days/week for 1 week. The first daily dose of MS-275 was given 1h before RT. Three fractions of 2 Gy were delivered the 1<sup>st</sup>, 3<sup>rd</sup> and 5<sup>th</sup> day for a total dose of 6 Gy. Mice were irradiated at room temperature using Elekta 6-MV photon linear accelerator, with a source-to-surface distance (SSD) of 100 cm. Tumor volumes were measured every 5 days for a period of 20 days after the first day of treatment with the HDACi. During treatments, mice with distress signs were euthanized early according to protocol.

## 11. Evaluation of treatment response *in vivo*

The effects on tumor growth of different treatments were evaluated as follows: measuring tumor volume during and at the end of the experiment. Tumor volume was assessed every 4 days measurement with a Vernier caliper (lengthxwidth). The volume of the tumor was expressed in  $\text{mm}^3$  according to the formula  $\frac{4}{3}\pi r^3$ , measuring tumor weight at the end of the experiment and defining tumor progression (TP), the doubling of the tumor volume.

## 12. Statistical analysis and data analysis

Each experiment was performed in triplicate and the results were expressed as the mean  $\pm$ SD. Data normal distribution was confirmed by Shapiro-Wilk, D'agostino and Pearson and Kolmogorov-Smirnov tests. Real-time PCR experiments were evaluated by one-way (ANOVA) with a Tukey's



post hoc test using  $2^{-\Delta\Delta C_t}$  values for each sample. Flow cytometry data were analyzed by ANOVA with a Bonferroni post hoc test. All analyses were performed using the SAS System (SAS Institute Inc., Cary, NC, USA) and GraphPad Prism 6.1.

## RESULTS

### IN VITRO

#### 1. Activity levels of class I HDACs in RMS subtypes

The expression levels of class I HDACs (HDAC1, 2, 3 and 8) were evaluated by RT-qPCR in RD (ERMS), RH30 (ARMS) and in HMSC (human mesenchymal stromal cells) as the basal counterpart. Compared to HMSC, in RD cells the expression of HDAC1, HDAC2, HDAC3 and HDAC8 was reduced by  $98.9\pm 0.21\%$ ,  $99.5\pm 0.043\%$ ,  $72.9\pm 3.9\%$  and  $95.2\pm 0.7\%$ , respectively (Fig. 1. a). Also in RH30 cells HDACs transcript levels were downregulated compared to basal cells by  $68.7\pm 2.5\%$ ,  $33.5\pm 4.5\%$ ,  $87.3\pm 1.3\%$  and  $97.3\pm 0.8\%$ , respectively (Fig. 1. b).

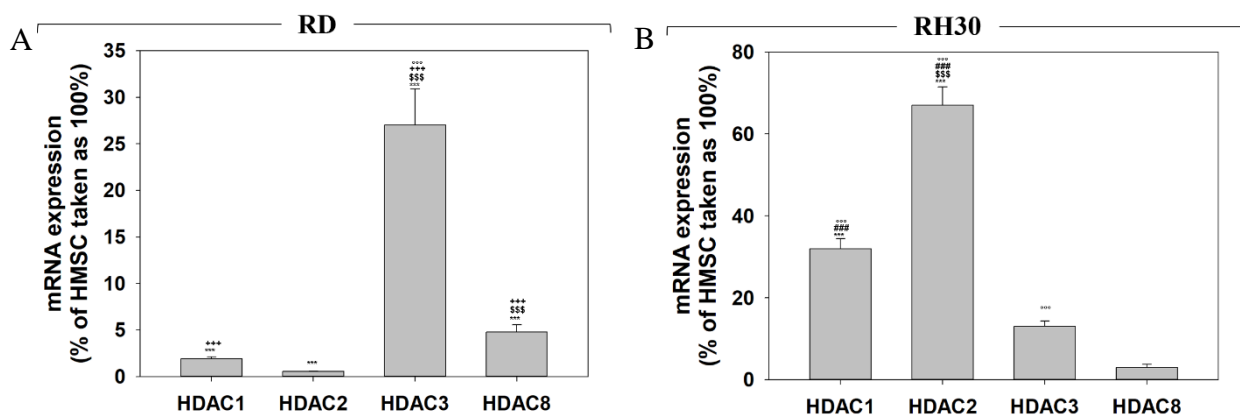


**Fig. 1** Expression of class I HDACs in ERMS and ARMS cell lines.

A. HDAC1, 2, 3 and 8 transcript levels in RD (ERMS) vs. HMSC, set at 100%.

B. HDAC1, 2, 3 and 8 transcript levels in RH30 (ARMS) vs. HMSC, set at 100%

Results represent the mean values of three independent experiments  $\pm$ SD. Statistical significance:

\* $p\leq 0.05$ , \*\* $p\leq 0.01$ , \*\*\* $p\leq 0.001$  compared with HMSC cells;

$^{\circ}$  $p\leq 0.05$ ,  $^{\circ\circ}$  $p\leq 0.01$ ,  $^{\circ\circ\circ}$  $p\leq 0.001$  compared with HDAC1;

$^+$  $p\leq 0.05$ ,  $^{++}$  $p\leq 0.01$ ,  $^{+++}$  $p\leq 0.001$  compared with HDAC2;

$^{\#}$  $p\leq 0.05$ ,  $^{\#\#}$  $p\leq 0.01$ ,  $^{\#\#\#}$  $p\leq 0.001$  compared with HDAC3;

$^{\circ}$  $p\leq 0.05$ ,  $^{\circ\circ}$  $p\leq 0.01$ ,  $^{\circ\circ\circ}$  $p\leq 0.001$  compared with HDAC8.

#### 2. Viability assay of RMS cell lines:

##### 2.1. FK228 treatment reversibly and not efficiently controls tumor proliferation:

The concentration of FK228 able to inhibit 50% of cell viability ( $IC_{50}$ ) was  $1.4\pm 0.02$  nM in RD and  $0.6\pm 0.06$  nM in RH30 (Fig. 2. A). To study its ability to induce irreversible or reversible growth arrest and/or cells death, 4 days after treatment, FK228 was washed out (W/O) or not, and cells viability of adherent and floating cells assessed for the next 6 days. 4 days of treatment reduced the number of adherent cells by  $32.3\pm 2.6\%$  in RD and  $26.8\pm 3.1\%$  in RH30, and increased the number of floating cells, that resulted to be almost all dead. Where it was W/O, it rapidly restored RMS cell growth and reduced the number of floating/dead cells, how showed in fig. 2. B.

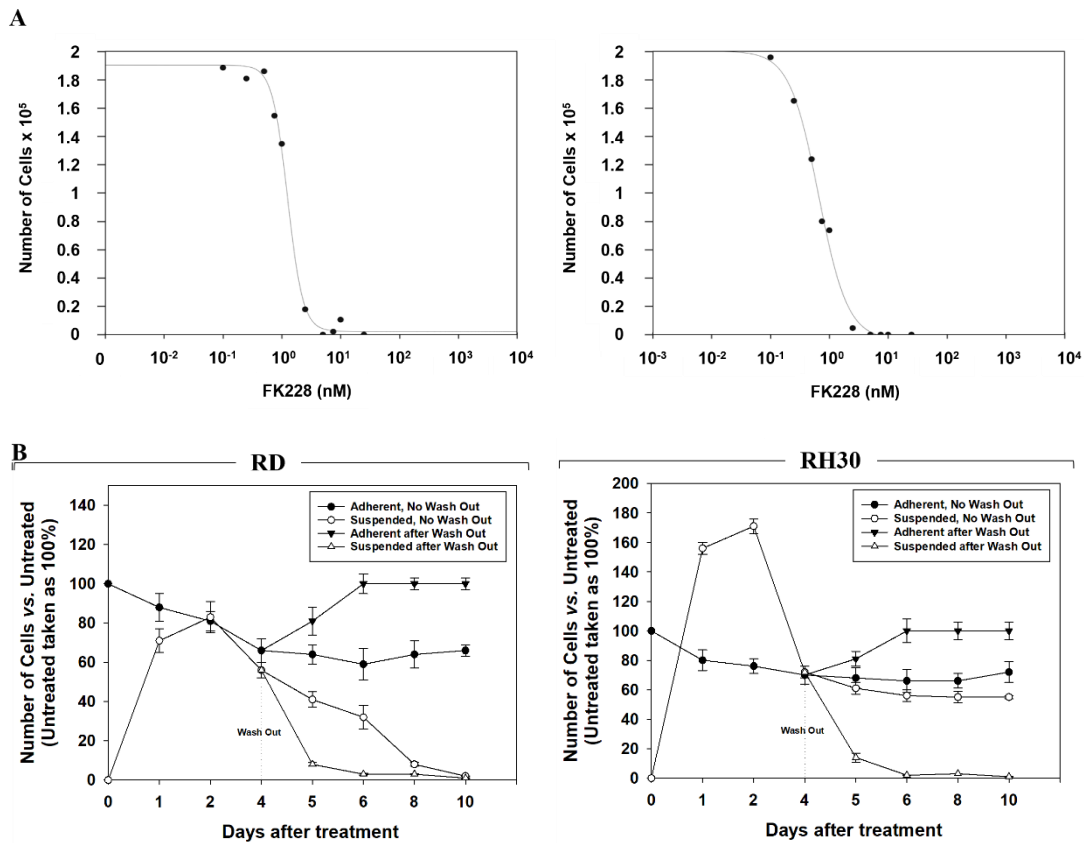


**Fig. 2** FK228 concomitantly induces reversible cell growth arrest, concomitant transient death in ERMS and ARMS cells.

A. Dose of FK228 able to reduce by 50% the cell viability of RD (Left Panel) and RH30 (Right Panel) cell lines treated for 24 h with increasing doses of FK228 (0, 1, 5, 10, and 20  $\mu$ M). Results represent the mean values of three independent experiments  $\pm$  SD;

B. Effect of FK228 on cell number of adherent and floating RD (Left Panel, FK228 1.4 nM) and RH30 (Right Panel, FK228 0.6 nM) cells treated for increasing times (1–10 days); after four days the drug washout was performed or not. Cell viability on floating cells was measured by trypan blue dye exclusion test. Percentage related to floating plot indicate cell death. Results represent the mean values of four independent experiments  $\pm$  SD. Statistical significance: \* $p \leq 0.05$ , \*\* $p \leq 0.01$ , \*\*\* $p \leq 0.001$  compared with the respective untreated cells.

## 2.2. MS-275 treatment induces growth arrest and cell death

The concentration of MS-275 able to inhibit the half of cell viability ( $IC_{50}$ ) at 24h, assessed by Tripian Blue exclusion assay, was 1  $\mu$ M in RD and 1.9  $\mu$ M in RH30 cell lines (fig. 3. A). These concentrations have been used in the experiments throughout the work. The effects of MS-275 on cell proliferation were assessed by counting adherent and floating RD and RH30 cells at different time points under 4 days of drug treatment followed or not by drug washout for a further 6 days. 4 days of treatment significantly reduced the number of adherent cells by  $86.2 \pm 3.4\%$  in RD and  $91.3 \pm 4.3\%$  in RH30 cells. Concomitantly, MS-275 increased the number of floating cells. Drug W/O did not restore the growth potential of RH30 cells, while RD cells slowly recovered (fig. 3. B). After 4 days of drug treatment, both RD and RH30 cells showed long cellular extensions, especially RH30 cells that seem to acquire a neuritic-like morphology (fig. 3. C). These findings suggest that MS-275 treatment resulted in both cytostatic and cytotoxic in the two RMS cell lines with a reversible on RD and irreversible on RH30 cells anti-proliferative effect.

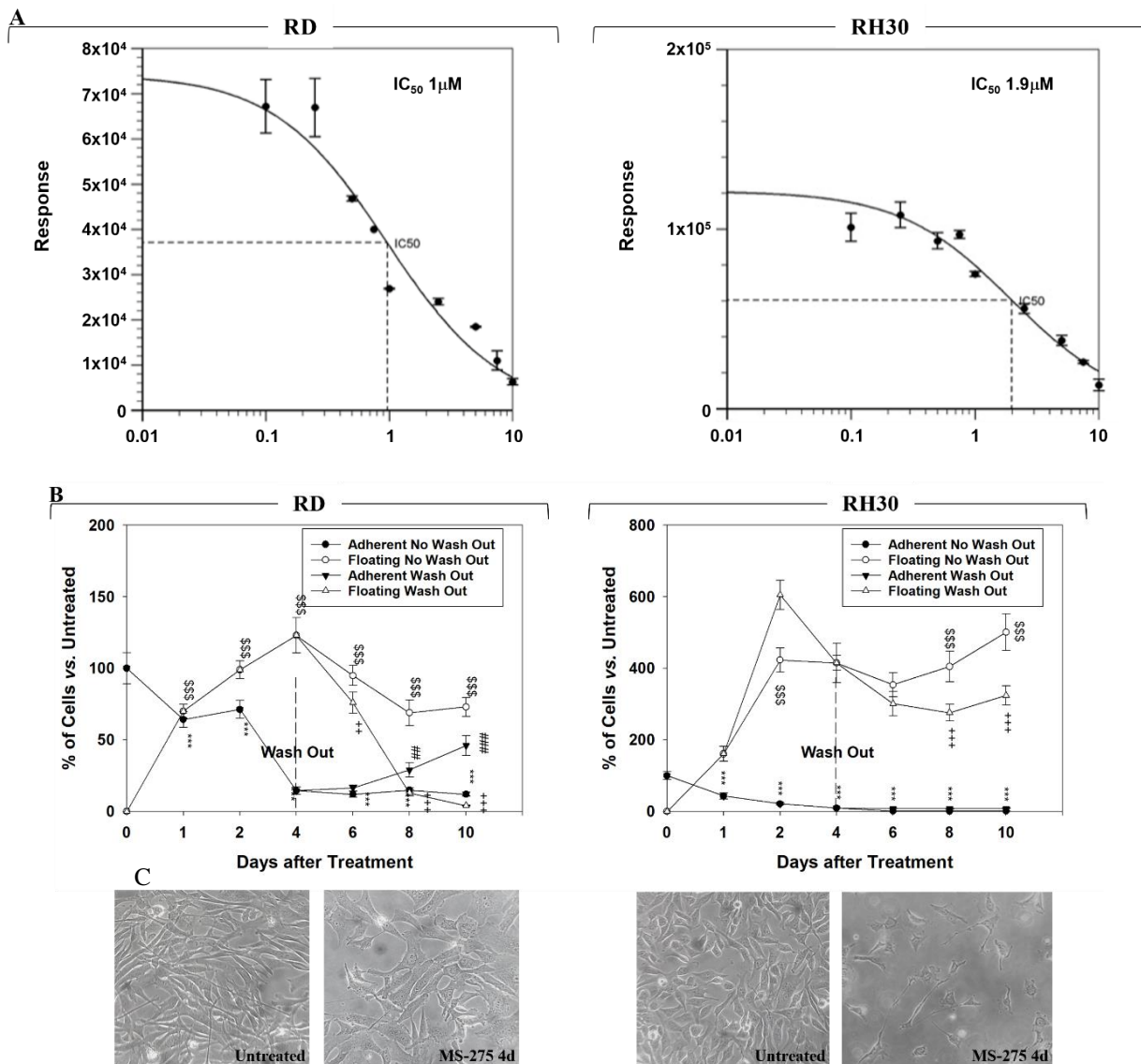


**Fig. 3** MS-275 induces reversible cell growth arrest in FN-RMS and FP-RMS cells.

- A. Dose of MS-275 able to reduce by 50% the cell survival of RD (Left) and RH30 (Right) cell lines was identified treating the cells for 24 h with increasing concentrations of the drug. Cell viability was measured by Trypan Blue dye exclusion test. Results represent the mean values of three independent experiments  $\pm$  SD.
- B. Effect of MS-275  $IC_{50}$  on cell number of adherent and floating RD (Left) and RH30 (Right) cells: after four days of treatment the drug was washed out or not and counts were performed for further 6 days. Surviving cells were counted using Trypan blue dye exclusion test. Results represent the mean values of four independent experiments  $\pm$  SD. Statistical significance: \*\*\* $p \leq 0.001$  vs. Untreated cells;  $^{\S}p \leq 0.05$ ,  $^{\S\S}p \leq 0.01$ ,  $^{\S\S\S}p \leq 0.001$  Washout vs. No Washout.
- C. Cellular morphology of RMS cells, RD (Left) and RH30 (Right), untreated or treated with MS-275 ( $IC_{50}$ ) for 4 days was analyzed under light microscope at 20X magnification.

### 3. FK228 reduced the mRNA expression levels of HDACs

Four days of FK228 significantly reduced the mRNA expression levels of HDAC1, HDAC2, HDAC3 and HDAC8 by  $56.3 \pm 4.2\%$ ,  $82.1 \pm 4.3\%$ ,  $67.9 \pm 4.1\%$  and  $69.4 \pm 1.4\%$  in RD and by  $73.2 \pm 1.9\%$ ,  $70.1 \pm 1.4\%$ ,  $65.8 \pm 1.1\%$  and  $87.1 \pm 0.2\%$  in RH30, respectively (fig. 4). The global activity of class I HDAC was also decreased by  $88.7 \pm 1.4\%$  in RD and  $71.2 \pm 1.6\%$  in RH30. Unfortunately, 24h after FK228 W/O, the expression and activity of HDACs were efficiently restored in both cell lines.

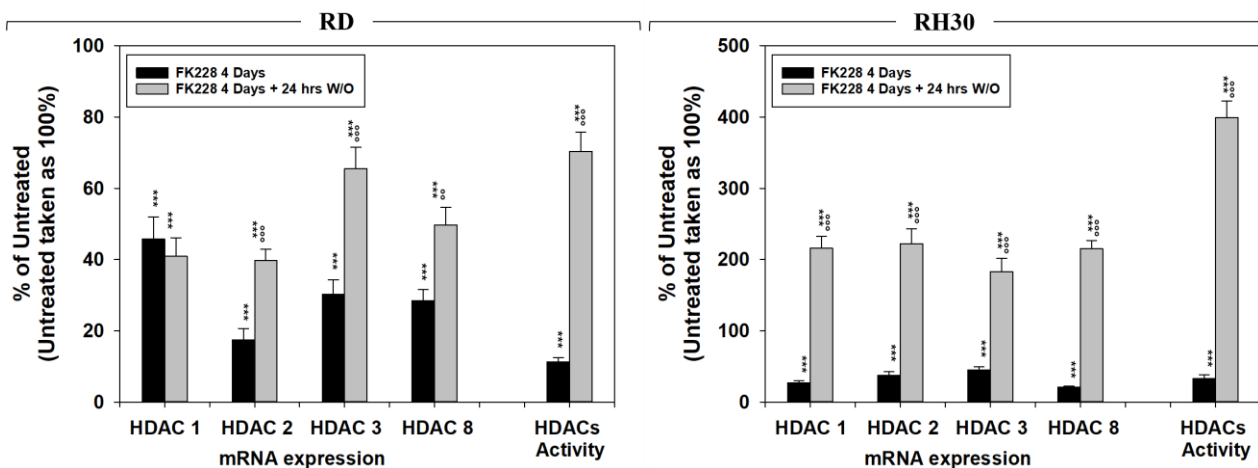


**Fig. 4** HDAC1, 2, 3 and 8 transcript levels and class I HDACs activity in RD (Left Panel, FK228 1.4 nM) and RH30 (Right Panel, 0.6 nM) cells treated for 4 days with FK228 and 24 h after FK228 washout. Transcript levels were measured by Q-PCR assays and GAPDH mRNA was used as an endogenous control. The relative mRNA expression levels are presented as the average fold changes in treated tumor cell lines vs. untreated cells, set at 1. Class I HDAC activity was measured by specific enzymatic assay and presented as the average fold changes in treated tumor cell lines vs. untreated cells, set at 1. Results represent the mean values of three independent experiments  $\pm$  SD. Statistical significance: \* $p \leq 0.05$ , \*\* $p \leq 0.01$ , \*\*\* $p \leq 0.001$  FK228 4 days vs. untreated cells,  $^{\circ}p \leq 0.05$ ,  $^{\circ\circ}p \leq 0.01$ ,  $^{\circ\circ\circ}p \leq 0.001$  FK228 4 days vs. FK228 washout.

#### 4. MS-275 downregulated transcript levels of HDACs

After 4 days of MS-275 treatment, RD cells downregulated the transcript levels of HDAC1 ~77%, HDAC2 ~60.5%, HDAC3 ~40.9%, HDAC8 ~25.9% and HDAC11 ~69%; also the global activity of HDACs is reduced by ~94.6%, how shows the figure 5. In RH30 cells the mRNA expression resulted totally repressed along with the global HDACs activity. 24h after the drug W/O, the expression of transcript and activity levels were restored and even up-regulated in the two cell lines.

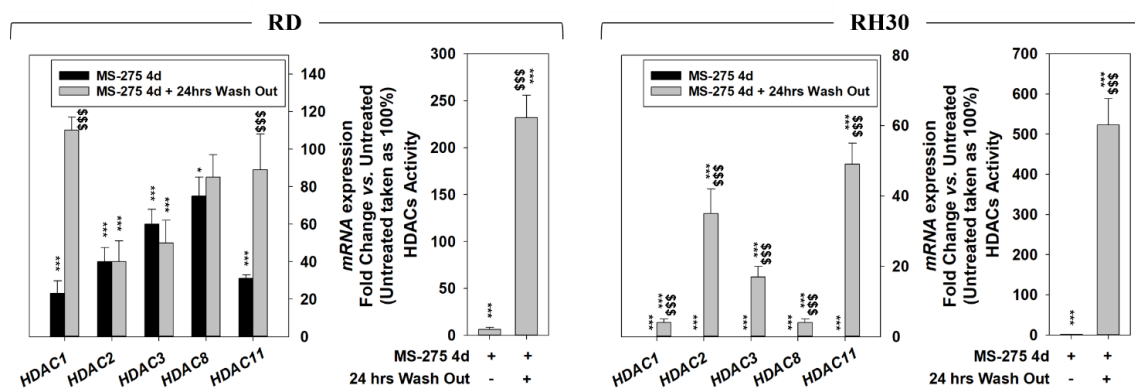


**Fig. 5** MS-275 reversibly reduces class I and IV HDACs expression and activity in FN-RMS and FP-RMS cells. HDAC1, 2, 3, 8 and 11 transcript levels in RD (Left) and RH30 (Right) cells treated for 4 days with MS-275 ( $IC_{50}$ ) followed by 24h of drug washout. Transcript levels were measured by qRT-PCR assays and GAPDH mRNA was used as endogenous control. The relative mRNA expression levels are presented as the average fold changes in treated tumor cell lines vs. untreated cells, set at 1. Results represent the mean values of three independent experiments  $\pm$  SD. Statistical significance: \* $p \leq 0.05$ , \*\* $p \leq 0.001$  vs. Untreated cells;  $^{\circ\circ\circ}p \leq 0.001$  Wash Out vs. No Wash Out.

#### 5. Cell cycle distribution and related molecular signature in RD and RH30 cells

##### 5.1. FK228 did not control efficiently tumor proliferation:

Cell cycle analysis by flow cytometry on RMS cells treated for 1, 2 and 4 days with FK228 (IC<sub>50</sub>) did not show any statistically significant change on cell cycle distribution, as described in figure 6.

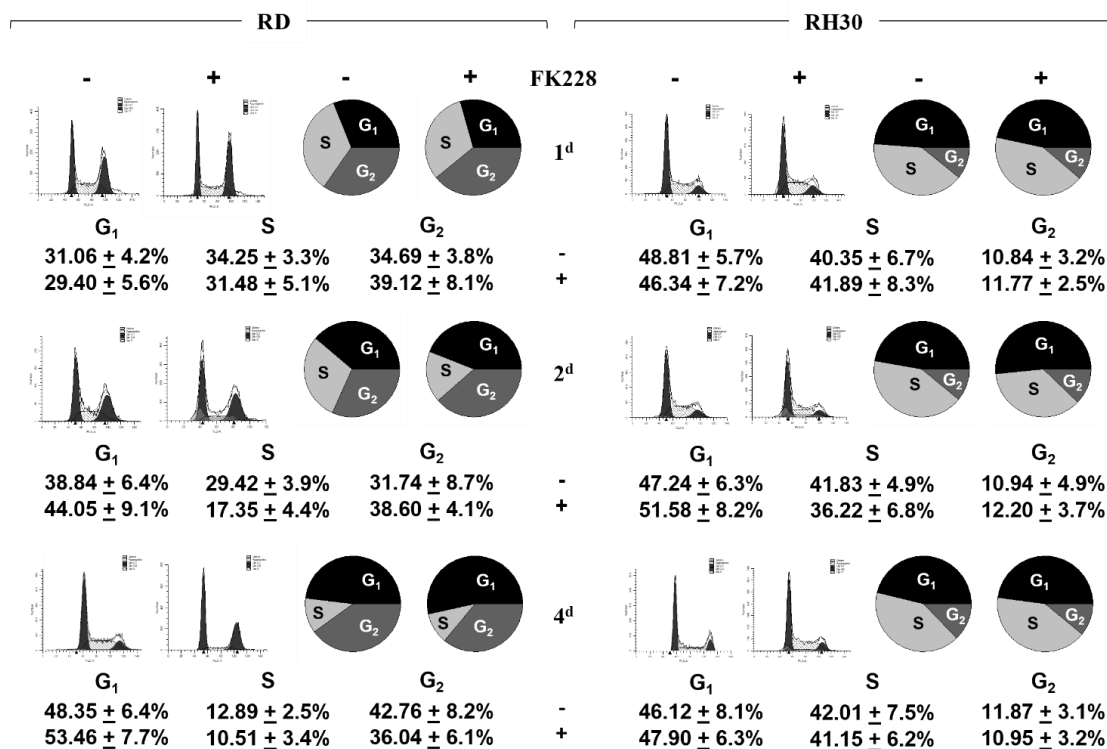


**Fig. 6** FK228 does not affect cell cycle distribution but induces cell cycle protein modulation. FACS analysis performed on RD (Left Panel, FK228 1.4 nM) and RH30 (Right Panel, 0.6 nM) cells untreated or treated for 1, 2 or 4 days. Representative of three different experiments.

At molecular level, the drug treatment upregulated the expression of several positive cell cycle regulators such as Cyclin-A (Cyc-A), b (Cyc-B), D1 (Cyc-D1) in both cell lines and c-Myc in RD and N-Myc in RH30 cells (fig. 7). These results indicated that FK228 is unable to contrast the proliferative properties of RMS cells. They also suggest that surviving cells are able to activate a molecular program potentially responsible for chemoresistance.

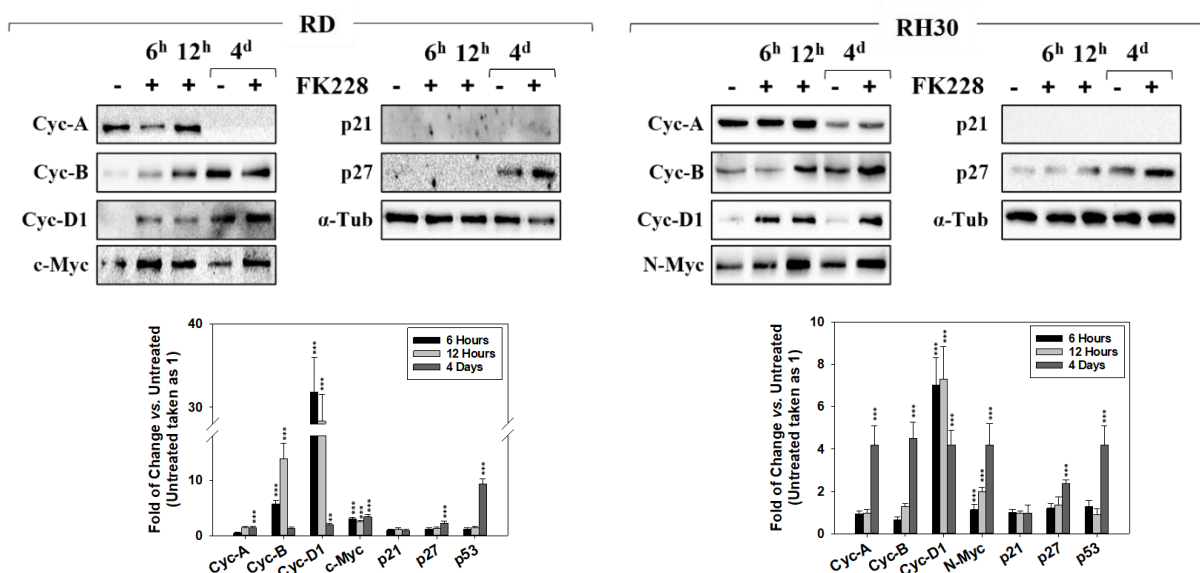


**Fig. 7** showing the percentage of cell cycle phases representing the mean value of four independent experiments. Cell lysates from RD (Left Panel, FK228 1.4 nM) and RH30 (Right Panel, 0.6 nM) cells treated for 6 h, 12 h and 4 days were analyzed by immunoblotting with specific ab for indicated proteins; α-Tubulin expression shows the loading of samples. Histograms represent the mean values of three independent experiments ± SD. Statistical significance: \*p<.05, \*\*p<.01, \*\*\*p<.001 FK228 4 days vs. untreated cells.

### 5.2. MS-275 affected cell cycle distribution:

Investigating the effects of MS-275 on cell cycle distribution by flow cytometry on RD and RH30 cells at 1, 2, 4 and 6 days post treatment, resulted a progressive reduction of cells in the S phase of the cell cycle to treated cells. Moreover, RD cells were accumulated in G<sub>1</sub> phase at days 2 and 4; then, after 6 days, they increased in the G<sub>2</sub> phase. Instead, RH30 cells showed a marked accumulation in the G<sub>1</sub> phase after 2 days from treatment, which was further increased up to 6 days (fig. 8).

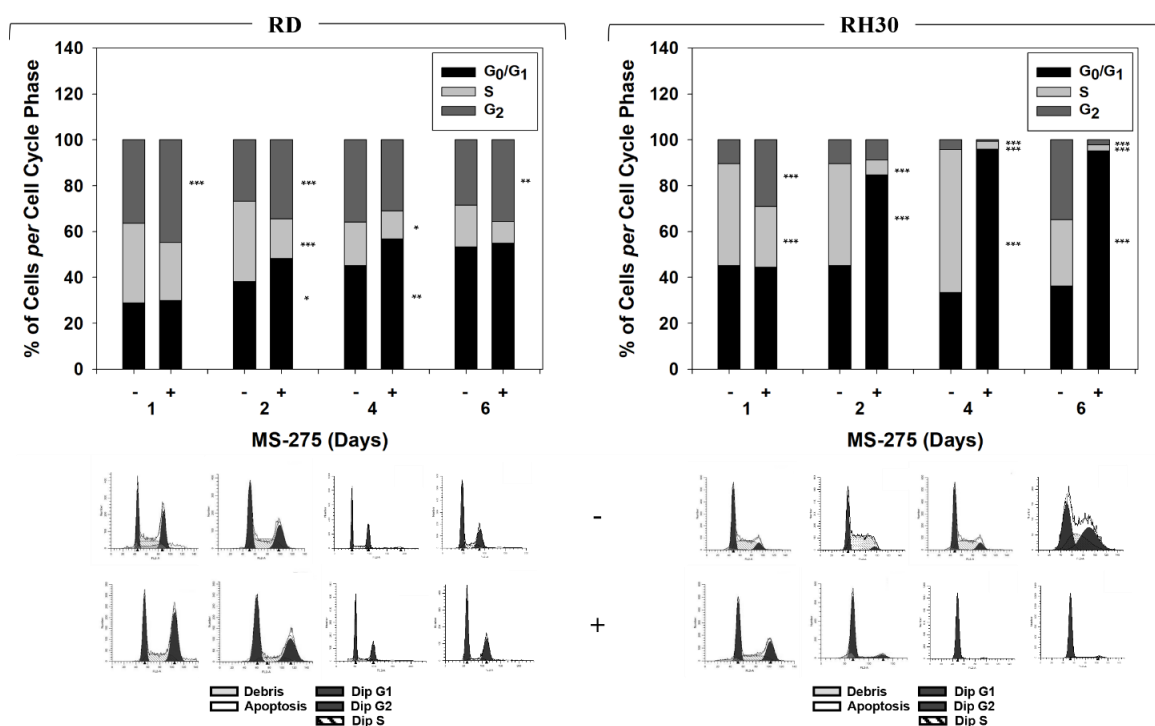


**Fig. 8** MS-275 affects cell cycle distribution. FACS analysis performed on RD (Left) and RH30 (Right) untreated or treated for 4 days with MS-275 (IC50). Data (Up) showing the percentage of cells in each cell cycle phase representing the mean value of three independent experiments. Histograms (Down) represent the mean values of three independent experiments  $\pm$  SD. Statistical significance: \*\*  $p \leq 0.01$ , \*\*\*  $p \leq 0.001$  vs. Untreated cells.

At the molecular level, after 24h and 4 days from treatment, in both RD and RH30 cells there is a downregulation of the expression of c-Myc (in RD) and N-Myc (in RH30), and of the cell cycle promoters Cyc-A, Cyc -B. Cyc-D1 was significantly downregulated but only in RH30. In addition, MS-275 upregulating the expression of the cell cycle negative controllers p21 and p27. The treatment is also able to reduced the activation of ERKs and AKTs in RD and RH30 respectively, how described figure 9. Altogether, these results suggest that MS-275 differently modulates the cell cycle distribution, even if it induces a similar modification in the expression of cell cycle molecular-related markers.

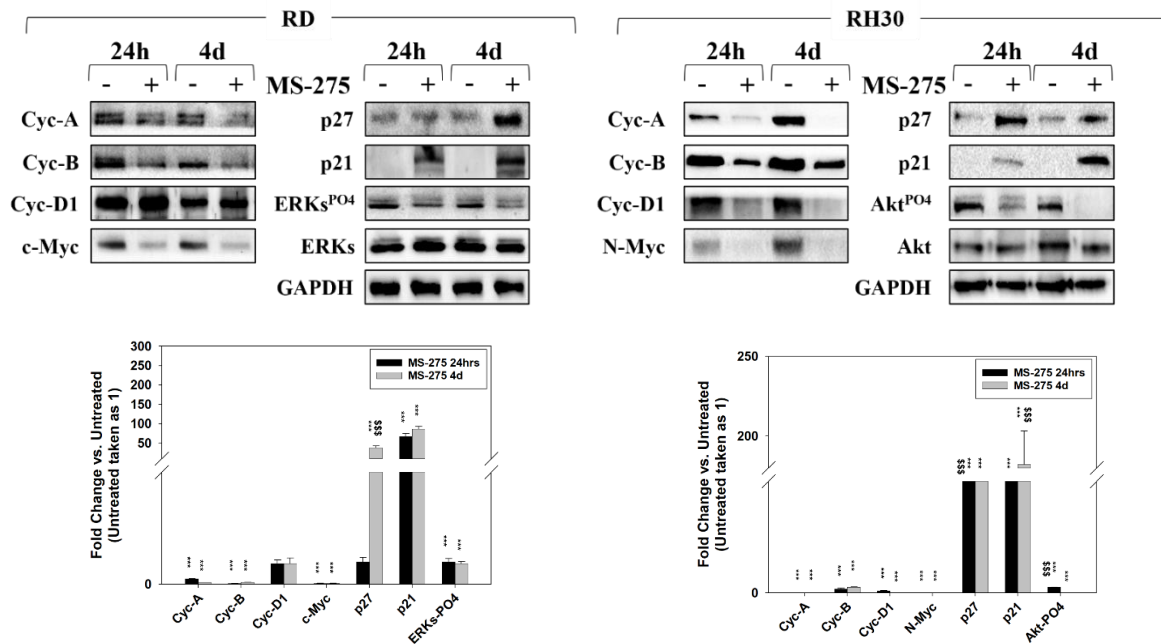
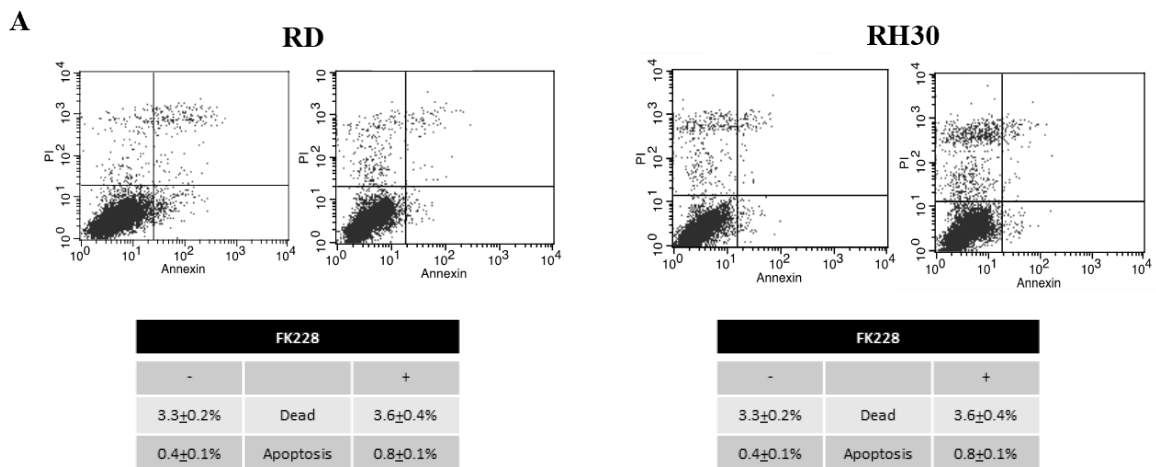


**Fig. 9** Cell lysates from RD (Left) and RH30 (Right) cells treated for 24 h and 4 days with MS-275 ( $IC_{50}$ ) were analyzed by immunoblotting with specific antibodies for the indicated proteins; GAPDH expression was used as a loading control. Histograms of densitometric analysis (Down) represent the mean values of three independent experiments  $\pm$  SD. Statistical significance: \*\*  $p \leq 0.01$ , \*\*\*  $p \leq 0.001$  vs. Untreated cells.

## 6. Apoptosis and PARP1 activity:

### 6.1. RMS cells activate anti-apoptotic and pro-surviving signals against FK228:

After 24h from drug treatment, it did not induce any significant increase in the number of apoptotic cells as show Annexin V positive cells (fig. 10. A) and the levels of Cleaved-Caspase 3 (fig. 11. A) in both RMS lines. On the other hand, FK228 significantly upregulated the protein levels of the anti-apoptotic Bcl-2 and Bcl-xL factors (fig. 11. A) and increased PARP1 activity (fig. 10. B) in both RD and RH30 cells. It also induced the phosphorylation/activation of ERKs and mTOR, and AKT in RD and RH30 respectively (fig. 11. B).





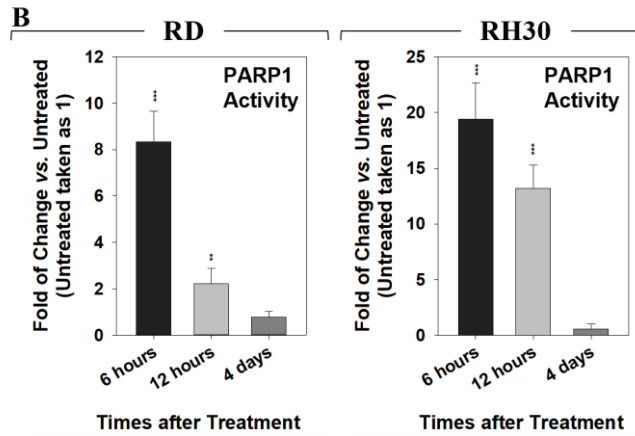


**Fig. 10** FK228 induces ROS-induced DSBs, triggers PARP1 but doesn't lead to apoptosis.

- A. Annexin V analysis performed on RD (Left Panel, FK228 1.4 nM) and RH30 (Right Panel, 0.6 nM) cells untreated or treated for 24h. Representative of three different experiments. Data (Lower Panel) showing the percentage of dead and apoptosis representing the mean value of three independent experiments.
- B. PARP1 activity assay performed on RD (Left Panel, FK228 1.4 nM) and RH30 (Right Panel, 0.6 nM) cells treated for 6, 12 h and 4 days. Histograms represent the mean values of three independent experiments  $\pm$  SD. Statistical significance: \* $p \leq .05$ , \*\* $p \leq .01$ , \*\*\* $p \leq .001$  FK228 4 days vs. untreated cells.

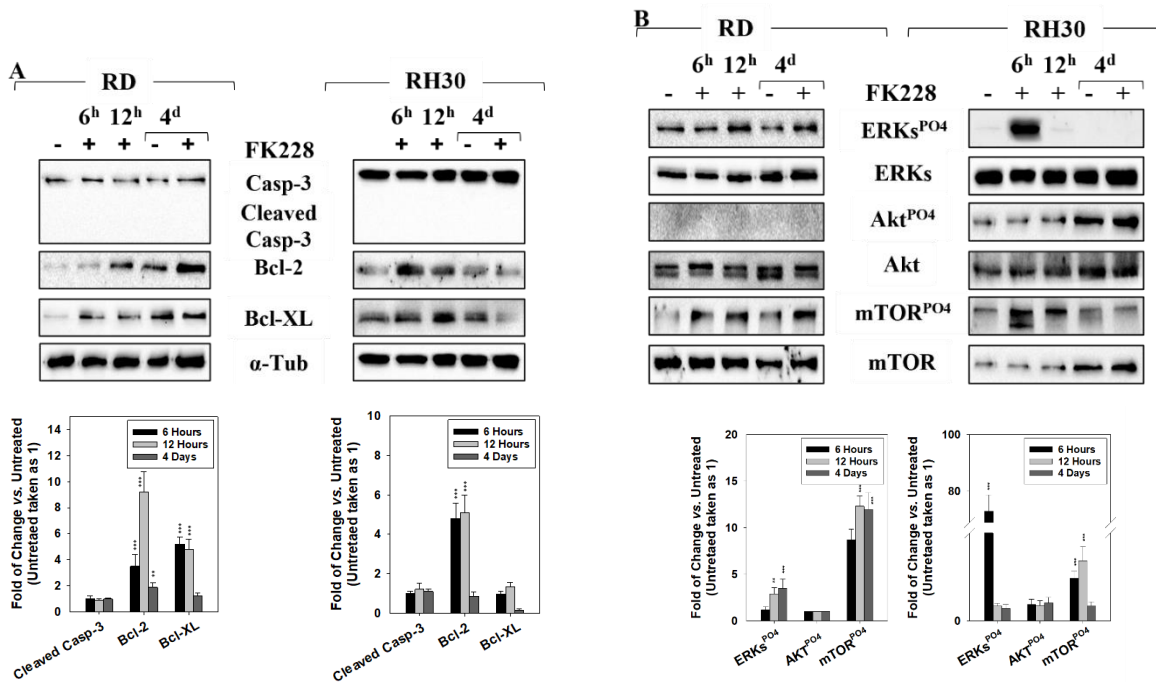


**Fig. 11** FK228 does not induce caspase cell death cascades and activates PI3K/Akt/mTOR and MAPKs/ERKs signals. Cell lysates from RD (Left Panel, FK228 1.4 nM) and RH30 (Right Panel, 0.6 nM) cells treated for 6h, 12h and 4 days were analyzed by immunoblotting with specific antibodies for indicated proteins;  $\alpha$ -Tubulin expression shows the loading of samples. Histograms represent the mean values of three independent experiments  $\pm$  SD. Panel shows immunoblotting representative of three different experiments. Statistical significance: \* $p \leq .05$ , \*\* $p \leq .01$ , \*\*\* $p \leq .001$  FK228 4 days vs. untreated cells.

Therefore, RMS cells seem to be able to survive to FK228 by activation of anti-apoptotic and pro-survival signals.

### 6.2. MS-275 induced non-apoptotic cell death:

The Annexin V cell staining on surviving cells was performed 24h after the treatment. The drug significantly increased the number of necrotic cells to ~18% in RD and to ~21% in RH30 cells compared to untreated cells. No significant difference was seen in the early (LR)



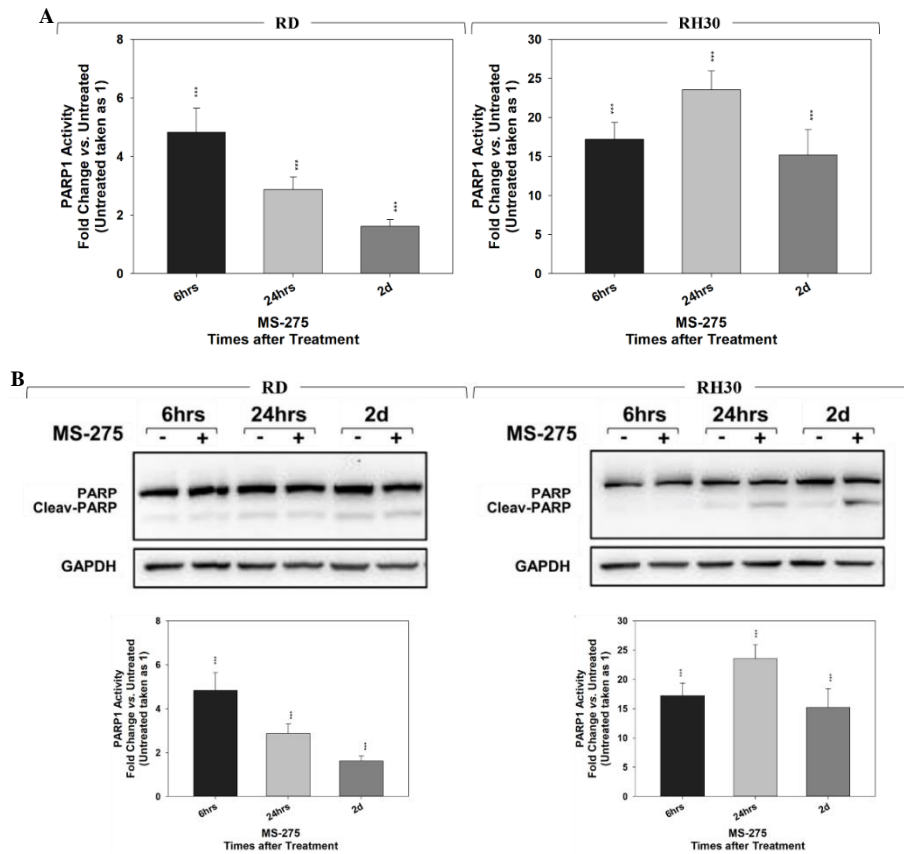


**Fig. 13** MS-275 induces PARP1 activation.

- A.** RD (Left) and RH30 (Right) cells treated with MS-275 IC<sub>50</sub> for 6h, 24h and 2 days were analyzed for PARP1 activity by a specific assay.
- B.** Cell lysates from RD and RH30 cells treated with MS275 IC<sub>50</sub> for 6h, 24h and 2 days were analyzed by immunoblotting with specific Ab for the indicated proteins; GAPDH expression was used as loading control of samples.
- Histograms of densitometric analysis represent the mean values of three independent experiments  $\pm$  SD. Statistical significance: \*\*\* $p < 0.001$  vs. untreated cells.

## 7. *In vitro* radiosensitive effects of HDACis in RMS cell lines

### 7.1. FK228 radiosensitize FP-RMS

#### 7.1.1. FK228 maintains DNA damage:

The ability of FK228 to radiosensitize RMS lines was assessed on parental (PR-RMS) and clinically relevant radioresistant RMS (RR-RMS) cell lines. Cells were pretreated or not with FK228 for 24h and irradiated with a single dose of 4 Gy. After irradiation, FK228 was W/O and colony formation assay performed. Drug treatment significantly reduced the ability of irradiated parental RH30 to form colonies by  $98.3 \pm 7.2\%$  compared to the untreated; improved also the therapeutic efficiency of RT by  $83.3 \pm 1.2\%$  than irradiated parental cells. Unfortunately, no radiosensitizing effects were detected in RD cells and in RR-RMS cell lines, how described figure 14. We also investigated the expression levels of  $\gamma$ -H2AX, a sensitive molecular marker of DNA damage and repair. It was assessed on RMS cells treated with FK228 for 6h, 12h and 4 days. The drug significantly increased  $\gamma$ -H2AX expression by  $11.3 \pm 1.4$  in 12h-treated RD

and by  $173.8 \pm 18.3$  in 6h-treated RH30. In any case,  $\gamma$ -H2AX levels returned to basal levels within 4 days of treatment in both RMS cell lines (fig. 15).

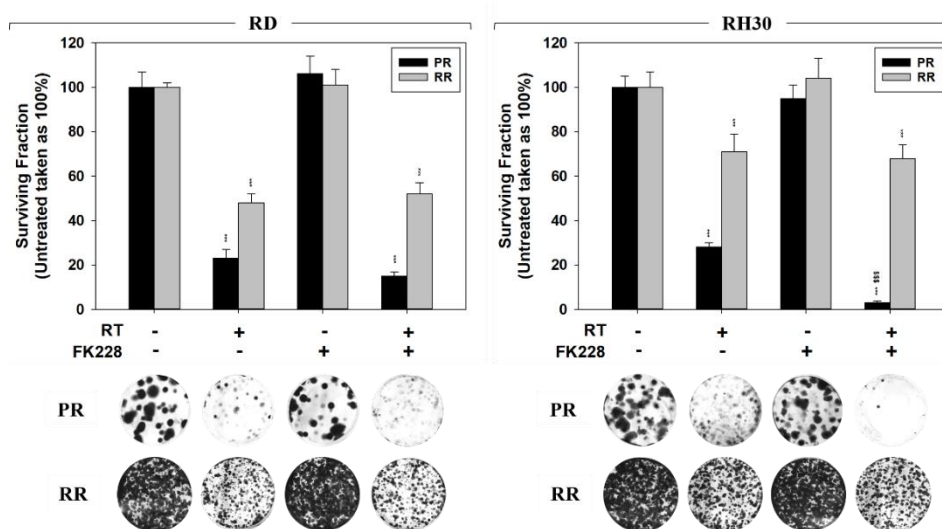


**Fig. 14** FK228 radiosensitizes ARMS cell lines by affecting the ability of RH30 cells to detoxify from RT-induced oxidative stress. Two hours after RT (4 Gy), cells were seeded at low concentration for colony assays or lysed for total protein extraction. Colony forming efficiency was calculated by crystal violet absorbance after 14 days of FK228/RT<sup>-</sup>, FK228<sup>+</sup>/RT<sup>-</sup>, FK228<sup>+</sup>/RT<sup>+</sup> or FK228<sup>-</sup>/RT<sup>+</sup> treatments (RD, Left Panel, FK228 1.4 nM and RH30, Right Panel, 0.6 nM). Results represent the mean values  $\pm$  SD of three independent experiments. Statistical significance: \*\*\* $p \leq 0.001$  FK228 4 days vs. untreated cells, <sup>sss</sup> $p \leq 0.05$  vs. RT.

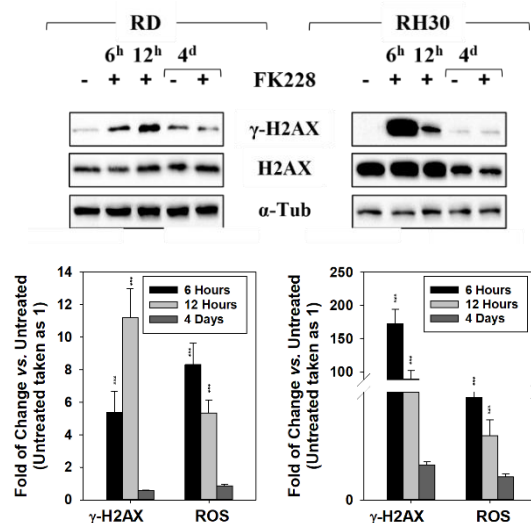


**Fig. 15** Cell lysates from RD (Left Panel, FK228 1.4 nM) and RH30 (Right Panel, 0.6 nM) cells treated for 6h, 12h and 4 days were analyzed by immunoblotting with specific ab for indicated proteins ( $\alpha$ -Tubulin expression shows the loading of samples) and mitochondrial superoxide anion production was assessed by MitoSox Red staining (ROS). Histograms represent the mean values of three independent experiments  $\pm$  SD. Panel shows immunoblotting representative of three different experiments. Statistical significance: \*\*\* $p \leq 0.001$  FK228 4 days vs. untreated cells.

### 7.1.2. FK228 reduce antioxidant ability of RMS:

RMS cells can efficiently activate antioxidant strategies to overcome RT toxicity. Pretreating them with FK228 we have obtained an enhanced of the ability of RT to induce ROS accumulation up to 6h post-RT. In RH30 cells ROS accumulation persisted up to 12h after RT, while in RD cells they were restored to baseline within 12h (fig. 15-16).

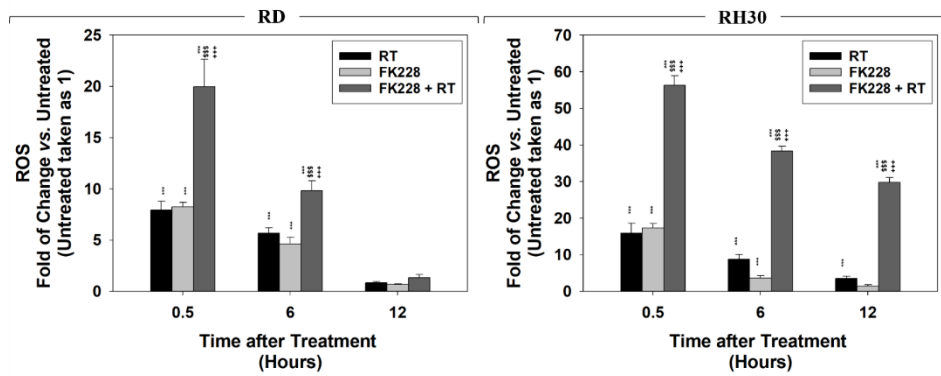


**Fig. 16** Mitochondrial super-oxide anion production was assessed by MitoSox Red staining, half hour (0.5h), 6h or 12h after RT. Statistical significance: \*\* $p \leq 0.01$ , \*\*\* $p \leq 0.05$  vs. untreated cells, <sup>SSS</sup> $p \leq 0.05$  vs. FK228, <sup>+++</sup> $p \leq 0.05$  vs. FK228+RT.

After this time, the mRNA expression levels of NRF2, SOD, CAT and GPx-4 were assessed. How showed in figure 17, RD cells pretreated with the drug activated more efficiently the transcription of NRF2 and CAT after RT, while there were no differences in RH30 cells. These results could be explained by the ability of RMS cells to efficiently activate antioxidant strategies to overcome RT toxicity, because the most RT-induced DSBs are triggered just by ROS. These evidences suggest that FK228 is able to radiosensitize the ARMS cells through mechanisms apparently unrelated to increased oxidative stress or reduced antioxidant response.

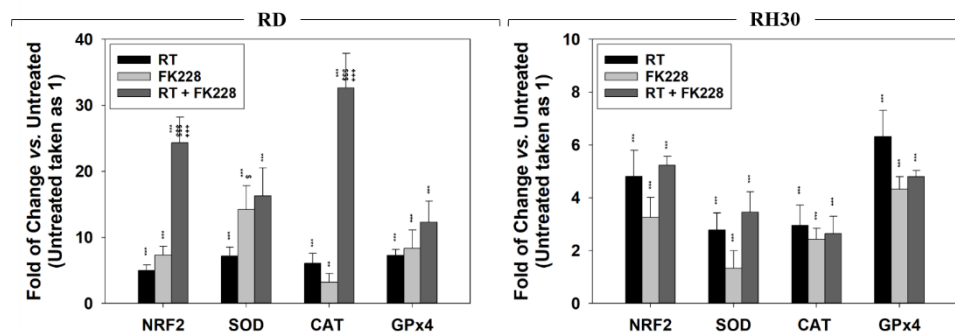


**Fig. 17** Gene expression of antioxidant enzymes superoxide dismutase (SOD-2), catalase (CAT), glutathione peroxidase (GPx-4) and nuclear factor erythroid 2 p45-related factor (NRF2) was investigated by real-time PCR, 12 h after RT. The gene expression was referenced to the ratio of the value of interest and basal conditions. The value of basal conditions was reported equal to 1. Single results are representative of three different experiments performed in triplicate. Statistical significance: \*\* $p \leq 0.01$ , \*\*\* $p \leq 0.05$  vs. untreated cells, <sup>S</sup> $p \leq 0.05$ , <sup>SSS</sup> $p \leq 0.05$  vs. FK228, <sup>+++</sup> $p \leq 0.05$  vs. FK228+RT.

### 7.1.3. FK228 impairs DSBs repair ability:

After the evaluation of  $\gamma$ H2AX levels, we investigated the ability of RMS cells to repair RT-induced DNA damage with and without FK228 treatment associated to RT. Observing in figure 18 DNA-PKCs, marker related to the Non-Homologous End Joining (NHEJ), and ATM, marker related to the Homologous Recombination (HR) DNA repair pathways, FK228 pretreatment significantly counteracted the phosphorylation/activation

of DNA-PKcs and ATM in RH30. In contrast, it did not significantly improve RT toxicity or modified the molecular response to RT of RD cells.

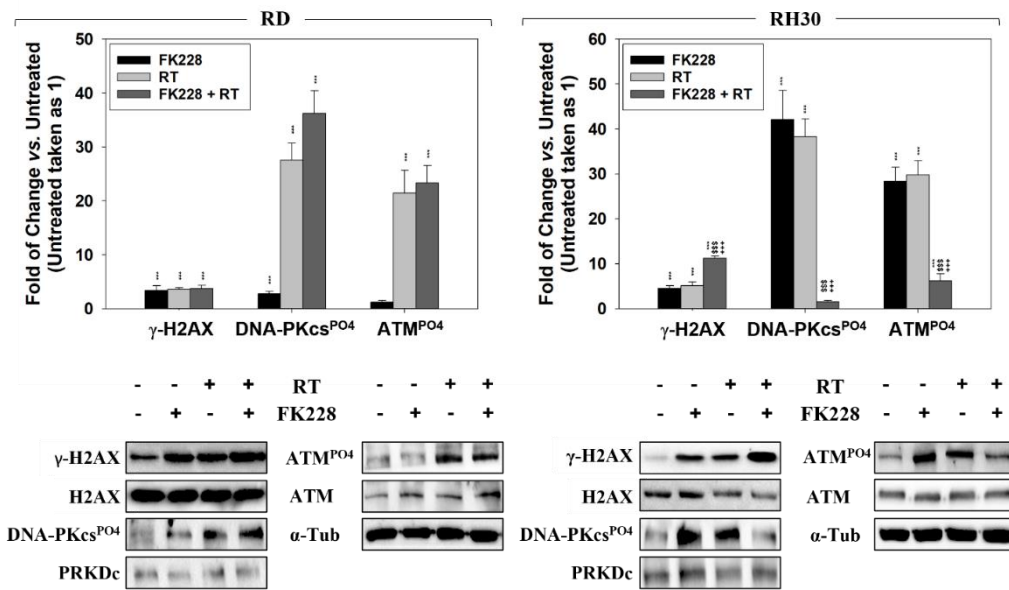


**Fig. 18** FK228 affects the ability of RH30 cells to repair RT-induced DSBs. Cell lysates from FK228<sup>-</sup>/RT<sup>-</sup>, FK228<sup>+</sup>/RT<sup>-</sup>, FK228<sup>-</sup>/RT<sup>+</sup> or FK228<sup>+</sup>/RT<sup>+</sup> treatments (RD, Left Panel, FK228 1.4 nM and RH30, Right Panel, 0.6 nM) were analyzed by immunoblotting with specific abs for indicated proteins;  $\alpha$ -Tubulin expression shows the loading of samples. Histograms (Upper Panel) represent the mean values of three independent experiments  $\pm$  SD. Statistical significance: \*\*\*p  $\leq$  0.05 vs. untreated cells, \$\$\$p  $\leq$  0.05 vs. FK228, +++p  $\leq$  0.05 vs. FK228+RT.

Studying the activity of key signal transduction pathways linked to RMS radioresistance did not show any significant difference. However, FK228 restrained the ability of RT to induce N-Myc expression in RH30 cells (fig. 19). Altogether, these results suggest that FK228 radiosensitizes ARMS cells also by affecting the DSBs repair network.

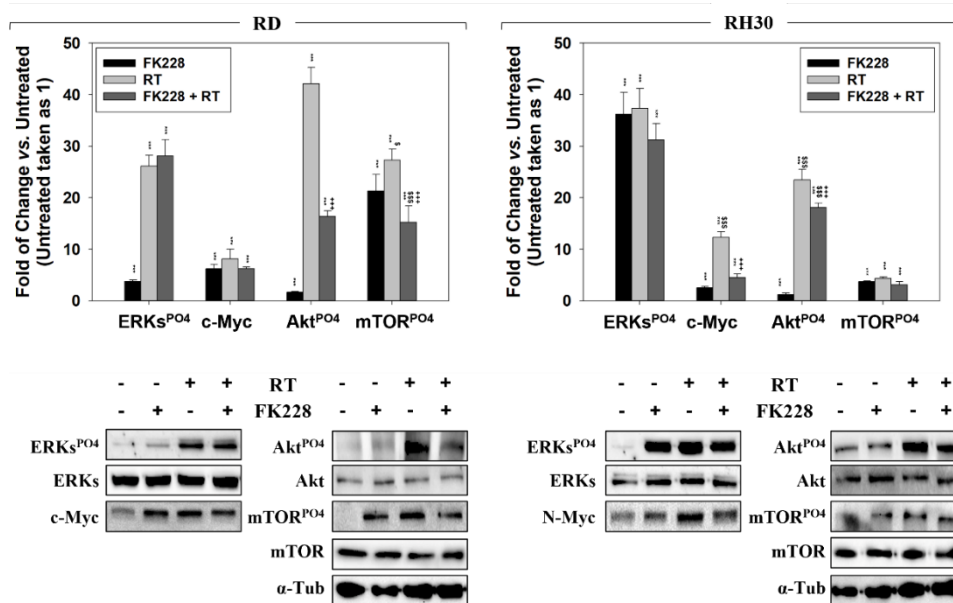


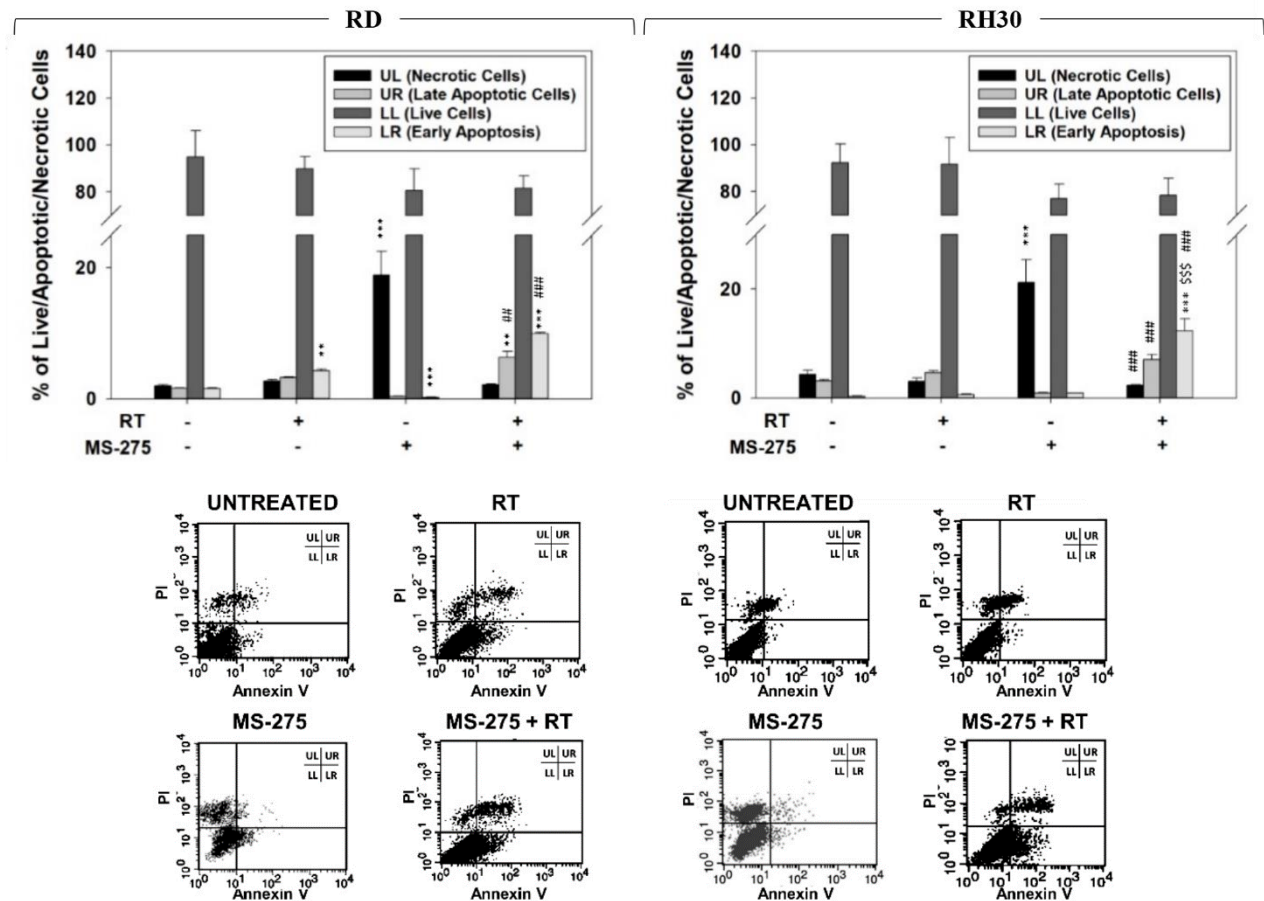
**Fig. 19** FK228 affects the ability of RH30 cells to repair RT-induced DSBs. Cell lysates from FK228<sup>-</sup>/RT<sup>-</sup>, FK228<sup>+</sup>/RT<sup>-</sup>, FK228<sup>-</sup>/RT<sup>+</sup> or FK228<sup>+</sup>/RT<sup>+</sup> treatments (RD, Left Panel, FK228 1.4 nM and RH30, Right Panel, 0.6 nM) were analyzed by immunoblotting with specific Abs for indicated proteins;  $\alpha$ -Tubulin expression shows the loading of samples. Panel shows representative immunoblotting of three independent experiments. Histograms (Upper Panel) represent the mean values of three independent experiments  $\pm$  SD. Statistical significance: \*\*\*p  $\leq$  0.05 vs. untreated cells, \$\$\$p  $\leq$  0.05, \$\$\$p  $\leq$  0.05 vs. FK228, +++p  $\leq$  0.05 vs. FK228+RT.

## 7.2. MS-275 radiosensitizes FP-RMS

### 7.2.1. MS-275 increase apoptosis in combination with RT:

The effects of MS-275 pre-treatment (24h) in inducing RT cell death and modifying cell cycle distribution were investigated by Annexin V cell staining and flow cytometry respectively, 24h after irradiation. Compared to RT alone, pre-treating RMS with the drug increased the size of apoptotic cells (fig.20.A) and induced accumulation in the G<sub>2</sub> phase of cell cycle (fig.20.B). These data indicate that the MS-275 predisposes both RD and RH30 to respond to radiation, even if it effectively radiosensitizes only RH30 cells. Furthermore, they also suggest a great ability of RD to repair radiation-induced damage and/or recover cell death.

A



B

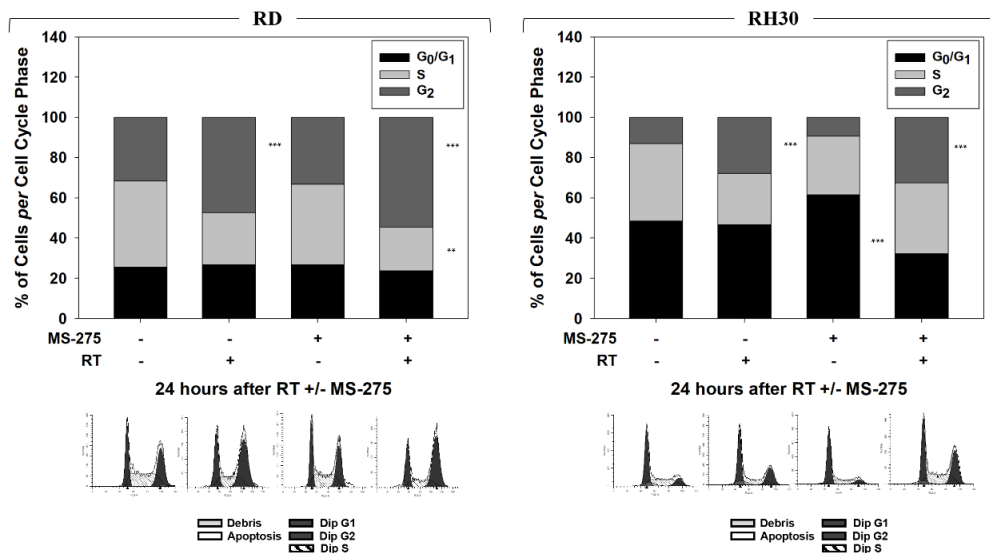


**Fig. 20** Pre-treating RMS with MS275 promotes RT-induced apoptosis.

- A.** Annexin V analysis performed after 24h of irradiation (4 Gy) on RD and RH30 cells untreated with MS275 IC<sub>50</sub>. Histograms (up) show the percentage of necrotic and apoptotic cells representing the mean value of three independent experiments. Representative FACS plots (Down) of three different experiments.
- B.** FACS analysis performed on RD and RH30 treated as in (A). Histograms show the percentage of cells in the cell cycle phases and represent the mean value of four independent experiments. The lower panel shows a representative FACS plot of one of three independent experiments.

Statistical significance: \*\* $p \leq 0.01$ , \*\*\* $p \leq 0.001$  vs. Untreated cells:

<sup>ss</sup> $p \leq 0.01$ , <sup>sss</sup> $p \leq 0.001$  vs. RT;

<sup>##</sup> $p \leq 0.01$ , <sup>###</sup> $p \leq 0.001$  vs. MS275.

### 7.2.2. MS-275 is able to induce DNA damage:

The ability of MS-275 to sensitize to RT was assessed through colony formation assay performed on RMS cells pre-treated for 24h with the drug and then irradiated with a dose of 4 Gy and imaged 6h later. RT treatment alone inhibited the capability of both cell lines to form colonies by  $82.8 \pm 4.7\%$  in RD and  $62.9 \pm 3.9\%$  in RH30. MS-275 as single agent reduced the colony formation ability by  $18.2 \pm 5.3\%$  in RD and  $64.1 \pm 4.9\%$  in RH30, and significantly increased the RT-induced toxicity in RH30 cells up to  $87.2 \pm 9.1\%$ . RD were not radiosensitized, how showed in figure 21. A. At molecular level the phosphorylation of H2AX ( $\gamma$ H2AX), a specific molecular marker of DNA damage, were assessed 6h after irradiation. The treatment with MS-275 markedly increased the ability of RT to upregulate  $\gamma$ H2AX but also do it as single agent (fig. 21. B), confirming the ability of HDACi to induce DNA damage.



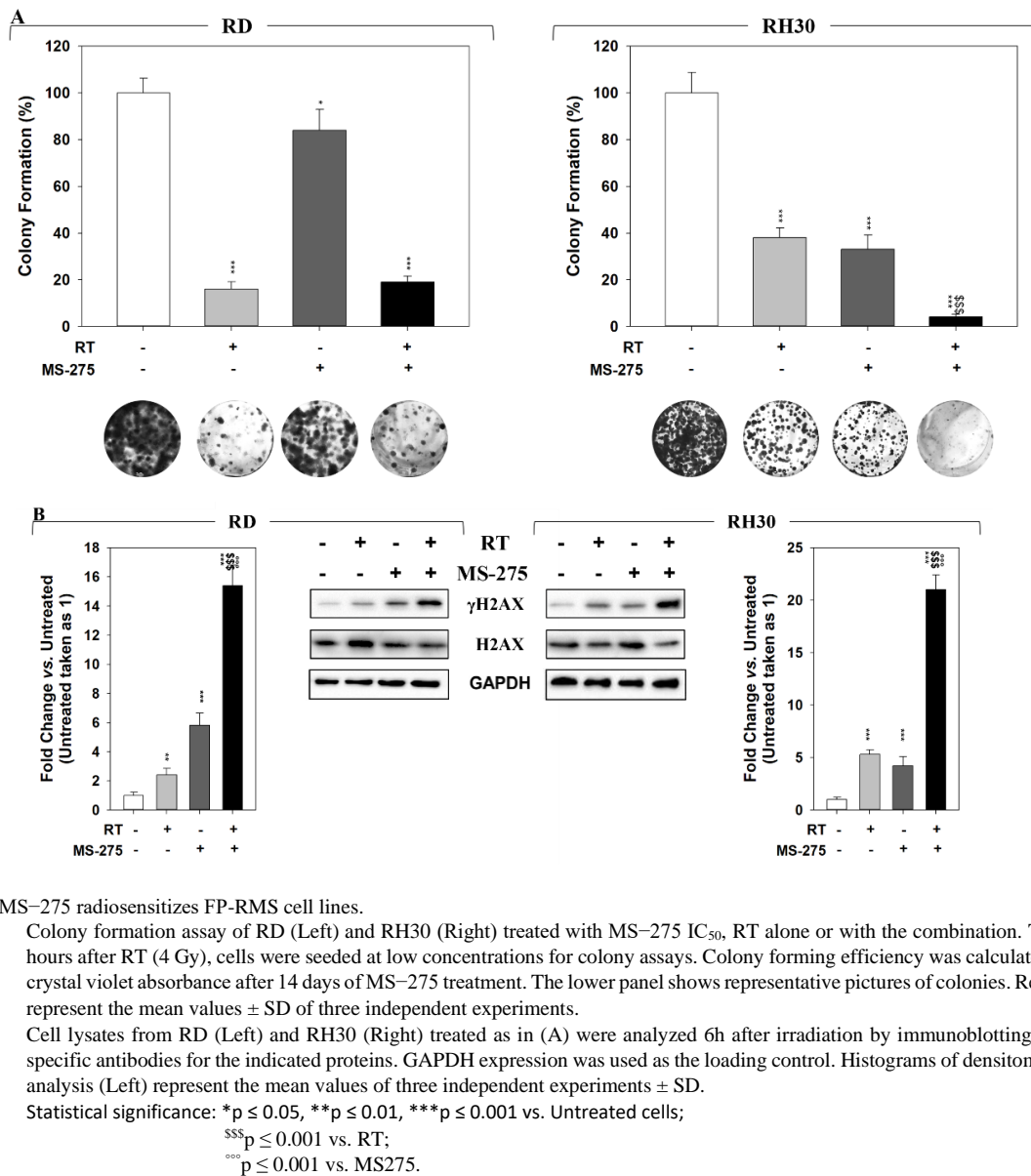


**Fig. 21** MS-275 radiosensitizes FP-RMS cell lines.

- A.** Colony formation assay of RD (Left) and RH30 (Right) treated with MS-275 IC<sub>50</sub>, RT alone or with the combination. Three hours after RT (4 Gy), cells were seeded at low concentrations for colony assays. Colony forming efficiency was calculated by crystal violet absorbance after 14 days of MS-275 treatment. The lower panel shows representative pictures of colonies. Results represent the mean values ± SD of three independent experiments.
- B.** Cell lysates from RD (Left) and RH30 (Right) treated as in (A) were analyzed 6h after irradiation by immunoblotting with specific antibodies for the indicated proteins. GAPDH expression was used as the loading control. Histograms of densitometric analysis (Left) represent the mean values of three independent experiments ± SD.

### 7.2.3. MS-275 impaires DNA damage repair system of FP-RMS from ROS accumulation induced by RT:

ROS are known as responsible for 2/3 of RT-induced DSBs. For first, observing the ROS production after administration of MS-275 and after the combination drug+RT, we noticed that ROS accumulation rapidly increased by RT and MS-275 as single treatments in both RD and RH30. But, while ROS induced by the drug were maintained throughout the experiment, the ROS levels due to RT returned to baseline 12h later. Pre-treating RMS cells with MS-275 further increased RT-induced ROS accumulation in both RD and RH30 cells and significantly reduced their ability to rapidly detoxify from ROS (fig. 22. B).

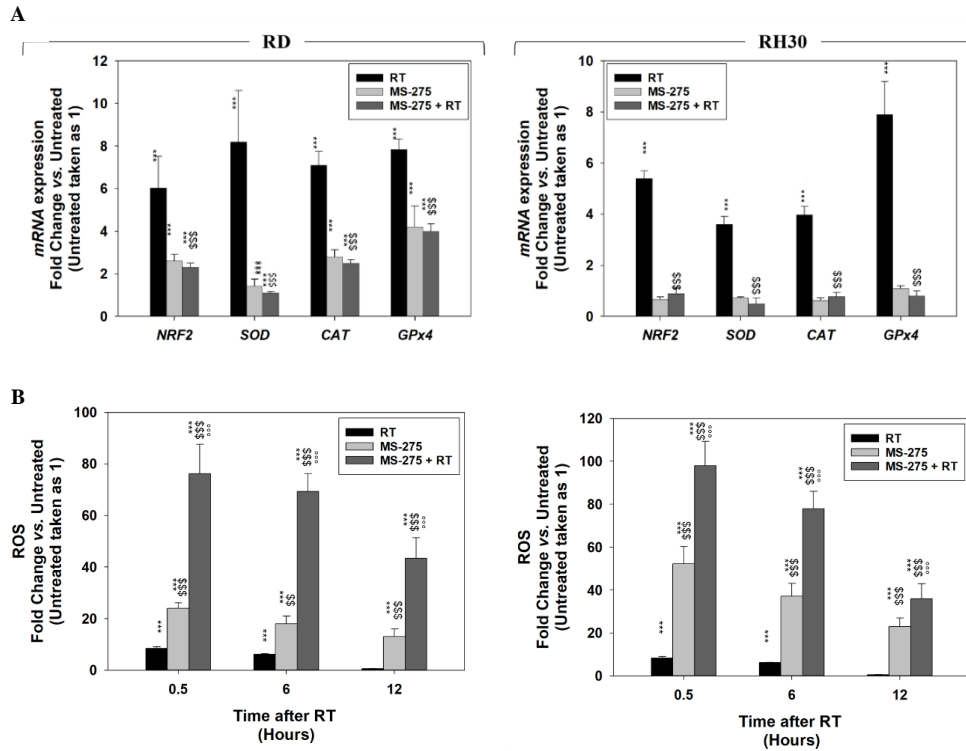


**Fig. 22** MS-275 inhibits anti-oxidant molecular response in both RMS cell lines. (A) RD (Left) and RH30 (Right) were treated with MS-275 ( $IC_{50}$ ) and RT (4 Gy) alone or pre-treated (24h) with MS-275 and then irradiated and values of three independent experiments  $\pm$  SD.

- A.** Gene expression of antioxidant enzymes superoxide dismutase (SOD-2), catalase (CAT), glutathione peroxidase (GPx)-4 and nuclear factor erythroid 2 p45-related factors (NRF2) were investigated by qRT-PCR, 12h after RT in cells treated. The gene expression was reported as fold change vs. untreated conditions reported equal to 1. Histograms are representative of three independent experiments performed in triplicate.
- B.** Mitochondrial superoxide anion production of RD (Left) and RH30 (Right) treated was assessed by MitoSox Red staining, half-hour (0.5), 6 or 12h after RT.
- Statistical significance: \*\*\* $p \leq 0.001$  vs. Untreated cells;  
 \$\$\$ $p \leq 0.001$  vs. RT;  
 °°° $p \leq 0.001$  vs. MS275.

About the DNA repair system, the phosphorylation/activation status of DNA-PKCs and ATM signaling were investigated. DNA-PKCs belong to the upstream of Non-Homologous End-Joining (NHEJ); ATM signaling belongs to Homologous Recombination (HR) DSBs repair pathways. MS-275 pretreatment failed in counteracting the RT-induced activation of DNA-PKCs-dependent NHEJ pathway in both cell lines. It was also not able to reduce the activation of ATM-dependent HR pathway in RD, but it reduced the ability of RH30 cells to activate the HR pathway (fig. 23). The anti-oxidant cell response was investigated assessing the expression of the key master regulator NRF2 and of its target genes: SOD, CAT and GPx4, 12h after irradiation in RMS cells pretreated or not with MS-275. The presence of the drug significantly blocked the mRNA accumulation of NRF2, SOD, CAT and GPx4 induced by RT (fig. 22. A). These results suggest that MS-275 acts as a radiosensitizer in FP-RMS cells by preferentially impairing the activation of HR-DSBs repair and the anti-oxidant response.

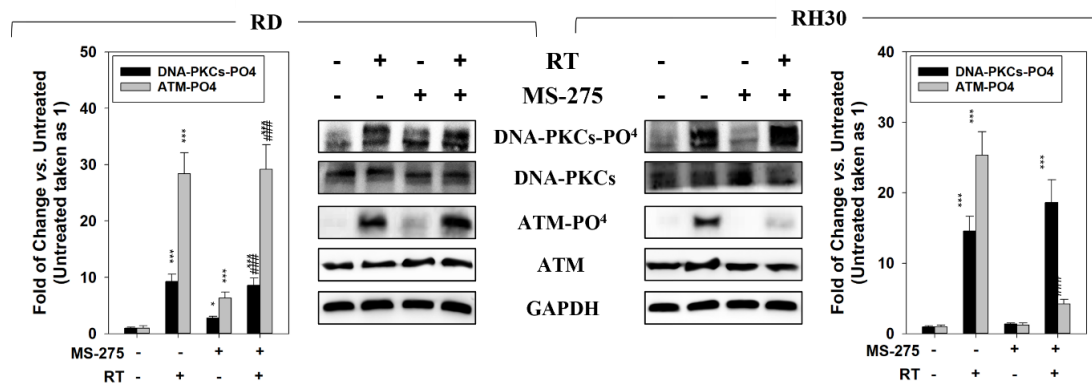


**Fig. 23** MS-275 counteracts the ability of RT to activate the HR-mediated DSBs repair pathway in RH30 and inhibits anti-oxidant molecular response in both RMS cell lines. RD (Left) and RH30 (Right) were treated with MS-275 ( $IC_{50}$ ) and RT (4 Gy) alone or pre-treated (24h) with MS-275 and then irradiated and values of three independent experiments  $\pm$  SD. Histograms are representative of three independent experiments performed in triplicate. Statistical significance: \*\*\* $p \leq 0.001$  vs. Untreated cells; <sup>sss</sup> $p \leq 0.001$  vs. RT; <sup>###</sup> $p \leq 0.001$  vs. MS-275.

## IN VIVO

### 8. *In vivo* radiosensitive effects of HDACis in RMS cell lines

#### 8.1. FK228 radiosensitizes ARMS:

For the *in vivo* experiments, treatment was performed after the animals had received RT and tumor volumes were measured every 5 day for a period of 20 days after the first treatment (fig. 24).

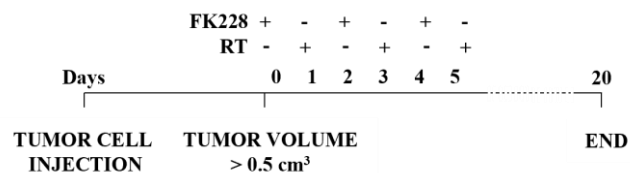


**Fig. 24** Treatment method for *in vivo* experiment.

Combining RT to FK228, the HDACi significantly improved RT therapeutic efficiency in RH30 xenografted mice by  $74.5 \pm 8.3\%$ . According to this result, tumor weights of RH30 xenografts from mice treated with the combination decreased significantly ranging from 75 to 90% reduction compared to controls. No difference in tumor growth and tumor weight was found after treatment with the combination in RD xenografts, as shown in figure 25. A,B. A curious fact is that FK228 as single agent did not reduce the rate of tumor growth both in RD and RH30 xenografted mice. Further, the number of mice showing tumor progression (TP) significantly differed across the groups. In the control group, TP occurred both in RD and RH30 xenografted mice within 5 days after the beginning of treatment. In the RT group, TP started from the 5<sup>th</sup> day and was completed within the 15<sup>th</sup> and 10<sup>th</sup> day after the beginning of treatment in RD and RH30 cells respectively. In the FK228 group, TP occurred within the 5<sup>th</sup> day and was completed within the 10<sup>th</sup> day after the beginning of treatment in both RD

and RH30 cells. When FK228 was combined with RT, TP started from the 5<sup>th</sup> day and was completed within the 15<sup>th</sup> day after the beginning of treatments in RD, while TP started from the 15<sup>th</sup> day and never completed in RH30 cells (fig. 25. C).

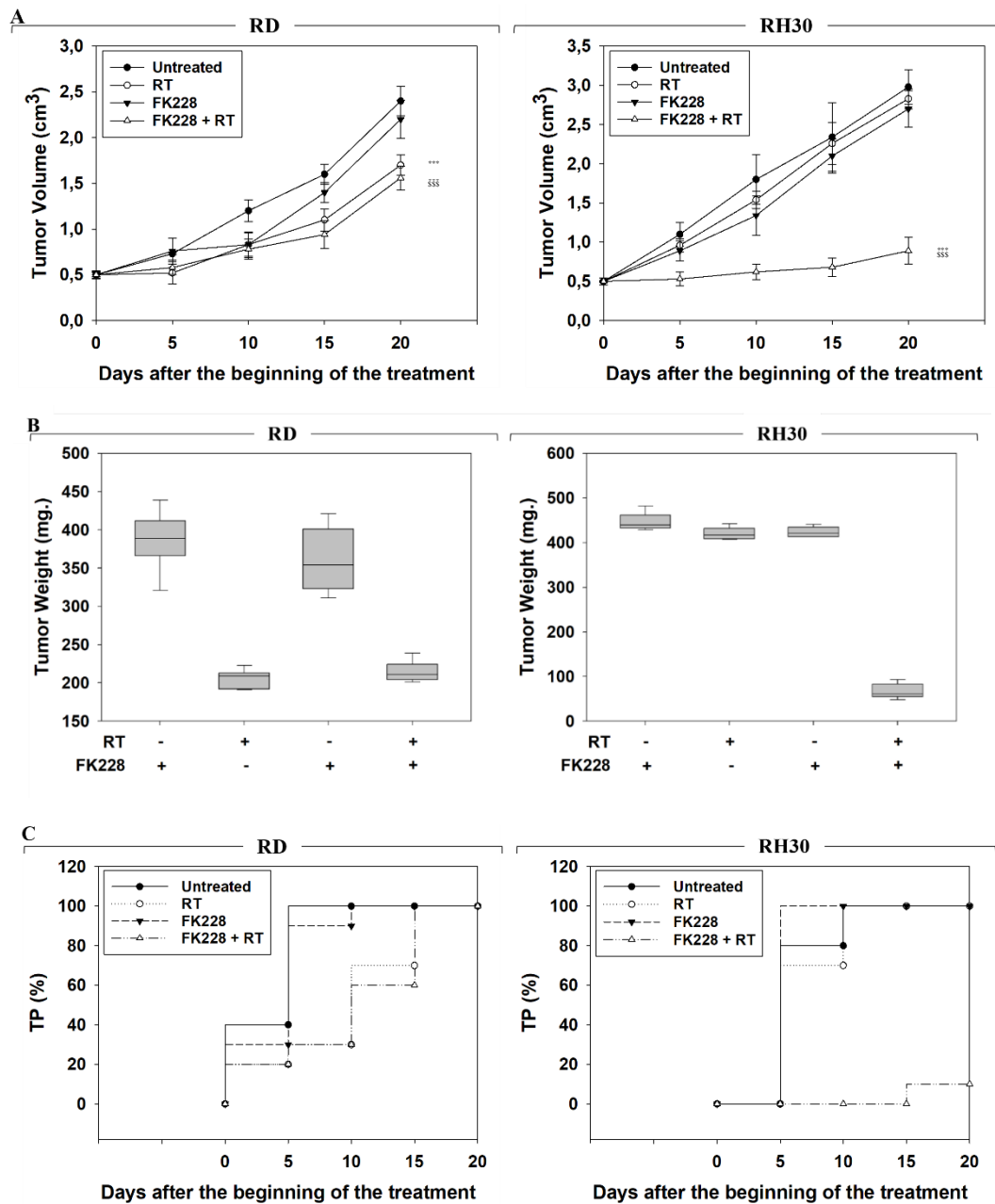


**Fig. 25** Effects of FK228 combined or not with irradiation on in vivo tumor growth.

- A.** Growth curve of tumor volumes from xenografted RD and RH30 cell lines, untreated (Untreated), FK228-treated irradiated (RT), FK228-pretreated and irradiated (RT + FK228). Tumor volumes were evaluated as describes in methods represent the mean  $\pm$  SEM of 10 mice. The panel shows the sequential treatments of xenografted mice started when tumors reached a volume of approximate 50 mm<sup>3</sup>. FK228 (1.2 mg/kg) was administered for before each irradiation, administered on alternate days. Results represent the mean values  $\pm$  SD. Statistical significance: \*\*\* $p \leq 0.001$  vs. untreated mice; <sup>sss</sup> $p \leq 0.001$  vs RT-treated mice.
- B.** Tumor weights in mice untreated or treated with FK228, RT or combined treatment.
- C.** Kaplan-Meier estimates for rates of progression for untreated, FK228, RT, or FK228 + RT combination in RMS-derived tumors.

These results highlight that FK228 efficiently radiosensitizes the RMS subtype *in vivo*.

## 8.2. MS-275 radiosensitizes FP-RMS cells:

*In vivo* experiments were then performed by subcutaneously injecting (s.c.) RMS cells in nude mice. When the tumor volume reached  $\sim 0.5 \text{ cm}^3$  ( $T_0$ ), mice were randomized into 4 groups of 8 animals each: vehicle, MS-275, RT, MS-275+RT. MS-275 as a single agent, 2.5 mg/kg, or vehicle (PBS) were administered intraperitoneally (i.p.) once daily for 5 consecutive days. Mice belonging to RT and MS-275+RT groups were irradiated with the dose of 2 Gy the 1<sup>st</sup>, 3<sup>rd</sup> and 5<sup>th</sup> day one hour after receiving MS-275, for a total dose of 6 Gy, as described in treatment scheme in figure 26. Tumor volumes were measured every 5 days for a period of 20 days after starting of the treatment. Compared to single treatments, combining RT and MS-275 significantly improve the therapeutic efficiency resulting in  $27.7 \pm 7.9\%$  volume reduction in RD and  $75.4 \pm 9.3\%$  in RH30 xenografts compared to RT alone. Comparing it to MS-275 alone, we obtained a reduction of  $43.5 \pm 8.2\%$  in RD and  $47.6 \pm 7.2\%$  in RH30 xenografts (fig. 27. A). Besides that, the combination completely prevented RH30 xenografts growth, while RD xenografts progressively increased over the course of the experiment. Accordingly, also tumor weights decreased significantly thank to the combination, compared to those of untreated and single treatments mice (fig. 27. B). About the TP, in RD the co-treatment xenografted mice, it resulted complete within the 15<sup>th</sup> day after the beginning of treatment. Strikingly, no TP occurred in RH30 xenografted mice with co-treatment, as can be seen in figure 27. C. These evidences indicate the ability of MS-275 to radiosensitize preferentially the FP-RMS subtype.

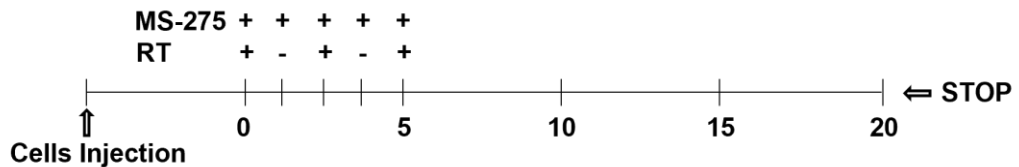
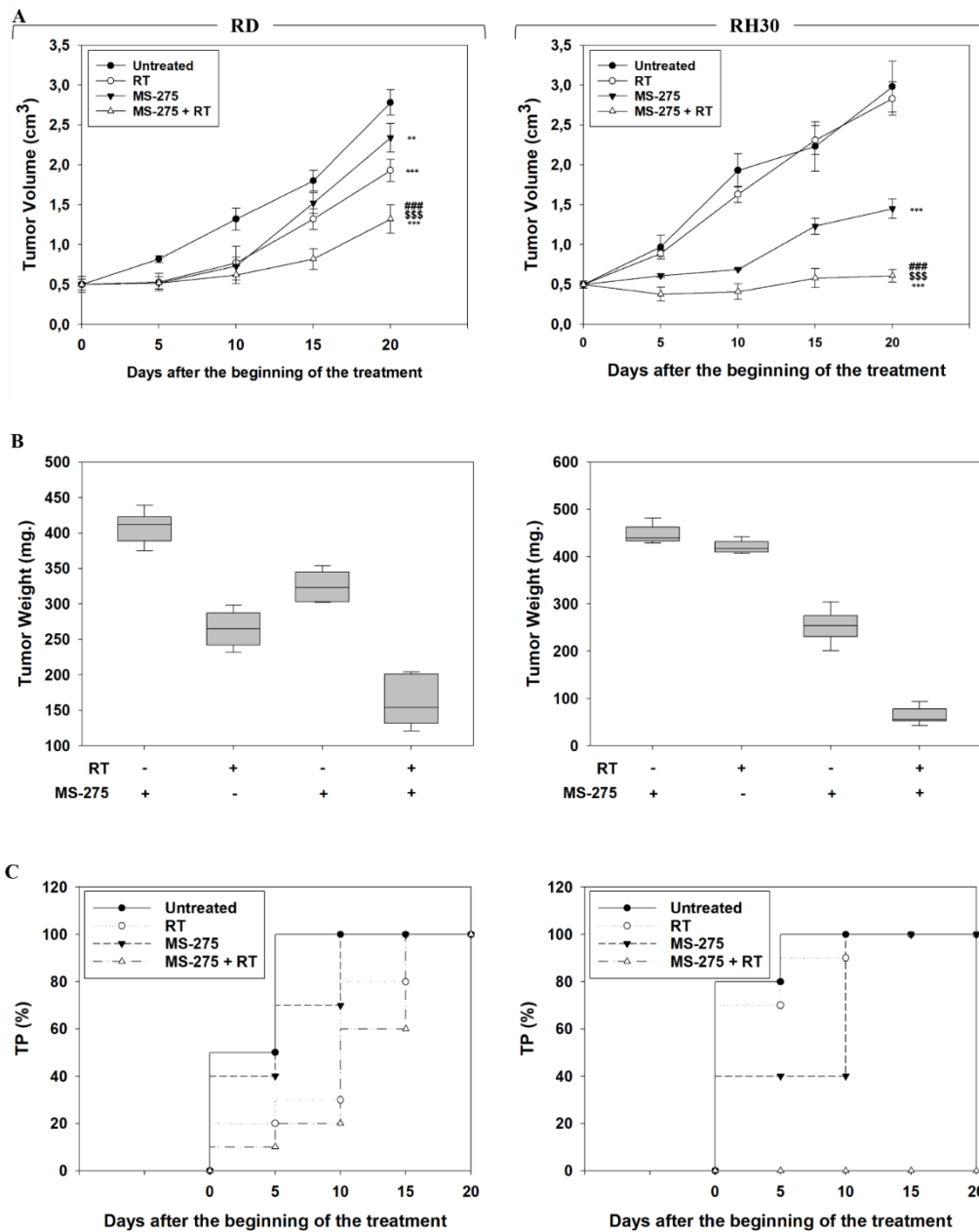


Fig. 26 Treatment method for *in vivo* experiment.



**Fig. 27** Effects of MS-275 combined or not with irradiation on *in vivo* tumor growth.

- A.** Growth curve of tumor volumes from xenografted RD and RH30 cell lines, untreated, MS-275-treated, irradiated (RT), MS-275-pre-treated and irradiated (RT + MS-275). Tumor volumes were evaluated as described in methods and represent the mean  $\pm$  SEM of 8 mice per group. The graphs show the sequential treatments of xenografted mice started when tumors reached a volume of approximately  $0.5 \text{ cm}^3$ . Results represent the mean values  $\pm$  SD. Statistical significance: \*\* $p \leq 0.01$ , \*\*\* $p \leq 0.001$  vs. Untreated mice; \$\$\$ $p \leq 0.001$  vs. RT-treated mice; ### $p \leq 0.001$  vs. MS-275-treated mice.
- B.** Tumor weights mice injected with RD (Left) and RH30 (Right) and treated with MS-275 and RT alone or in combination.
- C.** Kaplan-Meier estimates for rates of progression for untreated, MS-275, RT, or MS-275 + RT combination in RMS-derived tumors.

## DISCUSSIONS

Studies suggest a cytoprotective role for PAX3-FOXO1 against radiation, chemotherapeutics and molecular targeted agents. It was demonstrated that the upregulation of the fusion oncoprotein during the G<sub>2</sub> phase promoted a cell cycle checkpoint adaptation allowing cells to transit from G<sub>2</sub> to mitosis despite DNA damage induced by radiation and chemotherapy<sup>25</sup>. Indeed, genetic knockdown of PAX3-FOXO1 was shown to improve the sensitivity to chemotherapeutics and radiation. In FP-RMS the fusion oncoprotein also interacts with the chromatin-related proteins such as HDACs and have been demonstrated to participate in the oncoprotein-driven epigenetic reprogramming<sup>55</sup>. So we shown that class I HDACs, known to play a key role to drive tumorigenesis in RMS<sup>62</sup>, resulted in global downregulation compared to human normal mesenchymal cells. Indeed, it was identified a transcriptional repressor complex involving the nuclear receptor corepressor (NCOR) and HDAC3 as a major suppressor of both FN- and FP-RMS differentiation<sup>68</sup>. In according, among class I HDACs, the most expressed were HDAC3 in RD and HDAC2 in RH30 cell line, belong to ERMS and ARMS respectively. Therefore, in a context of low general expression of HDAC class I, we assume that HDAC3 in RD and HDAC2 in RH30 could be the most pathogenically important even though a key role cannot be excluded for HDAC1 and HDAC8.

In the present work we investigated about FK228 (Romidepsin) and MS-275 (Entinostat), potent selective inhibitors of class I HDACs<sup>77</sup> and class I and IV HDAC<sup>67</sup> respectively. These HDACis are already approved for the clinical use<sup>70</sup> and herein, we have investigated the therapeutic potential of FK228 in RMS as monotherapy and in combination with RT.

Molecularly targeted and standard cytotoxic drugs often induce concomitant growth arrest and cell death. This double effect depends on tumor heterogeneity, whereby within the same tumor there are subpopulations exhibiting different sensitivity to therapies<sup>91</sup>. In case of FP-RMS the fusion proteins cause a decrease in the expression of p21 and facilitates cancer cell proliferation. Treatment with HDACi Romidepsin induced p21 and prevent the fusions, regulate also the expression of cell-cycle genes such as cyclin D1, Cdk4, and Cdk6 inducing cell-cycle arrest in actively or abnormally proliferating cancer cells<sup>92</sup>.

Using low concentrations of FK228, we obtained a reduction of the cell viability and an affect in RMS proliferation and, as showed by washout experiments, the growth arrest that was reversible for both RD and RH30 cells. About this reversibility, we hypothesized that while FK228 efficiently killed a subpopulation of sensitive RMS, surviving cells could activate molecular mechanisms of resistance to HDACi, has already been described for other tumor types<sup>93</sup>. The presence of the drug FK228 induced non-apoptotic cell death. RMS cells upregulated the expression of Bcl-2 and Bcl-XL, negative controllers of apoptotic cell death, and the drug activated PARP1 signaling, known to mediate non-apoptotic cell death. These evidences suggest that FK228 could trigger PARP1-mediated

non-apoptotic cell death in sensitive cells while surviving cells counteract the apoptotic stimulus upregulating Bcl-2 and Bcl-XL, as already described in other cell lines<sup>94</sup>.

Potential mechanisms of resistance to FK228 could be the early and stable upregulation of cell cycle positive regulators cyclin-A, -B, -D1, c-Myc and N-Myc, as well as of the cyclin-dependent kinase inhibitor p27, which was associated to the lack of changes in cell cycle distribution of RMS cells. The upregulation of cyclins and Myc family members has been shown to promote chemoresistance whilst the upregulation of p27, potentially triggered by Bcl-XL and Bcl-2, could be required to maintain a proliferative quiescence status and/or sustain chemoresistance<sup>95</sup>. Even the downregulation of class I HDACs induced by FK228 and its overexpression after the drug washout, could be strategies to acquire a more aggressive/chemoresistant phenotype<sup>93</sup>. Therefore, RMS seems to have multiple strategies capable of counteracting the potential cytotoxic action of FK228.

About MS-275, it was demonstrated that also Entinostat can act as PAX3-FOXO1 modulator, because of its coregulators such as HDAC1 and HDAC2. The drug was able to reduce the fusion oncoprotein expression and to reduce tumor growth<sup>96</sup>. Accordingly, MS-275 induced growth arrest, that W/O experiments showed to be irreversible in FP-RMS RH30 cell line. The drug led a drastic modification on cell cycle distribution, the treated cells rapidly arrested in the G<sub>1</sub> phase and continued to die after W/O. FN-RMS did not undergo major changes in cell cycle distribution but exhibited similar changes at the molecular level. MS-275 downregulated the expression of cell cycle positive regulators: Cyclin-A, -B, D1 and upregulated the expression of the cyclin-dependent kinase inhibitors: p21 and p27 in both RMS cell subtypes. Furthermore, it downmodulated the activation of MEKs/ERKs in RD and AKTs in RH30, which have been respectively shown to be among the key-master regulator signaling of FN- and FP-RMS<sup>97</sup>. The distinct RH30 cells response to MS-275 compared to FK228 could be related to a difference at the molecular level: the strong decrease of N-Myc levels<sup>96</sup>. N-Myc is, indeed, one of the key core regulatory transcription factors (CR TFs) crucial for the maintenance of the FP-RMS tumorigenic phenotype, whose lack determines the concomitant downregulation of all the other CR TFs and the death of cancer cells<sup>97</sup>. Also in RD cell line, MS-275 is able to hit proliferation regulatory pathways leading to a marked reduction of c-Myc, an oncogene down-stream to the RAS pathway mutated in this cell line<sup>98</sup>. However, this modulation affected mildly the survival of RD cells, which still retained their ability to form growing colonies. This aspect deserves to be clarified in future studies to define whether the RAS pathway remains partially active under drug treatment. Entinostat was also shown to counteract cell migration/invasion and stemness and to induce a transient induction of myogenic differentiation<sup>85</sup>.

About cell death, also MS-275 induced necrosis potentially mediated by the activation of PARP1. Indeed, as happening for the FK228, both surviving FP-RMS and FN-RMS cells upregulated the expression of Bcl-2 and Bcl-XL. Here this mechanism was not sufficient to prevent FP-RMS RH30



cell death but could be strategic for FN-RMS RD cells to counteract the cytotoxic potential of HDAC inhibition and, therefore, could represent a potential further target for future investigation on HDACi-based combination approaches.

Moreover, HDACi promotes cancer cell death also by inducing ROS accumulation and consequent DSBs<sup>99</sup>. In agreement, FK228 induced ROS accumulation and  $\gamma$ H2AX (a marker for DSBs) upregulation in RMS cells. Accordingly, also MS-275 increased the accumulation of ROS in both cell lines and upregulated the phosphorylation of H2AX. The major problem about this pathway seems to be the efficient activation, by RMS cells, of ROS detoxifying mechanisms and pro-surviving signals such as PI3K-AKT-mTOR and MAPK pathways<sup>100</sup>. Thus, as shown for other cancer types<sup>64-65</sup>, combining PI3K or MAPKs inhibitors could be a strategy to overcome FK228/MS-275 resistance. From here the decision to combining the HDACis with RT and to observe their radiosensitizing ability.

RT kills cancer cells by inducing, directly or indirectly, DSBs through ROS accumulation<sup>101</sup>. Combining FK228 with RT more efficiently increased ROS accumulation compared to RT alone. However, while RD cells hyper-activated the transcription of NRF2 and CAT antioxidant genes and the activation of the DNA damage response (DDR), RH30 cells failed to do so and showed radiosensitization. Notably, FK228 did not affect the ability of irradiated RD and RH30 cells to activate the pathways that sustain RMS radioresistance. The ability of FK228 to radiosensitize ARMS, but not ERMS, was also confirmed *in vivo*. Combining FK228 and RT, more effectively than single agents, reduced tumor volume and weight and prevented the progression of tumors in RH30 xenografted mice. Also MS-275 combined with RT, compared to single treatments, drastically impaired the clonogenic survival of FP-RMS but not FN-RMS cells, even though significantly increased  $\gamma$ H2AX in both. The agent drastically increased the ROS production and accumulation induced by RT, counteracted the ability of cells to detoxify from oxidative stress and enhancing their RT-dependent accumulation in the G<sub>2</sub> phase of the cell cycle. The presence of the drug restrained the ability of RMS cells to upregulate the expression of NRF2 and of its related downstream targets CAD, SOD and GPx4, mediators of the antioxidant response, usually activated by ionizing radiation and responsible for radioresistance<sup>92</sup>. Notably, MS-275 counteracted the expression of the entire RT-induced molecular antioxidant axis in both cell lines, differently from FK228. This finding suggests that FP-RMS cells have radioresistance mechanisms independent from the ROS detoxification mechanisms<sup>102</sup>, an aspect that deserves further investigations.

In line with our findings, also other recent reports pointed out the *in vitro* and *in vivo* efficacy of Entinostat and Romidepsin as radiosensitizers in FP-RMS models. This HDACi property was related to the ability to promote a high and persistent ROS production, to impair DNA repair and radiation-induced ROS detoxifying mechanisms<sup>92;96</sup>. In addition, a transient downregulation of the class I and

IV HDACs has been suggested to participate in entinostat and romidepsin radio-sensitizing activities. One possible reason for the no one type of effect in ERMS by FK228 could be the inability of the drug to inhibit HDAC3. Indeed, the drug has been shown to inhibit HDAC1, HDAC2 and HDAC8 but no data have still been shown for HDAC3. Therefore, considering that HDAC3 is the most represented class I HDAC in ERMS, where it plays a crucial anti-differentiation oncogenic role, its non- or very low inhibition by FK228 could explain the failure of treatment in this RMS subtype. Furthermore, in combination with RT, the agent triggered DNA-PKCs activation, which is known to phosphorylate/activate HDAC3<sup>103</sup>. Thus, this drug could promote the activation of a loop that could support the uncontrolled activation of HDAC3 in ERMS cells.

Instead, about MS-275, it probably was not able to radio-sensitize ERMS subtype because of the activation of NHEJ pathway of DDR. We found that the drug counteracted RT-induced activation of HR signaling in FP-RMS cells but did not affect DNA-PKCs activation in both the subtypes. Therefore, the inability of MS-275 to radio-sensitize RMS cells seems to depend on its ability to counteract the full activation of both NHEJ and HR DSBs repair pathways induced by RT. On the other hand, RH30 radio-sensitization appears to be related to the ability of MS-275 to prevent activation of the HR pathway, known to be the most important repair pathway and the last resource for DSBs repair. Indeed, HR has been shown to play a key role to repair a wide variety of toxic lesions caused by many anticancer treatments, so its inactivation result in an increased sensitivity to anticancer treatments<sup>99</sup>. Interestingly, in FP-RMS, HR activation resulted counteracted by MS275 at least until six hours after irradiation, time interval commonly known to be sufficient for DNA repair in normal but not in cancer cells<sup>104</sup>. So, six hours represent the minimum time in which surviving neoplastic cells can be more easily killed by subsequent irradiation<sup>58</sup>. Thus the MS-275 would favor the radio-sensitization to subsequent fractions of RT.

The ability of MS-275 to radio-sensitize FP-RMS was also confirmed *in vivo* by using RMS xenograft models. Pre-treating mice with MS-275 before RT completely prevent tumor growth as well as tumor progression in RH30 xenografted mice. This result could have a great impact also considering that RH30 cells *in vivo* are completely unresponsive to RT and modestly respond to MS-275. Notably, contrary to *in vitro* data, the drug radio-sensitized FN-RMS *in vivo* even if the tumor masses only slowed their growth rate, continuing to grow over time. A possible explanation for this discrepancy between *in vitro* and *in vivo* data could be given by the radiobiological concept of redistribution, which characterizes the functioning of the dose<sup>105</sup>. It has been shown that cells arrested in G<sub>2</sub> are more radiosensitive and consecutive fractions of RT, each of which can induce arrest in G<sub>2</sub>, can thus be progressively more and more effective. Here, the pre-treatment with MS-275 increased the percentage of the cells in G<sub>2</sub> making them more sensitive to the subsequent RT fractions. Further, other mechanisms could be involved in the *in vivo* response of FN-RMS cells, such as the ability of HDACi

to inhibit angiogenesis or tumor microenvironment<sup>106</sup>. Future experiments are needed to better understand the *in vivo* effects of MS-275 in FN-RMS in order to identify further strategies that definitively radio-sensitize this tumor subtype.

Finally, it cannot be excluded that the remarkable radio-sensitizing effects of MS-275 especially on FP-RMS RH30 cells, could be, at least in part, related to the blockade of the only representative of class IV HDAC inhibited by the drug as HDAC11. This could be in line with the aberrant expression of this class of HDACs in this RMS subtype<sup>107</sup>. These findings mean that HDAC11 could be a rising star in epigenetics and potential therapeutic target for cancer treatment. However, this hypothesis needs to be exploited in the future.

## CONCLUSIONS

Rhabdomyosarcoma is the most common soft tissue sarcoma in children/adolescents less than 18 years of age, with an annual incidence of 1-2/million. Multidisciplinary care and multimodal therapies, such as surgery, chemotherapy and/or radiotherapy represent currently the gold standard to treat RMS but resistance to treatments often determines failure and poor survival. With the development and refinement of multimodal treatments regimes, survival has improved substantially for many children with RMS. However, the survival of those diagnosed with widely metastatic or relapsed disease continues to be very low, so functional approaches and new molecular targets will be needed to further improve the outcome of this disease. According to the literature, RMS is characterized by an aberrant epigenetic regulation. So, in this study we have been the purpose to targeting this mechanism throughout the use of HDACi, that are successfully used as single agents in some cancer types, and observed their antitumoral effects in *in vitro* and *in vivo* models.

Herein, class I HDACi, FK228, monotherapy showed limited effects in treating RMS as single agent, but its combination with RT resulted in radiosensitization of ARMS, that is FP-RMS cells. Instead, targeting class IV HDAC, as HDAC11, could be a better strategy, seeing the effects of MS-275 on cell growth of FP-RMS cell line. Indeed, increasing evidence indicates HDAC11 as a rising star in epigenetics and potential therapeutic target for cancer treatment. Likely FK228 and also MS-275 showed excellent results if it is combined with RT especially on FP-RMS RH30 cells. Therefore, these results suggest that targeting class I and IV HDACs could be a potential combination-based therapeutic strategy to treat and radiosensitize FP-RMS, the intrinsically radio-resistant and most aggressive type of RMS.

However, deeper studies are needed to clarify the potential of combined HDACi and RT in cancer, since it has been recently reported that adaptation mechanism to radiation leading to radioresistance can be caused by pan-HDAC inhibition.

## BIBLIOGRAPHY

1. V. Damerell, M.S. Pepper, S. Prince, Molecular mechanisms underpinning sarcomas and implications for current and future therapy, *Signal Transduct. Target Ther.* 26 (1) (2021) 246–265, <https://doi.org/10.1038/s41392-021-00647-8>.
2. Taylor BS, Barretina J, Maki RG, Antonescu CR, Singer S, Ladanyi M. Advances in sarcoma genomics and new therapeutic targets. *Nature reviews Cancer* 2011 8;11(8):541–57.
3. J.A. Perry, B.K.A. Seong, K. Stegmaier, Biology and therapy of dominant fusion oncoproteins involving transcription factor and chromatin regulators in sarcomas, *Ann. Rev. Cancer Biol.* 3 (1) (2019) 299–321.
4. Barr FG. Gene fusions involving PAX and FOX family members in alveolar rhabdomyosarcoma. *Oncogene* 2001 9 10;20(40):5736–46. [PubMed: 11607823]
5. S.X. Skapek, A. Ferrari, A.A. Gupta, P.J. Lupo, E. Butler, J. Shipley, F.G. Barr, D. S. Hawkins, Rhabdomyosarcoma, *Nat. Rev. Dis. Primers* 5 (1) (2019), <https://doi.org/10.1038/s41572-018-0051-2>.
6. Mary E. Olanich, Frederic G. Barr A CALL TO ARMS: TARGETING THE PAX3-FOXO1 GENE IN ALVEOLAR RHABDOMYOSARCOMA *Expert Opin Ther Targets.* 2013 May ; 17(5): 607–623. doi:10.1517/14728222.2013.772136.
7. Simone Hettmer, Corinne M. Linardic, Anna Kelsey, Erin R. Rudzinski, Christian Vokuhl, Joanna Selfe, Olivia Ruhen, Jack F. Shern, Javed Khan, Alexander R. Kovach, Philip J. Lupo, Susanne A. Gatz, Beat W. Schäfer, Samuel Volchenbourn, Véronique Minard-Colin, Ewa Koscielniak, Douglas S. Hawkins, Gianni Bisogno, Monika Sparber-Sauer, Rajkumar Venkatramani, Johannes H.M. Merks, Janet Shipley. Molecular testing of rhabdomyosarcoma in clinical trials to improve risk stratification and outcome: A consensus view from European paediatric Soft tissue sarcoma Study Group, Children’s Oncology Group and Cooperative Weichteilsarkom-Studiengruppe. *European Journal of Cancer* 172 (2022) 367e386
8. Andrea Stuart and Jayant Radhakrishnan. Rhabdomyosarcoma. [*Indian J Pediatr* 2084; 71 (4) : 331-337]
9. Rudzinski E.R., Anderson J.R., Hawkins D.S., Skapek S.X., Parham D.M., Teot L.A. The World Health organization classification of skeletal muscle tumors in pediatric rhabdomyosarcoma: a report from the children's oncology group. *Arch Pathol Lab Med.* 2015; 139: 1281-1287Cinzia Lanzi, Giuliana Cassinelli. Combinatorial strategies to potentiate the efficacy of HDAC inhibitors in fusion-positive sarcomas. *Biochemical Pharmacology* 198 (2022) 114944.
10. De Giovanni C, Landuzzi L, Nicoletti G, Lollini PL, Nanni P. Molecular and cellular biology of rhabdomyosarcoma. *Future Oncol* 2009 11;5(9):1449–75. [PubMed: 19903072]
11. Shern J.F., Chen L., Chmielecki J., Wei J.S., Patidar R., Rosenberg M., Ambrogio L., Auclair D., Wang J., Song Y.K., Tolman C., Hurd L., Liao H., Zhang S., Bogen D., Brohl A.S., Sindiri S., Catchpoole D., Badgett T., Getz G., Mora J., Anderson J.R., Skapek S.X., Barr F.G., Meyerson M., Hawkins D.S., Khan J. Comprehensive genomic analysis of rhabdomyosarcoma reveals a landscape of alterations affecting

- a common genetic axis in fusion-positive and fusion-negative tumors. *Cancer Discov.* 2014; 4: 216-231
12. S. Ognjanovic, A.M. Linabery, B. Charbonneau, J.A. Ross Trends in childhood rhabdomyosarcoma incidence and survival in the United States, 1975-2005 *Cancer*, 115 (2009), pp. 4218-4226
  13. Camero S, Cassandri M, Pomella S, Milazzo L, Vulcano F, Porrizzo A, Barillari G, Marchese C, Codenotti S, Tomaciello M, Rota R, Fanzani A, Megiorni F and Marampon F (2022) Radioresistance in rhabdomyosarcomas: Much more than a question of dose. *Front. Oncol.* 12:1016894. doi: 10.3389/fonc.2022.1016894
  14. Shern JF, Chen L, Chmielecki J, et al. , Comprehensive genomic analysis of rhabdomyosarcoma reveals a landscape of alterations affecting a common genetic axis in fusion-positive and fusion-negative tumors. *Cancer Discov*, 2014. 4(2): p. 216–31. [PubMed: 24436047]
  15. Sia J, Szmyd R, Hau E, Gee HE. Molecular mechanisms of radiation-induced Cancer cell death: a primer. *Front Cell Dev Biol.* 2020;13:41.
  16. Francesco Petragano, Ilaria Pietrantonì, Simona Camero, Silvia Codenotti, Luisa Milazzo, Francesca Vulcano, Giampiero Macioce, Ilenia Giordani, Paolo Tini, Sara Cheleschi, Giovanni Luca Gravina, Claudio Festuccia, Alessandra Rossetti, Simona Delle Monache, Alessandra Ordinelli, Carmela Ciccarelli, Annunziata Mauro, Barboni Barbara, Cristina Antinozzi, Amalia Schiavetti, Roberto Maggio, Luigi Di Luigi, Antonella Polimeni, Cinzia Marchese, Vincenzo Tombolini, Alessandro Fanzani, Nicola Bernabò, Francesca Megiorni and Francesco Marampon. Clinically relevant radioresistant rhabdomyosarcoma cell lines: functional, molecular and immune-related characterization. Clinically relevant radioresistant rhabdomyosarcoma cell lines: functional, molecular and immune-related characterization. *Journal of Biomedical Science* (2020) 27:90
  17. Li H., Sisoudiya S.D., Martin-Giacalone B.A., Khayat M.M., Dugan-Perez S., Marquez-Do D.A., Scheurer M.E., Muzny D., Boerwinkle E., Gibbs R.A., Chi Y.Y., Barkauskas D.A., Lo T., Hall D., Stewart D.R., Schiffman J.D., Skapek S.X., Hawkins D.S., Plon S.E., Sabo A., Lupo P.J. Germline cancer predisposition variants in pediatric rhabdomyosarcoma: a report from the children's oncology group. *J Natl Cancer Inst.* 2021; 113: 875-883
  18. Narasimhan P. Agaram, M.B.B.S. Evolving Classification of Rhabdomyosarcoma. *Histopathology.* 2022 January ; 80(1): 98–108. doi:10.1111/his.14449.
  19. Skapek S.X., Anderson J., Barr F.G., Bridge J.A., Gastier-Foster J.M., Parham D.M., Rudzinski E.R., Triche T., Hawkins D.S. PAX-FOXO1 fusion status drives unfavorable outcome for children with rhabdomyosarcoma: a children's oncology group report. *Pediatr Blood Cancer.* 2013; 60: 1411-1417
  20. Williamson D, Missiaglia E, de Reynies A, Pierron G, Thuille B, Palenzuela G, et al. Fusion gene negative alveolar rhabdomyosarcoma is clinically and molecularly indistinguishable from embryonal rhabdomyosarcoma. *Journal of clinical oncology: official journal of the American Society of Clinical Oncology* 2010 5 1;28(13):2151–8. [PubMed: 20351326]

21. D.E. El Demellawy, J. McGowan-Jordan, J. de Nanassy, E. Chernetsova, A. Nasr, Update on molecular findings in rhabdomyosarcoma, *Pathology* 49 (3) (2017) 238–246, <https://doi.org/10.1016/j.pathol.2016.12.345>.
22. Heske C.M., Chi Y.Y., Venkatramani R., Li M., Arnold M.A., Dasgupta R., Hiniker S.M., Hawkins D.S., Mascarenhas L. Survival outcomes of patients with localized FOXO1 fusion-positive rhabdomyosarcoma treated on recent clinical trials: a report from the Soft Tissue Sarcoma Committee of the Children's Oncology Group. *Cancer*. 2021; 127: 946-956
23. M. Buckingham, F. Relaix, PAX3 and PAX7 as upstream regulators of myogenesis, *Semin. Cell Dev. Biol.* 44 (2015) 115–125, <https://doi.org/10.1016/j.semcdb.2015.09.017>.
24. A. Coomans de Brach`ene, J.B. Demoulin, FOXO transcription factors in cancer development and therapy, *Cell. Mol. Life Sci.* 73 (6) (2016) 1159–1172, <https://doi.org/10.1007/s00018-015-2112-y>.
25. M. Wachtel, B.W. Sch` afer, PAX3-FOXO1: Zooming in on an “undruggable” target, *Semin. Cancer Biol.* 50 (2018) 115–123, <https://doi.org/10.1016/j.semcancer.2017.11.006>.
26. K. Kikuchi, S. Hettmer, M.I. Aslam, J.E. Michalek, W. Laub, B.A. Wilky et al., Cell-cycle dependent expression of a translocation-mediated fusion oncogene mediates checkpoint adaptation in rhabdomyosarcoma, *PLoS Genet.* 10 (1) (2014) e1004107, doi: 10.1371/journal.pgen.1004107.
27. A.D. Marshall, G.C. Grosveld, Alveolar rhabdomyosarcoma - the molecular drivers of PAX3/7-FOXO1-induced tumorigenesis, *Skelet Muscle.* 2 (1) (2012) 25, <https://doi.org/10.1186/2044-5040-2-25>.
28. Shern JF, Selfe J, Izquierdo E, et al. , Genomic Classification and Clinical Outcome in Rhabdomyosarcoma: A Report From an International Consortium. *J Clin Oncol*, 2021: p. JCO2003060.
29. Williamson D., Lu Y.J., Gordon T., Sciot R., Kelsey A., Fisher C., Poremba C., Anderson J., Pritchard-Jones K., Shipley J. Relationship between MYCN copy number and expression in rhabdomyosarcomas and correlation with adverse prognosis in the alveolar subtype. *J Clin Oncol.* 2005; 23: 880-888
30. P.R. Pandey, B. Chatterjee, M.E. Olanich, J. Khan, M.M. Miettinen, S.M. Hewitt, et al., PAX3-FOXO1 is essential for tumour initiation and maintenance but not recurrence in a human myoblast model of rhabdomyosarcoma, *J. Pathol.* 241 (5) (2017) 626–637, <https://doi.org/10.1002/path.4867>.
31. Dietz KN, Miller PJ, Iyengar AS, Loupe JM, Hollenbach AD. Identification of serines 201 and 209 as sites of Pax3 phosphorylation and the altered phosphorylation status of Pax3-FOXO1 during early myogenic differentiation. *Int J Biochem Cell Biol* 2011 6;43(6):936–45. [PubMed: 21440083]
32. Linardic CM. PAX3-FOXO1 fusion gene in rhabdomyosarcoma. *Cancer Lett* 2008 10 18;270(1): 10–8. [PubMed: 18457914]
33. Liu L., Wu J., Ong S.S., Chen T. Cyclin-dependent kinase 4 phosphorylates and positively regulates PAX3-FOXO1 in human alveolar rhabdomyosarcoma cells. *PLoS One.* 2013; 8: e58193
34. Gryder B.E., Yohe M.E., Chou H.C., Zhang X., Marques J., Wachtel M., Schaefer B., Sen N., Song Y., Gualtieri A., Pomella S., Rota R., Cleveland A., Wen X., Sindiri S., Wei J.S., Barr F.G., Das S., Andresson T., Guha R., Lal-Nag M., Ferrer M., Shern J.F., Zhao K., Thomas C.J., Khan J. PAX3-FOXO1 establishes

- myogenic super enhancers and confers BET bromodomain vulnerability. *Cancer Discov.* 2017; 7: 884-899
35. Dyson K.A., Stover B.D., Grippin A., Mendez-Gomez H.R., Lagmay J., Mitchell D.A., Sayour E.J. Emerging trends in immunotherapy for pediatric sarcomas. *J Hematol Oncol.* 2019; 12: 78
36. Sultan I, Qaddoumi I, Yaser S, et al. , Comparing adult and pediatric rhabdomyosarcoma in the surveillance, epidemiology and end results program, 1973 to 2005: an analysis of 2,600 patients. *J Clin Oncol.* 2009. 27(20): p. 3391–7. [PubMed: 19398574]
37. Anke E.M. van Erp, Yvonne M.H. Versleijen-Jonkers, Winette T.A. van der Graaf, and Emmy D.G. Fleuren. Targeted Therapy–based Combination Treatment in Rhabdomyosarcoma. *Mol Cancer Ther;* 17(7) July 2018
38. Seki M., Nishimura R., Yoshida K., Shimamura T., Shiraishi Y., Sato Y., Kato M., Chiba K., Tanaka H., Hoshino N., Nagae G., Shiozawa Y., Okuno Y., Hosoi H., Tanaka Y., Okita H., Miyachi M., Souzaki R., Taguchi T., Koh K., Hanada R., Kato K., Nomura Y., Akiyama M., Oka A., Igarashi T., Miyano S., Aburatani H., Hayashi Y., Ogawa S., Takita J. Integrated genetic and epigenetic analysis defines novel molecular subgroups in rhabdomyosarcoma. *Nat Commun.* 2015; 6: 7557
39. Renshaw J., Taylor K.R., Bishop R., Valenti M., De Haven Brandon A., Gowan S., Eccles S.A., Ruddle R.R., Johnson L.D., Raynaud F.I., Selfe J.L., Thway K., Pietsch T., Pearson A.D., Shipley J. Dual blockade of the PI3K/AKT/mTOR (AZD8055) and RAS/MEK/ERK (AZD6244) pathways synergistically inhibits rhabdomyosarcoma cell growth in vitro and in vivo. *Clin Cancer Res.* 2013; 19: 5940-5951
40. Rong Fan, MD; David M. Parham, MD; Larry L. Wang, MD, PhD. An Integrative Morphologic and Molecular Approach for Diagnosis and Subclassification of Rhabdomyosarcoma. *Arch Pathol Lab Med—Vol 146, August 2022*
41. Simona Camero, Lucrezia Camicia, Francesco Marampon, Simona Ceccarelli, Rajeev Shukla, Olga Mannarino, Barry Pizer, Amalia Schiavetti, Antonio Pizzuti, Vincenzo Tombolini, Cinzia Marchese, Carlo Dominicia, Francesca Megiornic. BET inhibition therapy counteracts cancer cell survival, clonogenic potential and radioresistance mechanisms in rhabdomyosarcoma cells. *Cancer Letters* 479 (2020) 71–88
42. Schulz A, Meyer F, Dubrovska A, Borgmann K. Cancer stem cells and radioresistance: DNA repair and beyond. *Cancers (Basel).* 2019;11:E862.
43. Rossetti A., Petragano F., Milazzo L. , Vulcano F., Macioce G., Codenotti G., Cassandri M., Pomella S., Cicchetti F., Fasciani I., Antinozzi C., Di Luigi L., Festuccia C., De Felice F., Vergine M., Fanzani A., Rota R., Maggio R., Polimeni A., Tombolini V., Gravina G.L., and Marampon F. Romidepsin (FK228) fails in counteracting the transformed phenotype of rhabdomyosarcoma cells but efficiently radiosensitizes, in vitro and in vivo, the alveolar phenotype subtype. *INTERNATIONAL JOURNAL OF RADIATION BIOLOGY* 2021, VOL. 97, NO. 7, 943–957  
<https://doi.org/10.1080/09553002.2021.1928786>



44. Pomella, S.; Porrazzo, A.; Cassandri, M.; Camero, S.; Codenotti, S.; Milazzo, L.; Vulcano, F.; Barillari, G.; Cenci, G.; Marchese, C.; et al. Translational Implications for Radiosensitizing Strategies in Rhabdomyosarcoma. *Int. J. Mol. Sci.* 2022, 23, 13281. <https://doi.org/10.3390/ijms232113281>
45. Huang R-X, Zhou P-K. DNA Damage response signaling pathways and targets for radiotherapy sensitization in cancer. *Signal Transduct Target Ther* (2020) 5:60. doi: 10.1038/s41392-020-0150-x
46. Mladenov E, Magin S, Soni A, Iliakis G. DNA Double-strand break repair as determinant of cellular radiosensitivity to killing and target in radiation therapy. *Front Oncol* (2013) 3:113. doi: 10.3389/fonc.2013.00113
47. Francesco Marampon, Silvia Codenotti, Francesca Megiorni, Andrea Del Fattore, Simona Camero, Giovanni Luca Gravina, Claudio Festuccia, Daniela Musio, Francesca De Felice, Valerio Nardone, Anna Natalizia Santoro, Carlo Dominici, Alessandro Fanzani, Luigi Pirtoli, Antonella Fioravanti, Vincenzo Tombolini, Sara Cheleschi, Paolo Tini. NRF2 orchestrates the redox regulation induced by radiation therapy, sustaining embryonal and alveolar rhabdomyosarcoma cells radioresistance. *Journal of Cancer Research and Clinical Oncology* (2019) 145:881–893
48. S. Codenotti, F. Faggi, R. Ronca, P. Chiodeli, E. Grillo, M. Guescini, F. Megiorni, F. Marampon, A. Fanzani, Caveolin-1 enhances metastasis formation in a human model of embryonal rhabdomyosarcoma through Erk signaling cooperation, *Cancer Letters*, <https://doi.org/10.1016/j.canlet.2019.02.013>.
49. Camero S, Ceccarelli S, de Felice F, Marampon F, Mannarino O, Camicia L, et al. PARP inhibitors affect growth, survival and radiation susceptibility of human alveolar and embryonal rhabdomyosarcoma cell lines. *J Cancer Res Clin Oncol* (2019) 145:137–52. doi: 10.1007/s00432-018-2774-6
50. Marampon F, Gravina GL, di Rocco A, Bonfili P, di Staso M, Fardella C, et al. MEK/ERK inhibitor U0126 increases the radiosensitivity of rhabdomyosarcoma cells In vitro and In vivo by downregulating growth and DNA repair signals. *Mol Cancer Ther* (2011) 10:159–68. doi: 10.1158/1535-7163.MCT-10-0631
51. Pajonk F, Vlashi E, McBride WH. Radiation resistance of cancer stem cells: The 4 r's of radiobiology revisited. *Stem Cells* (2010) 28:639–48. doi: 10.1002/stem.318
52. Perrone C, Pomella S, Cassandri M, Pezzella M, Milano GM, Colletti M, et al. MET inhibition sensitizes rhabdomyosarcoma cells to NOTCH signaling suppression. *Front Oncol* (2022) 12:835642. doi: 10.3389/fonc.2022.835642
53. Garcia-Guede A, Vera O, Ibáñez-de-Caceres I. When oxidative stress meets epigenetics: Implications in cancer development. *Antioxidants* (2020) 9:468. doi: 10.3390/antiox9060468
54. Marampon F, di Nisio V, Pietrantonio I, Petragliano F, Fasciani I, Scicchitano BM, et al. Pro-differentiating and radiosensitizing effects of inhibiting HDACs by PXD-101 (Belinostat) in in vitro and in vivo models of human rhabdomyosarcoma cell lines. *Cancer Lett* (2019) 461:90–101. doi: 10.1016/j.canlet.2019.07.009
55. Kim J-G, Park M-T, Heo K, Yang K-M, Yi J. Epigenetics meets radiation biology as a new approach in cancer treatment. *Int J Mol Sci* (2013) 14:15059–73. doi: 10.3390/ijms140715059

56. B.A. Nacev, K.B. Jones, A.M. Intlekofer, J.S.E. Yu, C.D. Allis, W.D. Tap, M. Ladanyi, T.O. Nielsen, The epigenomics of sarcoma, *Nat. Rev. Cancer* 20 (10) (2020) 608–623, <https://doi.org/10.1038/s41568-020-0288-4>
57. Chunlong Zhao, Hang Dong, Qifu Xu & Yingjie Zhang (2020): Histone deacetylase (HDAC) inhibitors in cancer: a patent review (2017-present), *Expert Opinion on Therapeutic Patents*, DOI: 10.1080/13543776.2020.1725470
58. Y. Liu, M. Yang, J. Luo and H. Zhou (2020) Radiotherapy targeting cancer stem cells “awakens” them to induce tumour relapse and metastasis in oral cancer. *International Journal of Oral Science*, 12:19; <https://doi.org/10.1038/s41368-020-00087-0>
59. M. Janaki Ramaiah, Anjana Devi Tangutur, Rajasekhar Reddy Manyam. Epigenetic modulation and understanding of HDAC inhibitors in cancer therapy. *Life Sciences* 277 (2021) 119504
60. Y. Li, E. Seto, HDACs and HDAC inhibitors in cancer development and therapy, *Cold Spring Harb. Perspect. Med.* 6 (10) (2016) a026831, <https://doi.org/10.1101/cshperspect.a026831>.
61. Jesse J. McClure, Xiaoyang Li, C. James Chou (2018). Advances and Challenges of HDAC Inhibitors in Cancer Therapeutics. *Advances in Cancer Research*, Volume 138 <https://doi.org/10.1016/bs.acr.2018.02.006>
62. Barneda-Zahonero, B., & Parra, M. (2012). Histone deacetylases and cancer. *Molecular Oncology*, 6(6), 579–589. <https://doi.org/10.1016/j.molonc.2012.07.003>.
63. Zagni C, Floresta G, Monciino G, et al. The Search for Potent, Small-Molecule HDACIs in Cancer Treatment: A Decade After Vorinostat. *Med Res Rev* 2017 Nov;37(6):1373-428.
64. F. Tang, E. Choy, C. Tu, F. Hornicek, Z. Duan, Therapeutic applications of histone deacetylase inhibitors in sarcoma, *Cancer Treat. Rev.* 59 (2017) 33–45, <https://doi.org/10.1016/j.ctrv.2017.06.006>.
65. A.C. West, R.W. Johnstone, New and emerging HDAC inhibitors for cancer treatment, *J. Clin. Invest.* 124 (1) (2014) 30–39, <https://doi.org/10.1172/JCI69738>.
66. Kai Gong, Maoqin Wang, Qiong Duan, Gang Li, Daojing Yong, Cailing Ren, Yue Li, Qijun Zhang, Zongjie Wang, Tao Sun, Huanyun Zhang, Qiang Tu, Changsheng Wu, Jun Fu, Aiyang Li, Chaoyi Song, Youming Zhang, Ruijuan Li. High-yield production of FK228 and new derivatives in a *Burkholderia* chassis. *Metabolic Engineering* 75 (2023) 131–142
67. Ryan, Q. C., Headlee, D., Acharya, M., Sparreboom, A., Trepel, J. B., Ye, J., et al. (2005). Phase I and pharmacokinetic study of MS-275, a histone deacetylase inhibitor, in patients with advanced and refractory solid tumors or lymphoma. *Journal of Clinical Oncology*, 23(17), 3912–3922. <https://doi.org/10.1200/JCO.2005.02.188>.
68. Phimmachanh M, Han JZR, O'Donnell YEI, Latham SL and Croucher DR (2020) Histone Deacetylases and Histone Deacetylase Inhibitors in Neuroblastoma. *Front. Cell Dev. Biol.* 8:578770. doi: 10.3389/fcell.2020.578770

69. Hontecillas-Prieto L, Flores-Campos R, Silver A, de Álava E, Hajji N and García-Domínguez DJ (2020) Synergistic Enhancement of Cancer Therapy Using HDAC Inhibitors: Opportunity for Clinical Trials. *Front. Genet.* 11:578011. doi: 10.3389/fgene.2020.578011
70. R.R. Shah, Safety and tolerability of histone deacetylase (HDAC) inhibitors in oncology, *Drug Saf.* 42 (2) (2019) 235–245, <https://doi.org/10.1007/s40264-018-0773-9>.
71. R.L. McIntyre, E.G. Daniels, M. Molenaars, R.H. Houtkooper and G.E. Janssens (2019) *EMBO Molecular Medicine* 11: e9854, 10.15252/emmm.201809854.
72. Tinka Haydn, Eric Metzger, Roland Schuele and Simone Fulda. Concomitant epigenetic targeting of LSD1 and HDAC synergistically induces mitochondrial apoptosis in rhabdomyosarcoma cells. *Cell Death and Disease* (2017) 8, e2879; doi:10.1038/cddis.2017.239
73. Xiangyang Liu, Grant C. Currens, Liang Xue and Yi-Qiang Cheng. Origin and bioactivities of thiosulfonated FK228. *Med. Chem. Commun.*, 2019, 10, 538
74. Ewa Lech-Maranda, Ewa Robak, Anna Korycka and Tadeusz Robak. Depsipeptide (FK228) as a Novel Histone Deacetylase Inhibitor: Mechanism of Action and Anticancer Activity. *Mini-Reviews in Medicinal Chemistry*, 2007, 7, 1062-1069
75. Wilson AJ, Lalani AS, Wass E, Saskowski J, Khabele D (2012) Romidepsin (FK228) combined with cisplatin stimulates DNA damage-induced cell death in ovarian cancer. *Gynecol Oncol* 127(3):579–586. <https://doi.org/10.1016/j.ygyno.2012.09.016>
76. Yehui Shi, Ying Fu, Xin Zhang, Gang Zhao, Yuan Yao, Yan Guo, Gang Ma, Shuai Bai, Hui Li. Romidepsin (FK228) regulates the expression of the immune checkpoint ligand PD-L1 and suppresses cellular immune functions in colon cancer. *Cancer Immunology, Immunotherapy* (2021) 70:61–73
77. Xiao, J. J., Foraker, A. B., Swaan, P. W., Liu, S., Huang, Y., Dai, Z., et al. (2005). Efflux of depsipeptide FK228 (FR901228, NSC-630176) is mediated by P-glycoprotein and multidrug resistance-associated protein 1. *The Journal of Pharmacology and Experimental Therapeutics*, 313(1), 268–276. <https://doi.org/10.1124/jpet.104.072033>
78. Shiraga, T., Tozuka, Z., Ishimura, R., Kawamura, A., & Kagayama, A. (2005). Identification of cytochrome P450 enzymes involved in the metabolism of FK228, a potent histone deacetylase inhibitor, in human liver microsomes. *Biological & Pharmaceutical Bulletin*, 28(1), 124–129
79. Furumai R, Matsuyama A, Kobashi N, Lee KH, Nishiyama M, Nakajima H, Tanaka A, Komatsu Y, Nishino N, Yoshida M, et al. 2002. FK228 (depsipeptide) as a natural prodrug that inhibits class I histone deacetylases. *Cancer Res.* 62:4916–4921.
80. Gore L, Rothenberg ML, O’Bryant CL, et al. A phase I and pharmacokinetic study of the oral histone deacetylase inhibitor, MS-275, in patients with refractory solid tumors and lymphomas. *Clin Cancer Res* 2008;14(14):4517-25
81. Jeffrey Knipstein & Lia Gore. Entinostat for treatment of solid tumors and hematologic malignancies. *Expert Opin. Investig. Drugs* (2011) 20(10):1455-1467
82. Acharya MR, Sparreboom A, Sausville EA, et al. Interspecies differences in plasma protein binding of MS-275, a novel histone deacetylase inhibitor. *Cancer Chemother Pharmacol* 2006;57(3):275—81

83. Rossana Ruiz, Luis E Ruez & Christian Rolfo. Entinostat (SNDX-275) for the treatment of non-small cell lung cancer. *Expert Opin. Investig. Drugs* (2015) 24(8).
84. Acharya MR, Karp JE, Sausville EA, et al. Factors affecting the pharmacokinetic profile of MS-275, a novel histone deacetylase inhibitor, in patients with cancer. *Invest New Drugs* 2006;24(5):367—75
85. Minnar CM, Chariou PL, Horn LA, et al. Tumor-targeted interleukin-12 synergizes with entinostat to overcome PD-1/ PD-L1 blockade-resistant tumors harboring MHC-I and APM deficiencies. *Journal for ImmunoTherapy of Cancer* 2022;10:e004561. doi:10.1136/ jtc-2022-004561
86. Andrew S. Truong, Mi Zhou, Bhavani Krishnan, Takanobu Utsumi, Ujjawal Manocha, Kyle G. Stewart, Wolfgang Beck, Tracy L. Rose, Matthew I. Milowsky, Xiaping He, Christof C. Smith, Lisa M. Bixby, Charles M. Perou, Sara E. Wobker, Sean T. Bailey, Benjamin G. Vincent, and William Y. Kim. Entinostat induces antitumor immune responses through immune editing of tumor neoantigens. *J Clin Invest.* 2021;131(16):e138560.
87. Vijayalaxmi G. Gupta, Jeff Hirst, Shariska Petersen, Katherine F. Roby, Meghan Kusch, Helen Zhou, Makena L. Clive, Andrea Jewell, Harsh B. Pathak, Andrew K. Godwin, Andrew J. Wilson, Marta Crispens, Emily Cybulla, Alessandro Vindigni, Katherine Fuh, Dineo Khabele. Entinostat, a selective HDAC1/2 inhibitor, potentiates the effects of olaparib in homologous recombination proficient ovarian cancer. *Gynecol Oncol.* 2021 July ; 162(1): 163–172. doi:10.1016/j.ygyno.2021.04.015.
88. Sonnemann J, Dreyer L, Hartwig M, et al. Histone deacetylase inhibitors induce cell death and enhance the apoptosis-inducing activity of TRAIL in Ewing’s sarcoma cells. *J Cancer Res Clin Oncol* 2007;133(11):847-58
89. Jaboin J, Wild J, Hamidi H, et al. MS27-275, an inhibitor of histone deacetylase, has marked in vitro and in vivo antitumor activity against pediatric solid tumors. *Cancer Res* 2002;62(21):6108—15
90. M.P. Phelps, J.N. Bailey, T. Vleeshouwer-Neumann, E.Y. Chen, CRISPR screen identifies the NCOR/HDAC3 complex as a major suppressor of differentiation in rhabdomyosarcoma, *Proc. Natl. Acad. Sci. U. S. A.* 113 (52) (2016) 15090–15095, <https://doi.org/10.1073/pnas.1610270114>.
91. Saito, A.; Yamashita, T.; Mariko, Y.; Nosaka, Y.; Tsuchiya, K.; Ando, T.; Suzuki, T.; Tsuruo, T.; Nakanishi, O. A synthetic inhibitor of histone deacetylase, MS-27-275, with marked in vivo antitumor activity against human tumors. *Proc. Natl. Acad. Sci. USA* 1999, 96, 4592–4597.
92. Hedrick E, Crose L, Linardic CM, Safe S. 2015. Histone deacetylase inhibitors inhibit rhabdomyosarcoma by reactive oxygen species dependent targeting of specificity protein transcription factors. *Mol Cancer Ther.* 14:2143–2153.
93. Lee JH, Choy ML, Marks PA. 2012. Mechanisms of resistance to histone deacetylase inhibitors. *Adv Cancer Res.* 116:39–86
94. Dutta C, Day T, Kopp N, van Bodegom D, Davids MS, Ryan J, Bird L, Kommajosyula N, Weigert O, Yoda A, et al. 2012. BCL2 suppresses PARP1 function and nonapoptotic cell death. *Cancer Res.* 72: 4193–4203.
95. J. Abraham, Y. Nunez- ~ Alvarez, ´ S. Hettmer, E. Carrio, ´ H.I. Chen, K. Nishijo, E. T. Huang, et al., Lineage of origin in rhabdomyosarcoma informs pharmacological response, *Genes Dev.* 28 (14) (2014) 1578–1591, <https://doi.org/10.1101/ gad.238733.114>.

96. M. Cassandri, S. Pomella, A. Rossetti, F. Petragnano, L. Milazzo, F. Vulcano, et al., MS-275 (Entinostat) promotes radio-sensitivity in PAX3-FOXO1 rhabdomyosarcoma cells, *Int. J. Mol. Sci.* 22 (19) (2021) 10671, <https://doi.org/10.3390/ijms221910671>.
97. Tonelli, R.; McIntyre, A.; Camerin, C.; Walters, Z.S.; Di Leo, K.; Selfe, J.; Purgato, S.; Missiaglia, E.; Tortori, A.; Renshaw, J.; et al. Antitumor activity of sustained N-myc reduction in rhabdomyosarcomas and transcriptional block by antigene therapy. *Clin. Cancer Res.* 2012, 18, 796–807.
98. Gravina, G.L.; Festuccia, C.; Popov, V.M.; Di Rocco, A.; Colapietro, A.; Sanità, P.; Delle Monache, S.; Musio, D.; De Felice, F.; Di Cesare, E.; et al. C-Myc Sustains Transformed Phenotype and Promotes Radioresistance of Embryonal Rhabdomyosarcoma Cell Lines. *Radiat. Res.* 2016, 185, 411–422.
99. Robert C, Rassool FV. 2012. HDAC inhibitors: roles of DNA damage and repair. *Adv Cancer Res.* 116:87–129.
100. Lombard DB, Cierpicki T, Grembecka J. 2019. Combined MAPK pathway and HDAC inhibition breaks melanoma. *Cancer Discov.* 9(4): 469–471.
101. Rahmani M, Aust MM, Benson EC, Wallace L, Friedberg J, Grant S. 2014. PI3K/mTOR inhibition markedly potentiates HDAC inhibitor activity in NHL cells through BIM- and MCL-1-dependent mechanisms in vitro and in vivo. *Clin Cancer Res.* 15(18):4849–4860.
102. N. Bharathy, N.E. Berlow, E. Wang, J. Abraham, T.P. Settlemeyer, J.E. Hooper, et al., The HDAC3-SMARCA4-miR-27a axis promotes expression of the PAX3:FOXO1 fusion oncogene in rhabdomyosarcoma, *Sci. Signal.* 11 (557) (2018) eaau7632, <https://doi.org/10.1126/scisignal.aau7632>.
103. Helleday, T. Homologous recombination in cancer development, treatment and development of drug resistance. *Carcinogenesis* 2010, 31, 955–960.
104. Begg, A.C.; Stewart, F.A.; Vens, C. Strategies to improve radiotherapy with targeted drugs. *Nat. Rev. Cancer* 2011, 239–253.
105. Boustani, J.; Grapin, M.; Laurent, P.A.; Apetoh, L.; Mirjole, C. The 6th R of radiobiology: Reactivation of anti-tumor immune response. *Cancers* 2019, 11, 860.
106. Ellis, L.; Hammers, H.; Pili, R. Targeting tumor angiogenesis with histone deacetylase inhibitors. *Cancer Lett.* 2009, 280, 145–153.
107. Liu, S.S.; Wu, F.; Jin, Y.M.; Chang, W.Q.; Xu, T.M. HDAC11: A rising star in epigenetics. *Biomed. Pharmacother.* 2020, 131, 110607.

